Further search for supersymmetry at $\sqrt{s} = 7$ TeV in final states with jets, missing transverse momentum, and isolated leptons with the ATLAS detector

G. Aad *et al.**
(ATLAS Collaboration)

(Received 23 August 2012; published 2 November 2012)

This work presents a new inclusive search for supersymmetry (SUSY) by the ATLAS experiment at the LHC in proton-proton collisions at a center-of-mass energy $\sqrt{s} = 7$ TeV in final states with jets, missing transverse momentum and one or more isolated electrons and/or muons. The search is based on data from the full 2011 data-taking period, corresponding to an integrated luminosity of 4.7 fb^{-1}. Single-lepton and multilepton channels are treated together in one analysis. An increase in sensitivity is obtained by simultaneously fitting the number of events in statistically independent signal regions, and the shapes of distributions within those regions. A dedicated signal region is introduced to be sensitive to decay cascades of SUSY particles with small mass differences (''compressed SUSY''). Background uncertainties are constrained by fitting to the jet-multiplicity distribution in background control regions. Observations are consistent with Standard Model expectations, and limits are set or extended on a number of SUSY models.

DOI: 10.1103/PhysRevD.86.092002 PACS numbers: 12.60.Jv, 13.85.Rm, 14.80.Ly

I. INTRODUCTION

Supersymmetry (SUSY) [1–9] is a candidate for physics beyond the Standard Model (SM). If strongly interacting supersymmetric particles are present at the TeV scale, they may be copiously produced in 7 TeV proton-proton collisions at the Large Hadron Collider [10]. In the minimal supersymmetric extension of the Standard Model (MSSM) [11–15] such particles decay into jets, leptons and the lightest supersymmetric particle (LSP). Jets arise in the decays of squarks and gluinos, while leptons can arise in decays involving charginos or neutralinos. A long-lived, weakly interacting LSP will escape detection, leading to missing transverse momentum ($\vec{p}_{\mathrm{T}}^{\,\mathrm{miss}}$ and its magnitude $E_{\mathrm{T}}^{\mathrm{miss}}$) in the final state. Significant $E_{\mathrm{T}}^{\mathrm{miss}}$ can also arise in scenarios where neutrinos are created somewhere in the SUSY decay cascade.

This paper presents a new inclusive search with the ATLAS detector for SUSY in final states containing jets, one or more isolated leptons (electrons or muons) and $E_{\mathrm{T}}^{\mathrm{miss}}$. Previous searches in these channels have been conducted by both the ATLAS [16–18] and CMS [19–22] collaborations. In this paper, the analysis is extended to 4.7 fb^{-1}, and single-lepton and multilepton channels (with jets and $E_{\mathrm{T}}^{\mathrm{miss}}$) are treated simultaneously. A signal region with a soft lepton and soft jets is introduced in order to probe SUSY decays involving small mass differences between the particles in the decay chain. A new, simultaneous fit to the yield in multiple signal regions and to the shapes of distributions within those signal regions is employed. Background uncertainties are constrained by fitting to the jet-multiplicity distribution in background control regions.

II. THE ATLAS DETECTOR

The ATLAS detector [23,24] consists of a tracking system (inner detector, ID) surrounded by a thin superconducting solenoid providing a 2 T magnetic field, electromagnetic and hadronic calorimeters and a muon spectrometer (MS). The ID consists of pixel and silicon microstrip detectors, surrounded by a straw-tube tracker with transition radiation detection (transition radiation tracker, TRT). The electromagnetic calorimeter is a lead liquid-argon (LAr) detector. Hadronic calorimetry is based on two different detector technologies, with scintillator tiles or LAr as active media, and with either steel, copper, or tungsten as the absorber material. The MS is based on three large superconducting toroid systems arranged with an eight-fold azimuthal coil symmetry around the calorimeters, and three stations of chambers for the trigger and for precise position measurements. The nominal pp interaction point at the center of the detector is defined as the origin of a right-handed coordinate system. The positive x axis is defined by the direction from the interaction point to the center of the LHC ring, with the positive y axis pointing upwards, while the beam direction defines the z axis. The azimuthal angle ϕ is measured around the beam axis and the polar angle θ is the angle from the z axis. The pseudorapidity is defined as $\eta = -\ln\tan(\theta/2)$. Transverse coordinates, such as the transverse momentum, p_{T}, are defined in the (x-y) plane.

*Full author list given at the end of the article.

III. SUSY SIGNAL MODELING AND SIMULATED EVENT SAMPLES

The SUSY models considered are minimal supergravity (MSUGRA) or constrained MSSM (CMSSM) [25,26], minimal gauge-mediated SUSY breaking (GMSB) [27–31] and a number of simplified models [32,33]. The MSUGRA/CMSSM model is characterized by five parameters: the universal scalar and gaugino mass parameters m_0 and $m_{1/2}$, a universal trilinear coupling parameter A_0, the ratio of the vacuum expectation values of the two Higgs doublets $\tan\beta$, and the sign of the Higgsino mass parameter μ. In this analysis, the values of m_0 and $m_{1/2}$ are scanned, and the other parameters are fixed as follows: $\tan\beta = 10$, $A_0 = 0$ and μ is taken to be positive. A diagram showing the decay of the associated production of a squark and a gluino is depicted in Fig. 1(a). Other diagrams representative for the SUSY models discussed in the following are shown in Figs. 1(b)–1(d).

The minimal GMSB model has six parameters: the SUSY breaking scale Λ, the mass scale of the messenger fields $M_{\rm mes}$, the number of messenger fields N_5, the scale of the gravitino coupling $C_{\rm grav}$, the ratio of the vacuum expectation values of the two Higgs doublets $\tan\beta$, and the sign of the Higgsino mass parameter μ. For the minimal GMSB model, the parameters $\tan\beta$ and Λ are scanned and the other parameters are assigned fixed values: $M_{\rm mes} = 250$ TeV, $N_5 = 3$, $C_{\rm grav} = 1$ and the sign of μ is taken to be positive. The mass scale of the colored superpartners is set by the parameter Λ, while the next-to-lightest SUSY particle (NLSP) is determined by a combination of Λ and $\tan\beta$. At low values of Λ, the NLSP is the lightest neutralino ($\tilde{\chi}_1^0$) while at the higher values of Λ where this search provides new sensitivity, the NLSP is a stau for $\tan\beta \gtrsim 10$ and a slepton of the first and second generation otherwise. The NLSP decays into its SM partner and a nearly massless gravitino. The gaugino and sfermion masses are proportional to N_5 and $\sqrt{N_5}$, respectively. The parameter $C_{\rm grav}$ determines the NLSP lifetime, set here such that all NLSPs decay promptly.

Several simplified models are considered in this paper. In the "one-step" models, SUSY production proceeds via either $pp \to \tilde{g}\,\tilde{g}$ or $pp \to \tilde{q}_L\tilde{q}_L^*$, where only left-handed squarks of the first and second generation are considered. The gluino decays to the neutralino LSP via $\tilde{g} \to q\bar{q}'\tilde{\chi}_1^\pm \to q\bar{q}'W^\pm\tilde{\chi}_1^0$, and the squark via $\tilde{q}_L \to q'\tilde{\chi}_1^\pm \to q'W^\pm\tilde{\chi}_1^0$, where the W boson can be real or virtual. The gluino and LSP masses are varied while the chargino mass is set to be halfway between them. In a variant of the one-step model, the LSP mass is held fixed at 60 GeV while the gluino (squark) and chargino masses are scanned.

In the "two-step" models, SUSY production proceeds via either $pp \to \tilde{g}\,\tilde{g}$ or $pp \to \tilde{q}_L\tilde{q}_L^*$, again where squarks of the first and second generation are considered. In the first class of two-step models all squarks and gluinos decay via a chargino: $\tilde{g} \to q\bar{q}'\tilde{\chi}_1^\pm$ and $\tilde{q}_L \to q'\tilde{\chi}_1^\pm$. The charginos decay via $\tilde{\chi}_1^\pm \to \ell\tilde{\nu}_L$ or $\tilde{\chi}_1^\pm \to \nu\tilde{\ell}_L$; in the case of third generation sleptons, the decay to the stau is via $\tilde{\chi}_1^\pm \to \nu\tilde{\tau}_1$. All three generations of sleptons and sneutrinos are allowed with equal probability, resulting in an equal branching ratio to sleptons and to sneutrinos. In the second class of two-step models, the gluinos or left-handed squarks decay either via a chargino ($\tilde{g} \to q\bar{q}'\tilde{\chi}_1^\pm$ or $\tilde{q}_L \to q'\tilde{\chi}_1^\pm$) or via a neutralino ($\tilde{g} \to q\bar{q}\tilde{\chi}_2^0$ or $\tilde{q}_L \to q\tilde{\chi}_2^0$). The events are generated such that one chargino and one neutralino are always present in the decays of the pair produced gluinos or left-handed squarks. Neutralino decays proceed via either $\tilde{\chi}_2^0 \to \ell\tilde{\ell}_L$ or $\tilde{\chi}_2^0 \to \nu\tilde{\nu}$. As in the first two-step model, all three generations of sleptons and sneutrinos are allowed with equal probability, resulting in a 50% branching ratio to sleptons and to sneutrinos. Finally, in the third class of two-step models without intermediate sleptons, the gluino and squark decay via $\tilde{g} \to q\bar{q}'\tilde{\chi}_1^\pm$ or $\tilde{q}_L \to q'\tilde{\chi}_1^\pm$; the decay of the chargino then proceeds via $\tilde{\chi}_1^\pm \to W^{(*)\pm}\tilde{\chi}_2^0 \to W^{(*)\pm}Z^{(*)}\tilde{\chi}_1^0$. This signature is realized in the MSSM in a parameter region where additional decay modes, not contained in the simplified model, may lead to a significant reduction of the cross section times branching fraction of the WZ signature.

In the first two types of two-step models, the chargino and neutralino have equal masses (again set to be halfway between the gluino/squark and LSP mass); the slepton and sneutrino masses are set to be equal and halfway between

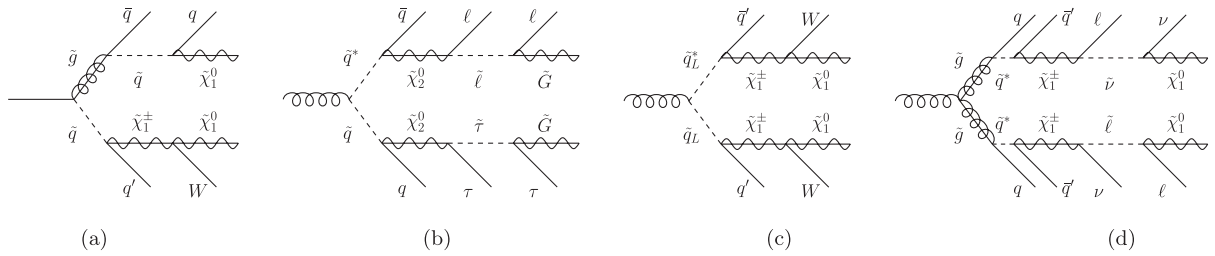

FIG. 1. Representative diagrams for the different SUSY models considered in this analysis: (a) MSUGRA/CMSSM model with $pp \to \tilde{q}\,\tilde{g}$ and subsequent decay of the squark via a chargino; (b) GMSB model with $pp \to \tilde{q}\tilde{q}^*$ and subsequent decay via sleptons and staus; (c) one-step simplified model with $pp \to \tilde{q}_L\tilde{q}_L^*$ and subsequent decay via charginos; (d) two-step simplified model with $pp \to \tilde{g}\,\tilde{g}$ and subsequent decays via charginos and sleptons or sneutrinos.

the chargino/neutralino and LSP masses. In the third two-step model, the $\tilde{\chi}_1^{\pm}$ mass is set halfway between the gluino/squark and LSP while the $\tilde{\chi}_2^0$ mass is set halfway between the chargino and LSP. In all the simplified models, the superpartners that have not been mentioned are decoupled by setting their masses to multi-TeV values.

Simulated event samples are used for estimating the signal acceptance, the detector efficiency, and for estimating many of the backgrounds (in most cases in association with data-driven techniques). The MSUGRA/CMSSM and minimal GMSB signal samples are generated with HERWIG++ 2.5.2 [34] and MRST2007LO* [35] parton distribution functions (PDFs); ISAJET 7.80 [36] is used to generate the physical particle masses. The simplified models are generated with one extra jet in the matrix element using MADGRAPH5 [37], interfaced to PYTHIA [38], with the CTEQ6L1 [39] PDF set; MLM matching [40] is done with a scale parameter that is set to one-fourth of the mass of the lightest sparticle in the hard-scattering matrix element. Signal cross sections are calculated in the MSSM at next-to-leading order in the strong coupling constant, including the resummation of soft gluon emission at next-to-leading-logarithmic accuracy (NLO + NLL) [41–45].

The simulated event samples for the SM backgrounds are summarized in Table I. The ALPGEN and MADGRAPH samples are produced with the MLM matching scheme. The ALPGEN samples are generated with a number of partons $0 \leq N_{\text{parton}} \leq 5$ in the matrix element, except for W + light-flavored jets which are generated with up to six partons. The $Wb\bar{b}$, $Wc\bar{c}$ and Wc cross sections shown are the leading-order values from ALPGEN multiplied by a K factor of 1.2, based on the K factor for light-flavored jets. For the final result, measured cross sections are used for the W/Z + heavy-flavor-jets samples [55]. The overlap between the heavy-flavored and light-flavored W/Z + jets samples is removed. The cross section for Z + jets with $10\ \text{GeV} < m_{\ell\ell} < 40\ \text{GeV}$ is obtained by assuming the same K factor as for $m_{\ell\ell} > 40$ GeV. The single-top cross sections are taken from MC@NLO; for the s and t channels, they are listed for a single lepton flavor.

The theoretical cross sections for W + jets and Z + jets are calculated with FEWZ [48] with the MSTW2008NNLO [56] PDF set. For the diboson cross sections, MCFM [52] with the MSTW2008NLO PDFs is used. The $t\bar{t}$ cross section is calculated with HATHOR 1.2 [47] using MSTW2008NNLO PDFs. The $t\bar{t} + W$ cross section is taken from Ref. [53]. The $t\bar{t} + Z$ cross section is the leading-order value multiplied by a K factor deduced from the NLO calculation at $\sqrt{s} = 14$ TeV [54].

Parton shower and fragmentation processes are simulated for the ALPGEN and MC@NLO samples using HERWIG [51] with JIMMY [57] for underlying event modeling; PYTHIA is used for the ACERMC single-top sample and $t\bar{t} + W/Z$. The PDFs used in this analysis are CTEQ6L1 for the ALPGEN and MADGRAPH samples, CT10 [58] for MC@NLO, and MRSTMCal (LO**) [59] for HERWIG. The underlying event tunes are the ATLAS AUET2B_LO** tunes [60].

The detector simulation [61] is performed using GEANT4 [62]. All samples are produced with a range of simulated minimum-bias interactions overlaid on the hard-scattering event to account for multiple pp interactions in the same beam crossing (pileup). The overlay also treats the impact

TABLE I. Simulated background event samples used in this analysis, with the corresponding production cross sections. The notation LO × K indicates that the process is calculated at leading order and corrected by a factor derived from the ratio of NLO to LO cross sections for a closely related process. The $t\bar{t}$, W + light-jets and Z + light-jets samples are normalized using the inclusive cross sections; the values shown for the W + light-jets and Z + light-jets samples are for a single lepton flavor. The single-top cross sections are listed for a single lepton flavor in the s and t channels. Further details are given in the text.

Physics process	Generator	Cross section (pb)	Calculation accuracy
$t\bar{t}$	ALPGEN 2.13 [46]	166.8	NLO + NLL [47]
$W(\rightarrow \ell\nu)$ + jets	ALPGEN 2.13 [46]	10460	NNLO [48]
$W(\rightarrow \ell\nu) + b\bar{b}$ + jets	ALPGEN 2.13 [46]	130	LO × K
$W(\rightarrow \ell\nu) + c\bar{c}$ + jets	ALPGEN 2.13 [46]	360	LO × K
$W(\rightarrow \ell\nu) + c$ + jets	ALPGEN 2.13 [46]	1100	LO × K
$Z/\gamma^*(\rightarrow \ell\ell)$ + jets ($m_{\ell\ell} > 40$ GeV)	ALPGEN 2.13 [46]	1070	NNLO [48]
$Z/\gamma^*(\rightarrow \ell\ell)$ + jets ($10\ \text{GeV} < m_{\ell\ell} < 40\ \text{GeV}$)	ALPGEN 2.13 [46]	3970	NNLO [48]
$Z/\gamma^*(\rightarrow \ell\ell) + b\bar{b}$ + jets ($m_{\ell\ell} > 40$ GeV)	ALPGEN 2.13 [46]	10.3	LO
Single-top (t chan)	ACERMC 3.8 [49]	7.0	NLO
Single-top (s chan)	MC@NLO 4.01 [50]	0.5	NLO
Single-top (Wt chan)	MC@NLO 4.01 [50]	15.7	NLO
WW	HERWIG 6.5.20 [51]	44.9	NLO [52]
WZ/γ^* ($m_{Z/\gamma^*} > 60$ GeV)	HERWIG 6.5.20 [51]	18.5	NLO [52]
$Z/\gamma^*Z/\gamma^*$ ($m_{Z/\gamma^*} > 60$ GeV)	HERWIG 6.5.20 [51]	5.96	NLO [52]
$t\bar{t} + W$	MADGRAPH5 [37]	0.169	NLO [53]
$t\bar{t} + Z$	MADGRAPH5 [37]	0.120	LO × K [54]

of pileup from beam crossings other than the one in which the event occurred. Corrections are applied to the simulated samples to account for differences between data and simulation for the lepton trigger and reconstruction efficiencies, momentum scale and resolution, and for the efficiency and mistag rates for b-quark tagging.

IV. OBJECT RECONSTRUCTION

This analysis is based on three broad classes of event selection: (i) a hard single-lepton channel that is an extension to higher masses of the previous search [16], (ii) a soft single-lepton channel geared towards SUSY models with small mass differences in the decay cascade, and (iii) a multilepton channel aimed at decay chains with higher lepton multiplicities. The event selection requirements are described in detail in Sec. VI. Here the final-state object reconstruction and selection are discussed.

A. Object preselection

The primary vertex [63] is required to be consistent with the beam spot envelope and to have at least five associated tracks; when more than one such vertex is found, the vertex with the largest summed $|p_T|^2$ of the associated tracks is chosen.

Electrons are reconstructed from energy clusters in the electromagnetic calorimeter matched to a track in the ID [64]. Preselected electrons are required to have $|\eta| < 2.47$ and pass a variant of the "medium" selection defined in Ref. [64] that differs mainly in having a tighter track-cluster matching in η, stricter pixel hit requirements, additional requirements in the TRT, and tighter shower-shape requirements for $|\eta| > 2.0$. These requirements provide background rejection close to the "tight" selection of Ref. [64] with only a few percent loss in efficiency with respect to medium. Preselected electrons are further required to pass a p_{T} requirement depending on the analysis channel: 10 GeV for the hard-lepton and multilepton channels, and 7 GeV in the soft-lepton channel.

Muons are identified either as a combined track in the MS and ID systems, or as an ID track matched with a MS segment [65,66]. Requirements on the quality of the ID track are identical to those in Ref. [16]. Preselected muons are required to have $|\eta| < 2.4$ and a p_{T} requirement that depends on the analysis channel: 10 GeV for the hard-lepton and multilepton channels, and 6 GeV in the soft-lepton channel.

Jets are reconstructed using the anti-k_t algorithm [67,68] with a radius parameter $R = 0.4$. Jets arising from detector noise, cosmic rays or other noncollision sources are rejected [69]. To account for the differences between the calorimeter response to electrons and hadrons, p_{T}- and η-dependent factors, derived from simulated events and validated with test beam and collision data, are applied to each jet to provide an average energy scale correction [69] back to particle level. Preselected jets are required to have $p_{\mathrm{T}} > 20$ GeV and $|\eta| < 4.5$. Since electrons are also reconstructed as jets, preselected jets which overlap with preselected electrons within a distance $\Delta R = \sqrt{(\Delta\eta)^2 + (\Delta\phi)^2} = 0.2$ are discarded.

B. Signal object selection

For the final selection of signal events, "signal" electrons are required to pass a variant of the "tight" selection of Ref. [64], providing 1%–2% gain in efficiency and slightly better background rejection. Signal electrons must have $|\eta| < 2.47$ and a distance to the closest jet $\Delta R > 0.4$. They are also required to satisfy isolation criteria: the scalar sum of the p_{T} of tracks within a cone of radius $\Delta R = 0.2$ around the electron (excluding the electron itself) is required to be less than 10% of the electron p_{T}.

Muons in the final selection (signal muons) are required to have $|\eta| < 2.4$ and $\Delta R > 0.4$ with respect to the closest jet. Further isolation criteria are imposed: the scalar sum of the p_{T} of tracks within a cone of radius $\Delta R = 0.2$ around the muon candidate (excluding the muon itself) is required to be less than 1.8 GeV. The p_{T} requirements for signal electrons and muons depend on the signal regions and are described in Sec. VI.

Signal jets are required to have $p_{\mathrm{T}} > 25$ GeV and $|\eta| < 2.5$. In addition, they are required to be associated with the hard-scattering process, by demanding that at least 75% of the scalar sum of the p_{T} of all tracks associated with the jet come from tracks associated with the primary vertex of the event. Jets with no associated tracks are rejected. The above requirements are applied to cope with the high pileup conditions of the 2011 data-taking, in particular the later part of the run.

The missing transverse momentum is computed as the negative of the vector sum of the p_{T} of all preselected electrons, preselected muons and preselected jets (after removing those overlapping with preselected electrons), and all calorimeter clusters with $|\eta| < 4.9$ that are not associated with any of the above-mentioned objects.

For approximately 20% of the 2011 data-taking period, an electronics failure created a region in the electromagnetic calorimeter, located at $0 < \eta < 1.4$ and $-0.8 < \phi < -0.6$, where no signals could be read out. Events with an electron in this region are vetoed for the entire data set, leading to an acceptance loss of less than 1% for signal events in the signal region. For jets, the amount of transverse energy (E_{T}) lost in the dead region can be estimated from the energy deposited in the neighboring calorimeter cells. If this lost E_{T} projected along the $E_{\mathrm{T}}^{\mathrm{miss}}$ direction amounts to more than 10 GeV and constitutes more than 10% of the $E_{\mathrm{T}}^{\mathrm{miss}}$, the event is rejected. The effect of the electronics failure is described in the detector simulation, and the loss of signal acceptance from this requirement is negligible.

Jets arising from b quarks are identified using information about track impact parameters and reconstructed secondary vertices [70]; the b-tagging algorithm is based on a neural network using the output weights of the JetFitter + IP3D, IP3D, and SV1 algorithms (defined in Ref. [70]) as input. The b-tagging requirements are set at an operating point corresponding to an average efficiency of 60% for b jets in simulated $t\bar{t}$ events, for which the algorithm provides a rejection factor of approximately 200–400 for light-quark and gluon jets (depending on the p_{T} of the jet) and a rejection of approximately 7–10 for charm jets.

V. TRIGGER AND DATA COLLECTION

The data used in this analysis were collected from March through October 2011, during which the instantaneous luminosity of the LHC reached $3.65 \times 10^{33}\ \mathrm{cm}^{-2}\,\mathrm{s}^{-1}$. The average number of interactions per beam crossing ranged from approximately 4 to 16 during the run, with an average of 10. After the application of beam, detector, and data-quality requirements, the total integrated luminosity is $4.7\ \mathrm{fb}^{-1}$. The uncertainty on the luminosity is determined to be 3.9% [71,72].

Three types of triggers were used to collect the data: electron, muon and $E_{\mathrm{T}}^{\mathrm{miss}}$. The electron trigger selects events containing one or more electron candidates, based on the presence of a cluster in the electromagnetic calorimeter, with a shower shape consistent with that of an electron. The transverse energy threshold at the trigger level was either 20 GeV or 22 GeV, depending on the instantaneous luminosity. For signal electrons satisfying $p_{\mathrm{T}} > 25$ GeV, the trigger efficiency is in the plateau region and ranges between 95% and 97%. In order to recover some of the efficiency for high-p_{T} electrons during running periods with the highest instantaneous luminosities, events were also collected with an electron trigger with looser shower-shape requirements but with a p_{T} threshold of 45 GeV.

The muon trigger selects events containing one or more muon candidates based on tracks identified in the MS and ID. The muon trigger p_{T} threshold was 18 GeV. During running periods with the highest instantaneous luminosities, the trigger requirements on the number of MS hits were tightened; in order to recover some of the resulting loss in efficiency, events were also collected with a muon trigger that maintained the looser requirement on the number of chamber hits but that required in addition a jet with p_{T} greater than 10 GeV. This jet requirement is fully efficient for jets with offline calibrated p_{T} greater than approximately 50 GeV. The muon triggers reach their efficiency plateaus below a signal muon p_{T} threshold of 20 GeV. The plateau efficiency ranges from about 70% for $|\eta| < 1.05$ to 88% for $1.05 < |\eta| < 2.4$.

The $E_{\mathrm{T}}^{\mathrm{miss}}$ trigger bases the bulk of its rejection on the vector sum of transverse energies deposited in projective trigger towers (each with a size of approximately $\Delta\eta \times \Delta\phi \sim 0.1 \times 0.1$ for $|\eta| < 2.5$ and larger and less regular in the more forward regions). A more refined calculation based on the vector sum of all calorimeter cells above threshold is made at a later stage in the trigger processing. The trigger required $E_{\mathrm{T}}^{\mathrm{miss}} > 60$ GeV, reaching its efficiency plateau for offline calibrated $E_{\mathrm{T}}^{\mathrm{miss}} > 180$ GeV. The efficiency on the plateau is close to 100%.

VI. EVENT SELECTION

Two variables, derived from the kinematic properties of the reconstructed objects, are used in the event selection. The transverse mass (m_{T}) computed from the momentum of the lepton (ℓ) and the missing transverse momentum ($\vec{p}_{\mathrm{T}}^{\mathrm{miss}}$), defined as

$$m_{\mathrm{T}} = \sqrt{2 p_{\mathrm{T}}^{\ell} E_{\mathrm{T}}^{\mathrm{miss}} (1 - \cos(\Delta\phi(\vec{\ell}, \vec{p}_{\mathrm{T}}^{\mathrm{miss}})))},$$

is useful in rejecting events containing a single W boson. The inclusive effective mass ($m_{\mathrm{eff}}^{\mathrm{inc}}$) is the scalar sum of the p_{T} of the leptons, the jets and $E_{\mathrm{T}}^{\mathrm{miss}}$:

$$m_{\mathrm{eff}}^{\mathrm{inc}} = \sum_{i=1}^{N_{\mathrm{lep}}} p_{\mathrm{T},i}^{\ell} + \sum_{j=1}^{N_{\mathrm{jet}}} p_{\mathrm{T},j} + E_{\mathrm{T}}^{\mathrm{miss}}$$

where the index i runs over all the signal leptons and j runs over all the signal jets in the event. The inclusive effective mass is correlated with the overall mass scale of the hard-scattering process and provides good discrimination against the SM background, without being too sensitive to the details of the SUSY decay cascade. The analysis in Ref. [16] used the three or four leading-p_{T} jets in the calculation of the effective mass; the additional jets used here improve the discrimination between signal and background. A second definition for the effective mass, denoted by m_{eff}, is based on the sum over the two, three, or four leading p_{T} jets, depending on the minimum number of jets required in a given signal region. This variable is used to compute the ratio $E_{\mathrm{T}}^{\mathrm{miss}}/m_{\mathrm{eff}}$ which reflects the fluctuations in the $E_{\mathrm{T}}^{\mathrm{miss}}$ as a function of the calorimeter activity in the event; the definition used here improves the rejection of the background from mismeasured jets.

This analysis is based on five signal regions, each tailored to maximize the sensitivity to different SUSY event topologies: (1,2) Signal regions requiring a hard lepton plus three or four jets are extensions of the previous analysis [16] to higher SUSY mass scales; these signal regions have been optimized for the MSUGRA/CMSSM model as well as for the bulk of the one-step simplified models with large mass difference (Δm) between the gluino and the LSP; (3) a soft-lepton signal region targets the simplified models with small Δm, where the hard leading jet comes from initial-state radiation (ISR); (4) a multilepton signal region with ≥ 2 jets is tailored to GMSB models; (5) a multilepton signal region with ≥ 4 jets is geared towards the two-step simplified models with

TABLE II. Overview of the selection criteria for the signal regions used in this analysis. The p_{T} selections for leptons are given for electrons (muons).

	Single lepton			Multilepton	
	3-jet	4-jet	Soft lepton	2-jet	4-jet
Trigger	Single electron or muon (+ jet)		Missing E_{T}	Single electron or muon (+ jet)	
N_{lep}	1	1	1	≥ 2	≥ 2
p_{T}^{ℓ} (GeV)	>25(20)	>25(20)	7 to 25 (6 to 20)	25 (20)	25 (20)
$p_{\mathrm{T}}^{\ell_2}$ (GeV)	<10	<10	<7(6)	>10	>10
N_{jet}	≥ 3	≥ 4	≥ 2	≥ 2	≥ 4
$p_{\mathrm{T}}^{\mathrm{jet}}$ (GeV)	>100, 25, 25	>80, 80, 80, 80	>130, 25	>200, 200	>50, 50, 50, 50
$p_{\mathrm{T}}^{4\mathrm{th\,jet}}$ (GeV)	<80	···	···	<50	···
$E_{\mathrm{T}}^{\mathrm{miss}}$ (GeV)	>250	>250	>250	>300	>100
m_{T} (GeV)	>100	>100	>100	···	···
$E_{\mathrm{T}}^{\mathrm{miss}}/m_{\mathrm{eff}}$	>0.3	>0.2	>0.3	···	>0.2
$m_{\mathrm{eff}}^{\mathrm{inc}}$ (GeV)	>1200	>800	···	···	>650

intermediate sleptons and sneutrinos. These signal regions are described in more detail and summarized in Table II.

(1) *Hard lepton plus three jets*. Events are selected with the electron and muon triggers. The number of signal leptons with $p_{\mathrm{T}} > 25(20)$ GeV for electrons (muons) is required to be exactly 1. Events containing additional signal leptons with $p_{\mathrm{T}} > 10$ GeV are rejected. The number of signal jets is required to be ≥ 3, with a leading jet satisfying $p_T > 100$ GeV and the other jets having $p_{\mathrm{T}} > 25$ GeV. Events with four or more jets are rejected if the fourth jet has $p_{\mathrm{T}} > 80$ GeV; this requirement keeps this signal region disjoint from the four-jet signal region. In addition, the following conditions are imposed: $m_{\mathrm{T}} > 100$ GeV, $E_{\mathrm{T}}^{\mathrm{miss}} > 250$ GeV, $E_{\mathrm{T}}^{\mathrm{miss}}/m_{\mathrm{eff}} > 0.3$, and $m_{\mathrm{eff}}^{\mathrm{inc}} > 1200$ GeV.

(2) *Hard lepton plus four jets*. The lepton requirements are the same as in the previous signal region. The number of signal jets is required to be ≥ 4, with the four leading jets satisfying $p_{\mathrm{T}} > 80$ GeV. In addition, the following requirements are applied: $m_{\mathrm{T}} > 100$ GeV, $E_{\mathrm{T}}^{\mathrm{miss}} > 250$ GeV, $E_{\mathrm{T}}^{\mathrm{miss}}/m_{\mathrm{eff}} > 0.2$, and $m_{\mathrm{eff}}^{\mathrm{inc}} > 800$ GeV.

(3) *Soft-lepton selection*. Events are selected with the $E_{\mathrm{T}}^{\mathrm{miss}}$ trigger. The number of signal leptons (electron or muon) is required to be exactly 1. Electrons are required to have $7\ \mathrm{GeV} < p_{\mathrm{T}} < 25$ GeV, and muons are required to be in the range $6\ \mathrm{GeV} < p_{\mathrm{T}} < 20$ GeV. Events containing an additional signal electron (muon) with $p_{\mathrm{T}} > 7(6)$ GeV are rejected. The number of signal jets is required to be ≥ 2, with the leading jet satisfying $p_{\mathrm{T}} > 130$ GeV and the second jet having $p_{\mathrm{T}} > 25$ GeV. In addition, the following conditions are required: $m_{\mathrm{T}} > 100$ GeV, $E_{\mathrm{T}}^{\mathrm{miss}} > 250$ GeV, and $E_{\mathrm{T}}^{\mathrm{miss}}/m_{\mathrm{eff}} > 0.3$. No explicit requirement on $m_{\mathrm{eff}}^{\mathrm{inc}}$ is applied.

(4) *Multilepton plus two jets*. Events are selected with the electron and muon triggers. Two or more signal leptons are required, with a leading electron (muon) with $p_T > 25(20)$ GeV and subleading leptons with $p_{\mathrm{T}} > 10$ GeV. The two leading leptons must have opposite charge. At least two signal jets with $p_{\mathrm{T}} > 200$ GeV are required. Events with four or more signal jets are rejected if the fourth leading jet has $p_{\mathrm{T}} > 50$ GeV; this requirement keeps this signal region disjoint from the multilepton plus four-jet signal region. In addition the $E_{\mathrm{T}}^{\mathrm{miss}}$ is required to be >300 GeV. No explicit requirements are made on $E_{\mathrm{T}}^{\mathrm{miss}}/m_{\mathrm{eff}}$ or $m_{\mathrm{eff}}^{\mathrm{inc}}$.

(5) *Multilepton plus four jets*. The lepton requirements are the same as in the multilepton plus two jets signal region. At least four signal jets with $p_{\mathrm{T}} > 50$ GeV are required. In addition, the following requirements are imposed: $E_{\mathrm{T}}^{\mathrm{miss}} > 100$ GeV, $E_{\mathrm{T}}^{\mathrm{miss}}/m_{\mathrm{eff}} > 0.2$, and $m_{\mathrm{eff}}^{\mathrm{inc}} > 650$ GeV.

In contrast to the previous analysis [16], no requirement on the azimuthal angle between the $E_{\mathrm{T}}^{\mathrm{miss}}$ vector and any of the jets is imposed as the background from multijet events is already low. This adds sensitivity to SUSY decay chains where the LSP is boosted along the jet direction.

VII. BACKGROUND ESTIMATION

The dominant sources of background in the single-lepton channels are the production of semileptonic and fully leptonic $t\bar{t}$ events, and W + jets where the W decays leptonically. For the multilepton channels, the main background sources are Z + jets and $t\bar{t}$. Other background processes which are considered are multijets, single-top, dibosons and $t\bar{t}$ plus vector bosons.

The major backgrounds are estimated by isolating each of them in a dedicated control region, normalizing the simulation to data in that control region, and then using the simulation to extrapolate the background expectations

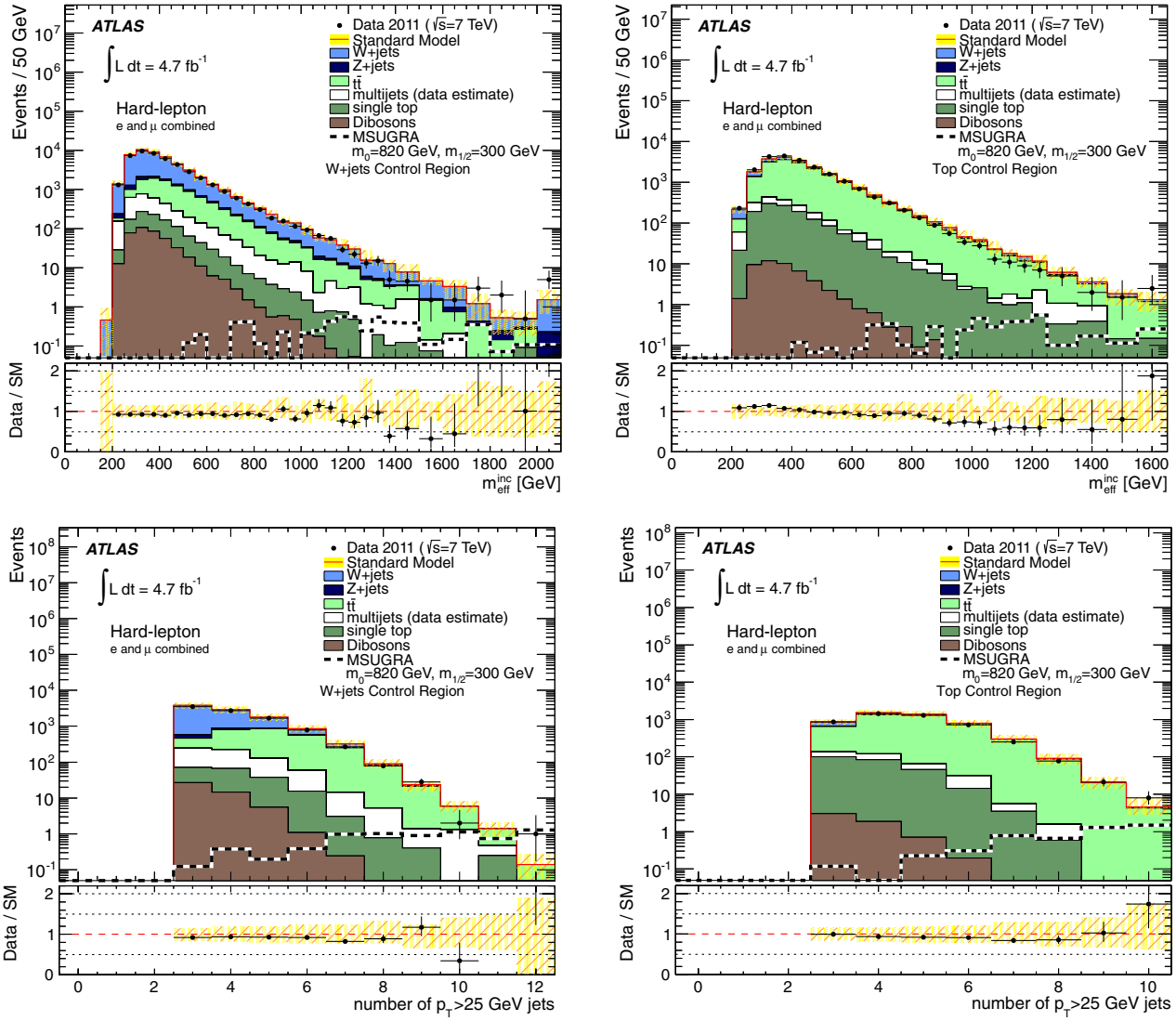

FIG. 2 (color online). Top panels: $m_{\mathrm{eff}}^{\mathrm{inc}}$ distribution in the W + jets (left) and $t\bar{t}$ (right) control regions for data and simulation for the single hard-lepton channels. Bottom panels: Distribution of the number of jets in the W + jets (left) and $t\bar{t}$ (right) control regions. In all plots, the last bin includes all overflows. The electron and muon channels are combined for ease of presentation. The "Data/SM" plots show the ratio between data and the total Standard Model expectation. The expectation for multijets is derived from the data. The remaining Standard Model expectation is entirely derived from simulation, normalized to the theoretical cross sections. The uncertainty band around the Standard Model expectation combines the statistical uncertainty on the simulated event samples with the systematic uncertainties on the jet energy scale, b tagging, data-driven multijet background, and luminosity. The systematic uncertainties are largely correlated from bin to bin. An example of the distribution for a simulated signal is also shown (not stacked); the signal point is chosen to be near the exclusion limit of the analysis in Ref. [16].

into the signal region. The multijet background is determined from the data by a matrix method described below. All other (smaller) backgrounds are estimated entirely from the simulation, using the most accurate theoretical cross sections available (Table I). To account for the cross contamination of physics processes across control regions, the final estimate of the background is obtained with a simultaneous, combined fit to all control regions, as described in Sec. IX.

Several correction factors are applied to the simulation. The p_T of the Z boson is reweighted based on a comparison of data with simulation in an event sample enriched in Z + jets events. The same correction factor is applied to W boson production and improves the agreement between data and simulation in the E_T^{miss} distribution. Other correction factors are derived during the combined fit. The relative normalization of the ALPGEN samples (W + jets, Z + jets and $t\bar{t}$) with different numbers of partons (N_{parton}) in the matrix element is adjusted by comparing the jet-multiplicity distributions in data and simulation in all control regions. A common set of corrections is obtained for the W + jets and Z + jets samples, and a separate set of

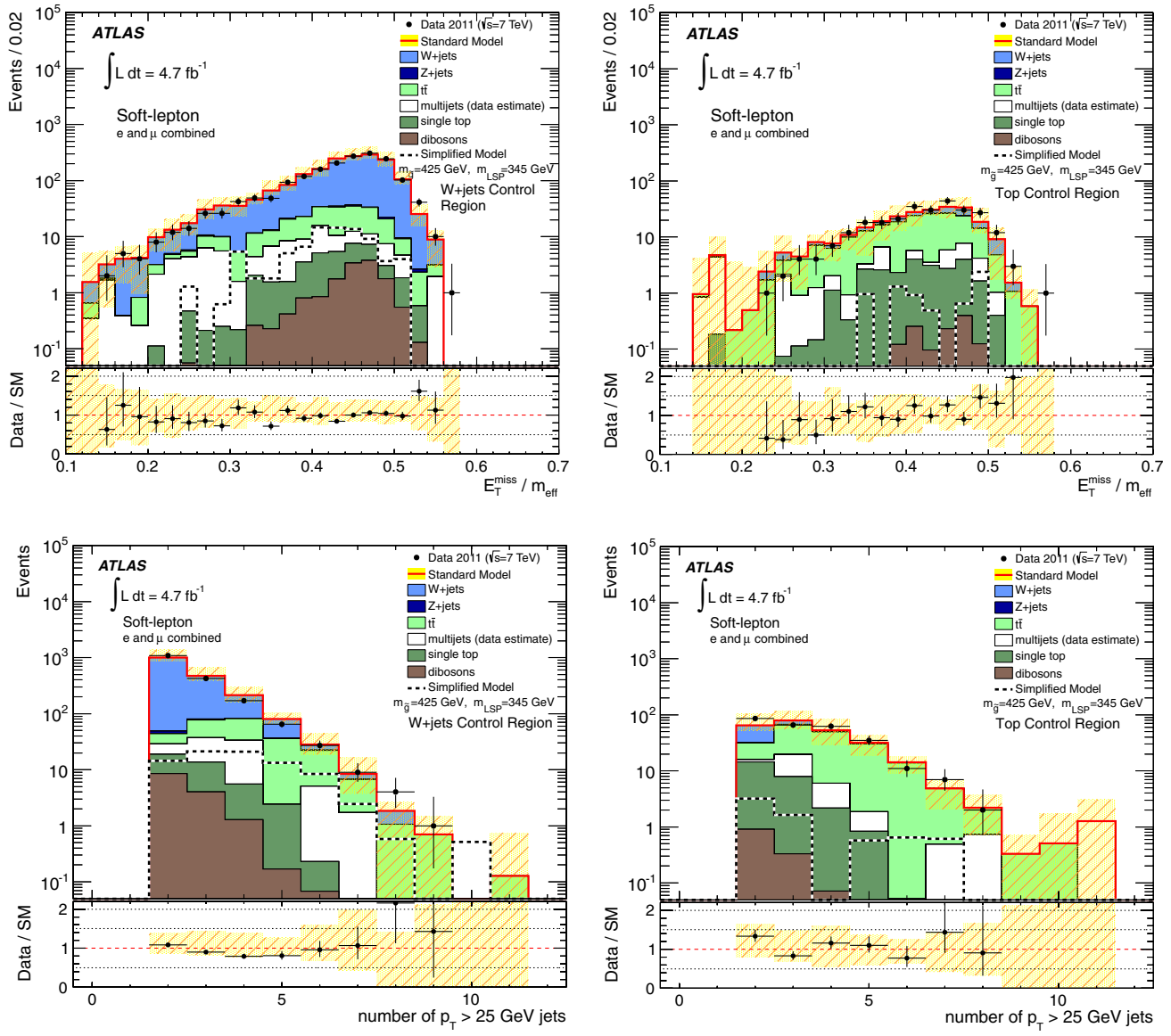

FIG. 3 (color online). Top panels: $E_{\mathrm{T}}^{\mathrm{miss}}/m_{\mathrm{eff}}$ distribution in the W + jets (left) and $t\bar{t}$ (right) control regions for data and simulation for the soft-lepton channel. Bottom panels: Jet-multiplicity distribution in the W + jets (left) and $t\bar{t}$ (right) control regions. In all distributions, electron and muon channels are combined. The "Data/SM" plots show the ratio between data and the total Standard Model expectation. The expectation for multijets is derived from the data. The remaining Standard Model expectation is entirely derived from simulation, normalized to the theoretical cross sections. The uncertainty band around the Standard Model expectation combines the statistical uncertainty on the simulated event samples with the systematic uncertainties on the jet energy scale, b tagging, data-driven multijet background, and luminosity. The systematic uncertainties are largely correlated from bin to bin. An example of the distribution for a simulated signal is also shown (not stacked); the signal point is near the exclusion limit of this analysis.

common corrections is obtained for semileptonic and fully leptonic $t\bar{t}$ decays. Neither the reweighting based on the p_T distribution of the Z boson nor the N_{parton} weights are applied in Figs. 2–4 below.

A. W/Z + jets and $t\bar{t}$ control regions

The W + jets and $t\bar{t}$ processes are isolated in control regions defined by the following requirements. For the hard single-lepton channel, ≥ 3 jets are required, with a leading jet $p_T > 80$ GeV and the other jets above 25 GeV. The lepton requirements are the same as in the signal region. The $E_{\mathrm{T}}^{\mathrm{miss}}$ is required to be between 40 and 150 GeV while the transverse mass is required to be between 40 and 80 GeV. Furthermore, the $m_{\mathrm{eff}}^{\mathrm{inc}}$ requirement is relaxed to be >500 GeV. The W + jets and $t\bar{t}$ control regions are distinguished by requirements on the number of b-tagged jets. For the W + jets control region, events are rejected if any of the three highest p_{T} jets is b tagged; the rejected events then define the $t\bar{t}$ control region. Table III summarizes

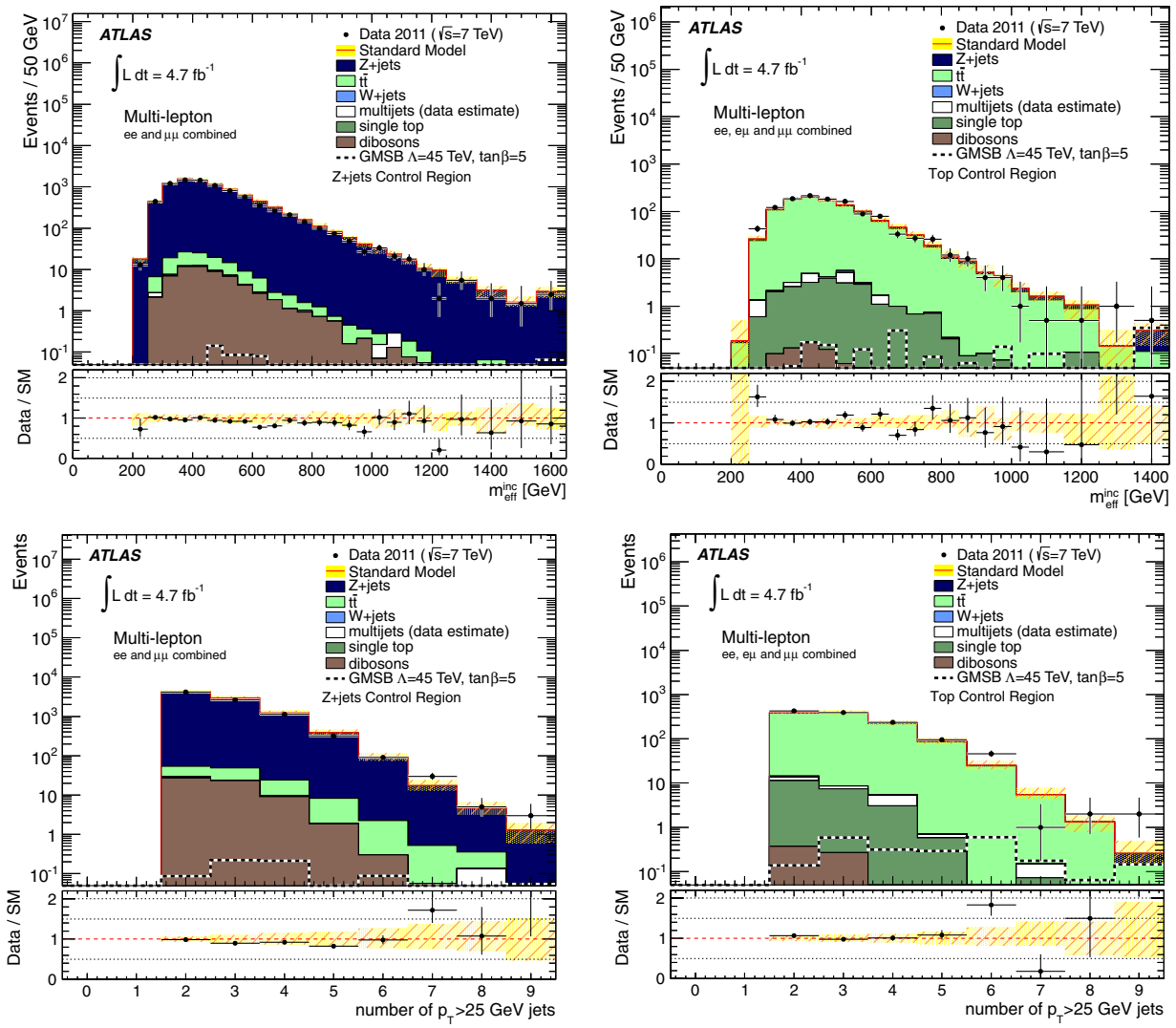

FIG. 4 (color online). Top panels: $m_{\rm eff}^{\rm inc}$ distribution in the Z + jets (left) and $t\bar{t}$ (right) control regions for data and simulation for the multilepton channels. Bottom panels: Distribution of the number of jets in the Z + jets (left) and $t\bar{t}$ (right) control regions; the last bin includes all overflows. The ee and $\mu\mu$ channels are combined for Z + jets and ee, $\mu\mu$ and $e\mu$ channels are combined for the $t\bar{t}$ distributions for ease of presentation. The "Data/SM" plots show the ratio between data and the total Standard Model expectation. The expectation for multijets is derived from the data. The remaining Standard Model expectation is entirely derived from simulation, normalized to the theoretical cross sections. The uncertainty band around the Standard Model expectation combines the statistical uncertainty on the simulated event samples with the systematic uncertainties on the jet energy scale, b tagging, data-driven multijet background, and luminosity. The systematic uncertainties are largely correlated from bin to bin. An example of the distribution for a simulated signal is also shown (not stacked); the signal point is chosen to be near the exclusion limit of the analysis in Refs. [82,83].

the control region definitions; Fig. 2 shows the composition of the W + jets and $t\bar{t}$ control regions as a function of $m_{\rm eff}^{\rm inc}$ and of the jet multiplicity. A discrepancy between simulation and data can be seen in the $m_{\rm eff}^{\rm inc}$ distribution. This effect is significantly reduced by the reweighting procedure discussed in Sec. VII B.

For the soft-lepton channel, the control region requirements on the leptons and jets are the same as in the signal region. However, the $E_{\rm T}^{\rm miss}$ is required to be between 180 GeV and 250 GeV and the transverse mass to be between 40 GeV and 80 GeV. The tighter $E_{\rm T}^{\rm miss}$ requirement, compared to the hard single-lepton control regions, is dictated by the trigger selection for this channel. Again, the W + jets and $t\bar{t}$ control regions are distinguished by the presence of b-tagged jets. For W + jets, events are rejected if any of the two highest $p_{\rm T}$ jets is b tagged; the rejected events form the $t\bar{t}$ control region. Figure 3 shows the composition of the W + jets and $t\bar{t}$ control regions for the soft-lepton channel as a function of $E_{\rm T}^{\rm miss}/m_{\rm eff}$ and the jet multiplicity. The significant contamination of $t\bar{t}$ background in the W + jets control sample at high jet multiplicity is taken into account in the combined fit to all backgrounds; uncertainties in the W + jets background at high jet multiplicity are suppressed

TABLE III. Overview of the selection criteria for the W + jets, Z + jets and $t\bar{t}$ control regions (CR). Only the criteria that are different from the signal selection criteria listed in Table II are shown.

	Hard lepton		Soft lepton		Multilepton	
	W CR	$t\bar{t}$ CR	W CR	$t\bar{t}$ CR	Z CR	$t\bar{t}$ CR
N_{jet}	≥ 3	≥ 3	≥ 2	≥ 2	≥ 2	≥ 2
$p_{\text{T}}^{\text{jet}}$ (GeV)	>80, 25, 25	>80, 25, 25	>130, 25	>130, 25	>80, 50 or >50, 50, 50, 50	>80, 50 or >50, 50, 50, 50
N_{jet} (b tagged)	0	≥ 1	0	≥ 1	···	≥ 1
$E_{\text{T}}^{\text{miss}}$ (GeV)	[40, 150]	[40, 150]	[180, 250]	[180, 250]	<50	[30, 80]
m_{T} (GeV)	[40, 80]	[40, 80]	[40, 80]	[40, 80]	···	···
$m_{\text{eff}}^{\text{inc}}$ (GeV)	>500	>500	···	···	···	···
$m_{\ell\ell}$ (GeV)	···	···	···	···	[81, 101]	<81 or >101

by the fact that $t\bar{t}$ becomes the dominant background in this region.

For the multilepton channels, the Z + jets control region is defined by requiring ≥ 2 jets with the two leading jets having $p_{\text{T}} > 80$ GeV and 50 GeV, respectively, or with four leading jets having $p_{\text{T}} > 50$ GeV. In addition, $E_{\text{T}}^{\text{miss}} < 50$ GeV and an opposite-sign, same-flavor dilepton pair with invariant mass between 81 GeV and 101 GeV are required. The lepton selection requirements are the same as in the signal region. The $t\bar{t}$ control region is defined with the same jet requirements as the Z + jets control region; at least one jet is required to be b tagged. In addition, $E_{\text{T}}^{\text{miss}}$ between 30 GeV and 80 GeV and a dilepton invariant mass outside the window [81,101] GeV are required. Figure 4 (top panels) shows the composition of the Z + jets and $t\bar{t}$ control regions for the multilepton channel as a function of $m_{\text{eff}}^{\text{inc}}$.

B. Reweighting of W + jets and Z + jets simulated samples

The samples of simulated W + jets and Z + jets events are reweighted as a function of the generated p_{T} of the vector boson. A common set of corrections to the p_{T} of the vector boson, applied to both W + jets and Z + jets samples, is found to improve the agreement between data and simulation for a number of variables ($E_{\text{T}}^{\text{miss}}$, $m_{\text{eff}}^{\text{inc}}$, and jet p_{T}).

The p_{T}^{Z} distribution is measured in data by selecting a sample with two oppositely charged, same-flavor leptons with an invariant mass between 80 GeV and 100 GeV, ≥ 3 signal jets with $p_{\text{T}} > 25$ GeV, and $m_{\text{eff}}^{\text{inc}} > 400$ GeV. The p_{T}^{Z} distribution in five bins of reconstructed p_{T} is compared to the ALPGEN simulation in five bins of generated p_{T}, with the first four bins ranging from 0 to 200 GeV and the last bin integrated above 200 GeV; the ratio of the two distributions is taken as the $p_{\text{T}}^{Z,\text{gen}}$-dependent weighting factor. The simulation employed here uses the cross sections listed in Table I. Only the systematic uncertainty from the jet energy scale is considered (in addition to statistical uncertainties) when computing the uncertainty on the weighting factors.

Figure 5 (top panels) shows the p_{T}^{Z} distribution before the application of the reweighting factors and after the final fit to all background control regions (described in Sec. IX), which includes the reweighting. The bottom half of the figure shows the $E_{\text{T}}^{\text{miss}}$ distribution in the hard-lepton W + jets control region (with the lower requirement on $E_{\text{T}}^{\text{miss}}$ set to 50 GeV and the upper requirement removed). Similar to p_{T}^{Z} and $E_{\text{T}}^{\text{miss}}$, the $m_{\text{eff}}^{\text{inc}}$ and jet p_{T} distributions are in good agreement with expectations after the reweighting.

C. Multijet background

Multijet events become a background when a jet is misidentified as an isolated lepton or when a real lepton appears as a decay product of hadrons in jets, for example, from b or c jets, and is sufficiently isolated. In the following, such leptonlike objects are collectively referred to as misidentified leptons. The multijet background in each signal region, and in the W + jets and $t\bar{t}$ control regions, where it is more significant, is estimated from the data following a matrix method similar to that employed in Ref. [16].

The multijet background from all sources (but separated by lepton flavor) is determined collectively. In the single-lepton channels, the multijet process is enhanced in control samples with all the signal region criteria applied but where the lepton isolation criteria are not imposed and the shower-shape requirements on electrons are relaxed. Defining N_{pass} and N_{fail} as the number of events in such a loose sample passing or failing the final lepton selection criteria, and defining N_{real} and N_{misid} as the number of real and the number of misidentified leptons, the following equations hold:

$$N_{\text{pass}} = \epsilon_{\text{real}} N_{\text{real}} + \epsilon_{\text{misid}} N_{\text{misid}},$$
$$N_{\text{fail}} = (1 - \epsilon_{\text{real}}) N_{\text{real}} + (1 - \epsilon_{\text{misid}}) N_{\text{misid}},$$

where ϵ_{real} is the relative identification efficiency for real leptons, and ϵ_{misid} is the misidentification efficiency for misidentified leptons. Solving the equations leads to

$$N_{\text{misid}}^{\text{pass}} = \epsilon_{\text{misid}} N_{\text{misid}} = \frac{N_{\text{fail}} - (1/\epsilon_{\text{real}} - 1) N_{\text{pass}}}{1/\epsilon_{\text{misid}} - 1/\epsilon_{\text{real}}}.$$

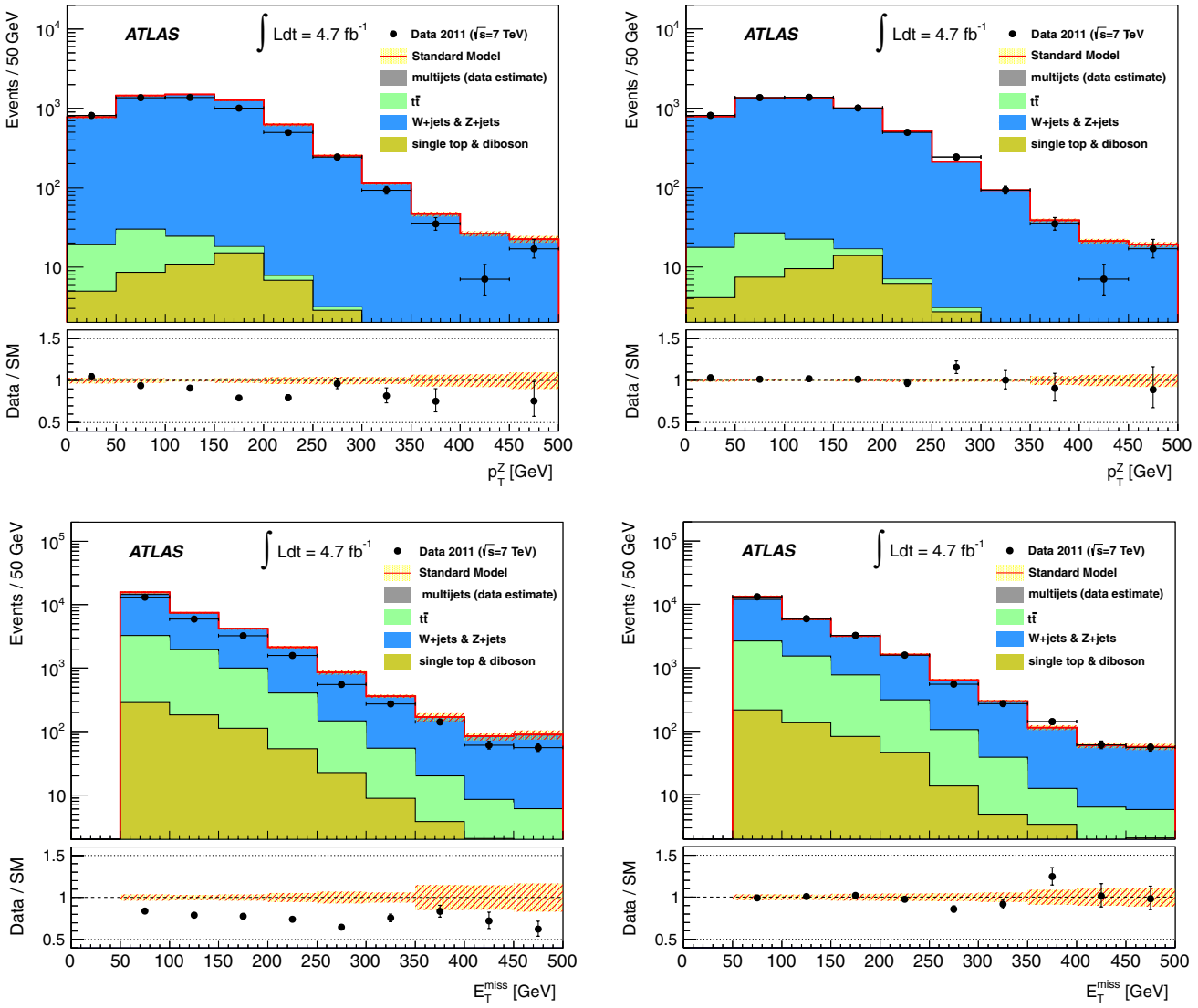

FIG. 5 (color online). Top panels: Distribution of the p_{T} of the Z boson in a region enhanced in Z + jets events (ee and $\mu\mu$ final states combined) before (left) the application of any reweighting factors, and after (right) the final fit to all background control regions (described in Sec. IX). Bottom panels: Distribution of $E_{\mathrm{T}}^{\mathrm{miss}}$ in the hard-lepton W + jets control region (electron and muon channels combined, lower requirement on $E_{\mathrm{T}}^{\mathrm{miss}}$ set to 50 GeV and upper requirement removed) before (left) application of reweighting factors and after (right) the final fit to all background control regions. Events in the overflow bin have not been plotted.

The efficiency ϵ_{real} is measured from data samples of $Z \to \ell\ell$ decays.

The lepton misidentification efficiency is obtained as follows. For electrons (muons) with $p_{\mathrm{T}} > 25(20)$ GeV $\epsilon_{\mathrm{misid}}$ is estimated with events containing at least one electron (muon) satisfying the relaxed criteria, and at least one signal jet with $p_{\mathrm{T}} > 30(60)$ GeV. In addition, for the electron case, $E_{\mathrm{T}}^{\mathrm{miss}} < 30$ GeV is required. For the muon case, the event is required to contain exactly one muon with $|d_0|/\sigma_{d_0} > 5$, where d_0 and σ_{d_0} are the transverse impact parameter and its uncertainty, respectively, measured with respect to the primary vertex. For the soft-lepton channel, the sample for deriving $\epsilon_{\mathrm{misid}}$ consists of events containing a same-sign and same-flavor lepton pair where the leptons satisfy the relaxed isolation criteria. The selection of a lepton pair allows the low-p_{T} region to be studied with a large data sample. The same-sign requirement reduces the dominance of b hadrons in the sample, providing a better mix of the different mechanisms by which leptons can be misidentified. One of the leptons is required to fail the signal lepton criteria to further enhance the background; the misidentification efficiency is measured with the other lepton. An additional veto around the Z boson mass is applied. In all channels, the electron misidentification efficiency is evaluated separately for samples enhanced (depleted) in heavy-flavor contributions by requiring (vetoing) a b-tagged jet in the event.

For the multilepton channels, the misidentification probabilities as determined above are applied to the number of events where two leptons pass the loose selection criteria. The contribution from processes where one lepton is real and the other misidentified has been studied in both simulation and data, using a generalization of the above matrix method to two leptons. Both methods give similar results; the final estimate is taken from the simulation.

D. Other backgrounds

The backgrounds from single-top, diboson and $t\bar{t}$ + vector boson production are estimated almost purely from simulation, as is the Z + jets background for the single-lepton channels. The background from cosmic-ray muons overlapping a hard-scattering event is estimated from a control sample with large z_0, defined as the distance in the z direction with respect to the primary vertex, evaluated at the point of closest approach of the muon to the primary vertex in the transverse plane. The extrapolated contribution to the signal region, $|z_0| < 5$ mm, is found to be negligible.

VIII. SYSTEMATIC UNCERTAINTIES

Systematic uncertainties have an impact on the expected background and signal event yields in the control and signal regions. These uncertainties are treated as nuisance parameters in a profile likelihood fit described in Sec. IX. The following systematic uncertainties on the reconstructed objects are taken into account. The jet energy scale (JES) uncertainty has been determined from a combination of test beam, simulation and *in situ* measurements from 2010 pp collision data [69]. Additional contributions from the higher luminosity and pileup in 2011 are taken into account. Uncertainties on the lepton identification, momentum/energy scale and resolution are estimated from samples of $Z \to \ell^+\ell^-$, $J/\psi \to \ell^+\ell^-$ and $W^\pm \to \ell^\pm\nu$ decays in data [64–66]. The uncertainties on the jet and lepton energies are propagated to the $E_{\mathrm{T}}^{\mathrm{miss}}$; an additional $E_{\mathrm{T}}^{\mathrm{miss}}$ uncertainty arising from energy deposits not associated with reconstructed objects is also included [73]. Uncertainties on the b-tagging efficiency are derived from dedicated data samples [74,75], e.g. containing muons associated with jets. Uncertainties on the light-flavor mistag rate are derived by examining tracks with negative impact parameter [76] while charm mistag uncertainties are obtained from data samples tagged by reconstructing D^* mesons [77].

Uncertainties in the matrix method for the determination of the multijet background include the statistical uncertainty in the number of events available in the various control samples, the difference in misidentification efficiency for electrons from heavy- versus light-flavored jets, the dependence of the misidentification efficiency on the jet multiplicity, and the uncertainty in the subtraction of other backgrounds from the samples used to estimate the misidentification efficiency.

Uncertainties from the identification efficiency for jets associated with the primary vertex and from the overlay of pileup in simulated events are both found to be negligible.

Theoretical modeling uncertainties in the simulation include the following contributions. In previous versions of the analysis, renormalization and factorization scale uncertainties were estimated by varying the corresponding parameters in the ALPGEN generator by a factor of 2, up and down from their nominal settings. Since these variations affect mostly the overall normalization of the cross sections for the samples with different values of N_{parton}, they are replaced here by a normalization of the individual light-parton bins to the data (see Sec. IX). Additional generator uncertainties arise from the parameter that describes the jet p_{T} threshold used in the matching ($p_{\mathrm{T,min}}$). This uncertainty is assessed by changing its default value from 15 GeV to 30 GeV; the difference is assigned as both a positive and negative uncertainty. Uncertainties arising from initial- and final-state radiation are taken into account by the variation of the MLM-matching parameter in multileg generators as well as by studying dedicated PYTHIA tunes with increased or decreased radiation [78]. Fragmentation/hadronization uncertainties are estimated by comparing HERWIG with PYTHIA. In order to vary the heavy-flavor fraction, the cross sections for $Wb\bar{b}$ + jets and $Wc\bar{c}$ + jets in Table I are scaled by 1.63 ± 0.76, while Wc + jets is scaled by 1.11 ± 0.35, based on correction factors derived from data [55]. The uncertainty on $Zb\bar{b}$ + jets is taken to be $\pm 100\%$. The uncertainties on the cross sections for $t\bar{t} + W$ and $t\bar{t} + Z$ are taken from the NLO calculations in Refs. [53,54].

The uncertainty in the signal cross section is taken from an envelope of cross section predictions using different PDF sets (including the α_{S} uncertainty) and factorization and renormalization scales, as described in Ref. [79]. For the simplified models, uncertainties in the modeling of initial-state radiation play a significant role for low gluino masses and for small mass differences in the decay cascade. These uncertainties are estimated by varying generator tunes in the simulation as well as by generator-level studies of $\tilde{g}\,\tilde{g}$ and $\tilde{q}\,\tilde{q}$ production with an additional ISR jet generated in the matrix element with MADGRAPH5.

The impact of these systematic uncertainties on the background yields and signal estimates is evaluated via an overall fit, described in Secs. IX and X.

IX. BACKGROUND FIT

The background in the signal region is estimated with a fit based on the profile likelihood method [80]. The inputs to the fit are as follows:

(1) The observed numbers of events in the W + jets (or Z + jets in the multilepton channels) and $t\bar{t}$ control regions, and the numbers expected from simulation. These are separated into seven jet-multiplicity bins,

TABLE IV. Overview of the selection criteria for the background validation regions (VR) for the single-lepton channels. Only the criteria that are different from the signal selection criteria listed in Table II are shown.

	Hard lepton			Soft lepton
	W VR	$t\bar{t}$ VR	High-m_{T} VR	
N_{jet}	≥ 3	≥ 3	≥ 3	≥ 2
$p_{\mathrm{T}}^{\mathrm{jet}}$ (GeV)	>80, 25, 25	>80, 25, 25	>80, 25, 25	>130, 25
N_{jet} (b tagged)	0	≥ 1	...	...
$E_{\mathrm{T}}^{\mathrm{miss}}$ (GeV)	[150, 250]	[150, 250]	[40, 250]	[180, 250]
m_{T} (GeV)	[40, 80]	[40, 80]	>100	[80, 100]
$m_{\mathrm{eff}}^{\mathrm{inc}}$ (GeV)	>500	>500	>500	...

ranging from three to nine jets for the hard-lepton channel, eight jet-multiplicity bins ranging from two to nine jets for the multilepton channels, and six bins ranging from two to seven jets for the soft-lepton channel. This information is shown in the bottom half of Figs. 2–4.

(2) Transfer factors (TF), derived from simulation, which are multiplicative factors that propagate the event counts for W + jets, Z + jets and $t\bar{t}$ backgrounds from one control region to another, or from one control region to the signal region. Typical values of the TFs from the control to the signal region are 10^{-2} and 10^{-4} for the soft- and hard-lepton channels, respectively.

(3) The number of multijet background events in all control and signal regions, as derived from the data.

(4) Expectations from simulation for the number of events from the minor backgrounds (single-top, diboson) in all control and signal regions.

For each analysis channel (hard-lepton, soft-lepton, multilepton) the event count in each bin of the control region is treated with a Poisson probability density function. The statistical and systematic uncertainties on the expected yields are included in the probability density function as nuisance parameters, constrained to be Gaussian with a width given by the size of the uncertainty. Approximately 150 nuisance parameters are included in the fit. Correlations in the nuisance parameters from bin to bin are taken into account where necessary. The Poisson probability density functions also include free parameters, for example to scale the expected contributions from the major backgrounds; these are described in more detail below. A likelihood is formed as the product of these probability density functions and the constraints on the nuisance parameters. Each lepton flavor (in the multilepton channel, each combination of flavors of the two leading leptons) is treated separately in the likelihood function. The free parameters and nuisance parameters are adjusted to maximize the likelihood. An important difference with respect to the analysis in Ref. [16] is the increase in the number of measurements, allowing the fit to be constrained. This has been used in this analysis to constrain the nuisance parameters for the jet energy scale and the uncertainty in the ALPGEN scale parameters from the shape information provided in the control regions.

The free parameters considered in the fit are as follows:

(1) $t\bar{t}$ background: Each $t\bar{t}$ sample, divided into N_{parton} bins (from 0 to 3, with the last being inclusive), is scaled by a free parameter. For each N_{parton} bin, a common parameter is used for semileptonic and dileptonic $t\bar{t}$ samples.

(2) W/Z background: Each W + jets and Z + jets sample, again divided into N_{parton} bins from 2 to 5, is scaled by a free parameter. The $N_{\mathrm{parton}} = 6$ bin for W + light-flavored jets shares its fit parameter with

TABLE V. Overview of the selection criteria for the background VR for the multilepton channels. Only the criteria that are different from the signal selection criteria listed in Table II are shown. For the two-jet validation regions, the fourth leading jet (if present) is required to have $p_T < 50$ GeV.

	Multilepton 2-jet		Multilepton 4-jet	
	Z VR	$t\bar{t}$ VR	Z VR	$t\bar{t}$ VR
N_{jet}	≥ 2	≥ 2	≥ 4	≥ 4
$p_{\mathrm{T}}^{\mathrm{jet}}$ (GeV)	>120, 120	>120, 120	>80, 50, 50, 50	>80, 50, 50, 50
N_{jet} (b tagged)	...	≥ 1	...	≥ 1
$E_{\mathrm{T}}^{\mathrm{miss}}$ (GeV)	[50, 100]	[100, 300]	[50, 100]	[80, 100]
$m_{\ell\ell}$ (GeV)	[81, 101]	<81 or >101	[81, 101]	<81 or >101

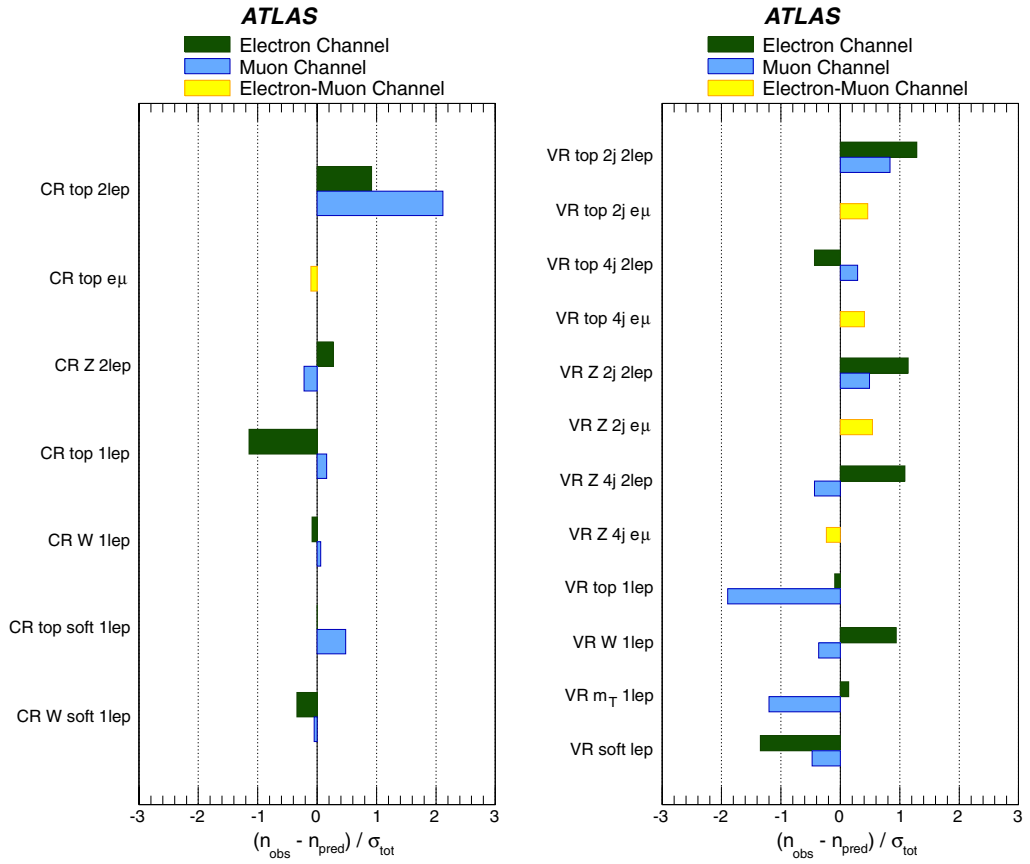

FIG. 6 (color online). Summary of the fit results in the control regions (left panel) and validation regions (right panel). The difference between the observed and predicted number of events, divided by the total (statistical and systematic) uncertainty on the prediction, is shown for each control and validation region.

$N_{\text{parton}} = 5$. The vector boson plus heavy-flavor samples share the same relative normalization parameters as the light-flavor samples. Only N_{parton} bins between 2 and 5 are allowed to float, as the lower multiplicity bins suffer from small numbers of events due to the jet and effective mass requirements.

The backgrounds from multijets and the subdominant backgrounds from single-top and diboson production are

TABLE VI. The observed numbers of events in the single-lepton signal regions, and the background expectations from the fit. The inputs to the fit are also shown; these consist of the data-driven multijet background estimate and the nominal expectations from simulation (MC), normalized to theoretical cross sections. The errors shown are the statistical plus systematic uncertainties.

Single lepton		Electron			Muon	
Number of events	3-jet	4-jet	Soft lepton	3-jet	4-jet	Soft lepton
Observed	2	4	11	1	2	14
Fitted bkg	2.3 ± 0.9	3.5 ± 0.9	14.0 ± 3.3	2.6 ± 0.8	1.5 ± 0.3	19 ± 5
Fitted top	0.4 ± 0.2	2.3 ± 0.6	3.8 ± 0.6	0.5 ± 0.2	1.3 ± 0.3	3.8 ± 0.8
Fitted W/Z + jets	1.5 ± 0.6	0.9 ± 0.2	5.8 ± 1.0	2.0 ± 0.6	0.2 ± 0.1	11.4 ± 2.3
Fitted other bkg	0.0 ± 0.0	$0.0^{+0.3}_{-0.0}$	0.6 ± 0.1	0.1 ± 0.1	0.0 ± 0.0	0.2 ± 0.1
Fitted multijet	0.3 ± 0.4	0.3 ± 0.4	3.8 ± 2.5	0.0 ± 0.0	0.0 ± 0.0	3.6 ± 2.5
MC exp. SM	2.7	5.3	14.2	2.8	2.4	18.0
MC exp. top	0.9	3.1	4.3	0.6	2.0	3.8
MC exp. W/Z + jets	1.5	1.3	5.5	2.0	0.3	10.5
MC exp. other bkg	0.0	0.5	0.5	0.2	0.1	0.1
Data-driven multijet	0.3	0.3	3.8	0.0	0.0	3.6

TABLE VII. The observed numbers of events in the multilepton signal regions, and the background expectations from the fit. The inputs to the fit are also shown; these consist of the data-driven multijet background estimate and the nominal expectations from simulation (MC), normalized to theoretical cross sections. The errors shown are the statistical plus systematic uncertainties.

Multilepton		2-jets			4-jets	
Number of events	ee	$\mu\mu$	$e\mu$	ee	$\mu\mu$	$e\mu$
Observed	0	0	1	8	12	18
Fitted bkg	0.3 ± 0.2	0.4 ± 0.2	0.7 ± 0.2	9.1 ± 1.5	11.7 ± 1.7	21 ± 3
Fitted top	0.1 ± 0.1	0.2 ± 0.1	0.6 ± 0.2	9.1 ± 1.4	11.1 ± 1.7	20 ± 3
Fitted W/Z + jets	0.1 ± 0.1	0.1 ± 0.0	0.0 ± 0.0	0.0 ± 0.0	0.2 ± 0.1	0.4 ± 0.1
Fitted other bkg	0.1 ± 0.1	0.1 ± 0.0	0.1 ± 0.0	0.0 ± 0.0	0.4 ± 0.1	0.6 ± 0.1
Fitted multijet	0.0 ± 0.0	0.0 ± 0.0	0.0 ± 0.0	0.0 ± 0.2	0.0 ± 0.0	0.0 ± 0.0
MC exp. SM	0.3	0.5	0.9	11.4	14.7	27.1
MC exp. top	0.2	0.3	0.7	11.1	13.9	26.0
MC exp. W/Z + jets	0.1	0.1	0.1	0.1	0.3	0.4
MC exp. other bkg	0.1	0.1	0.1	0.2	0.5	0.7
Data-driven multijet	0.0	0.0	0.0	0.0	0.0	0.0

allowed to float in the fit within their respective uncertainties.

Notable nuisance parameters in the fit are as follows:

(1) The uncertainty in the ALPGEN MLM-matching parameter $p_{\mathrm{T,min}}$ manifests itself in the relative normalization of the ALPGEN N_{parton} samples and in the jet p_{T} spectra within each sample. The change in the event counts in the array of all control regions, resulting from this shift in the relative normalization, is mapped to one parameter for both W + jets and Z + jets and a separate parameter for $t\bar{t}$.

(2) The uncertainty in the normalization of the $N_{\mathrm{parton}} = 0, 1$ bins for W + jets and Z + jets, due to uncertainties in renormalization and factorization scales, is treated by one nuisance parameter.

(3) The overall normalization of the vector boson plus heavy-flavor samples is assigned a nuisance parameter reflecting the uncertainty in the cross section.

(4) The uncertainty from the fit of the p_{T}^{Z} distribution is treated by assigning one nuisance parameter for each bin in true p_{T}. Four equal-width bins are used from 0 to 200 GeV, and one bin for $p_{\mathrm{T}} > 200$ GeV.

(5) The uncertainty due to the jet energy scale is considered in three jet p_{T} bins (25–40 GeV, 40–100 GeV and >100 GeV). The resulting uncertainty in the event counts in the array of all control regions is mapped to one nuisance parameter for each of the three jet p_{T} bins. The usage of three jet p_{T} bins prevents the fit from artificially overconstraining the jet energy scale.

A. Background fit validation

The background fit is cross-checked in a number of validation regions, situated between the control and signal regions, where the results of the background fit can be compared to observation. These validation regions are not used to constrain the fit. For the single hard-lepton channels, one common set of validation regions, which receives contributions from both three- and four-jet channels, is defined as follows:

(1) The W + jets validation region is identical to the W + jets control region for the three-jet channel except that the $E_{\mathrm{T}}^{\mathrm{miss}}$ requirement is changed to $150\,\mathrm{GeV} < E_{\mathrm{T}}^{\mathrm{miss}} < 250\,\mathrm{GeV}$ (from [40, 150] GeV).

(2) Similarly, the $t\bar{t}$ validation region is identical to the $t\bar{t}$ control region for the three-jet channel except for the change in the $E_{\mathrm{T}}^{\mathrm{miss}}$ requirement to 150 GeV $< E_{\mathrm{T}}^{\mathrm{miss}} <$ 250 GeV (from [40, 150] GeV).

TABLE VIII. Left to right: 95% CL upper limits on the visible cross section ($\langle\epsilon\sigma\rangle_{\mathrm{obs}}^{95}$) in the various signal regions, and on the number of signal events (S_{obs}^{95}). The third column (S_{exp}^{95}) shows the 95% CL upper limit on the number of signal events, given the expected number (and $\pm 1\sigma$ uncertainty on the expectation) of background events. The last column indicates the CL_B value, i.e. the observed confidence level for the background-only hypothesis.

Signal channel	$\langle\epsilon\sigma\rangle_{\mathrm{obs}}^{95}$ [fb]	S_{obs}^{95}	S_{exp}^{95}	CL_B
Hard electron, 3-jet	0.94	4.4	$4.3^{+2.0}_{-0.8}$	0.54
Hard muon, 3-jet	0.75	3.6	$4.2^{+2.0}_{-0.7}$	0.27
Hard electron, 4-jet	1.22	5.8	$5.3^{+2.6}_{-1.3}$	0.63
Hard muon, 4-jet	0.95	4.5	$3.8^{+1.3}_{-0.7}$	0.75
Soft electron	1.82	8.6	$10.4^{+4.2}_{-3.1}$	0.28
Soft muon	1.92	9.0	$12.5^{+5.4}_{-3.8}$	0.21
Multilepton, ee, 2-jet	0.71	3.3	3.5 ± 0.1	0.48
Multilepton, $\mu\mu$, 2-jet	0.76	3.6	3.5 ± 0.1	0.46
Multilepton, $e\mu$, 2-jet	0.83	3.9	$3.6^{+0.6}_{-0.2}$	0.85
Multilepton, ee, 4-jet	1.53	7.2	$7.7^{+3.2}_{-2.1}$	0.39
Multilepton, $\mu\mu$, 4-jet	1.93	9.1	$8.8^{+3.3}_{-3.0}$	0.55
Multilepton, $e\mu$, 4-jet	2.14	10.1	$11.5^{+4.8}_{-3.5}$	0.28

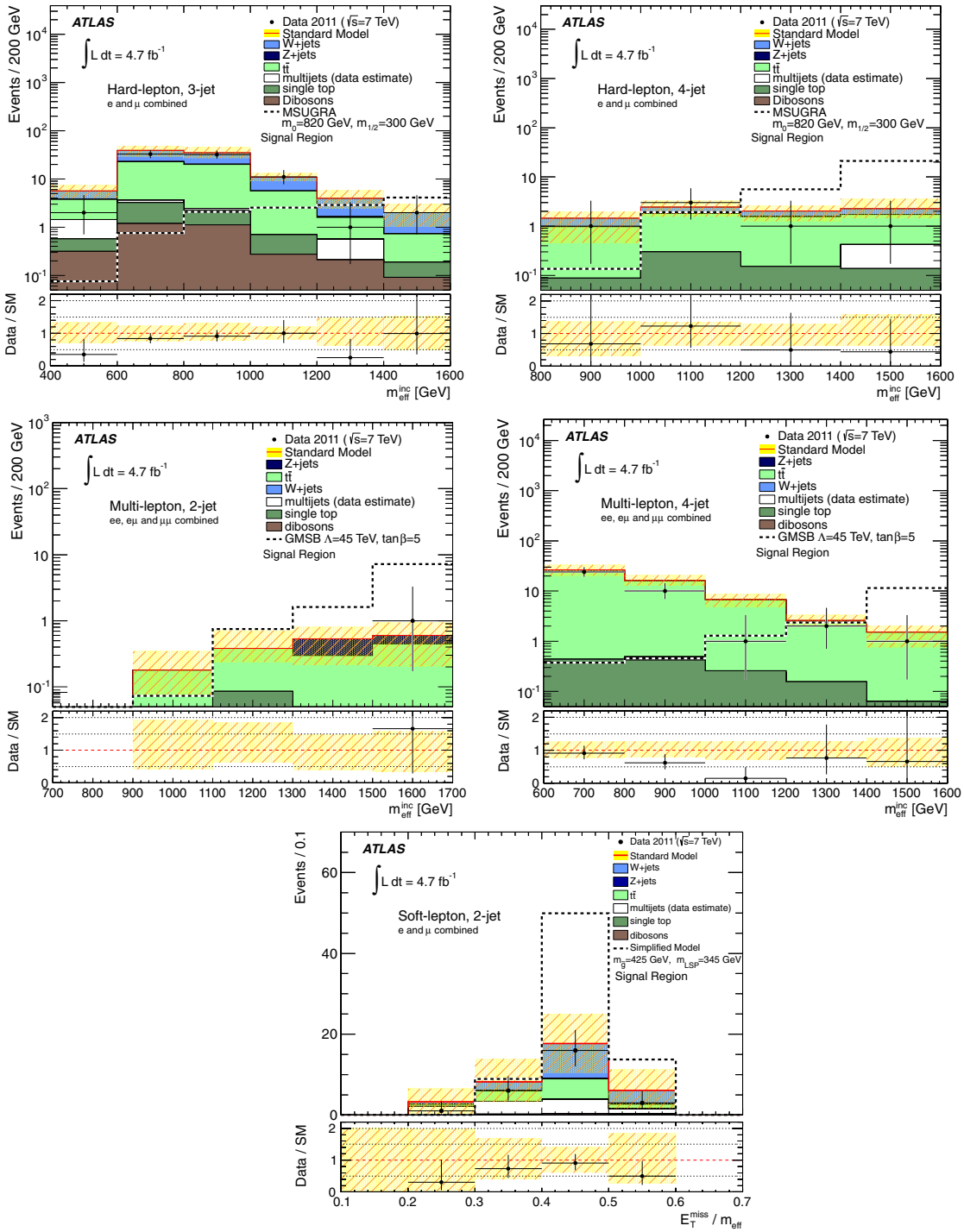

FIG. 7 (color online). Top and middle panels: Distribution of $m_{\mathrm{eff}}^{\mathrm{inc}}$ in the signal regions after all selection requirements except for that on the inclusive effective mass. Top left panel: hard-lepton, three-jet selection. Top right panel: hard-lepton, four-jet selection. Middle left panel: multilepton, two-jet selection. Middle right panel: multilepton, four-jet selection. The last $m_{\mathrm{eff}}^{\mathrm{inc}}$ bin includes all overflows. The lowest $m_{\mathrm{eff}}^{\mathrm{inc}}$ bins are affected by the minimum p_{T} requirements on jets and $E_{\mathrm{T}}^{\mathrm{miss}}$. Bottom panel: The $E_{\mathrm{T}}^{\mathrm{miss}}/m_{\mathrm{eff}}$ distribution in the soft-lepton signal region after all selection requirements except for that on $E_{\mathrm{T}}^{\mathrm{miss}}/m_{\mathrm{eff}}$. In all plots the different lepton flavors have been combined for ease of presentation. The ''Data/SM'' plots show the ratio between data and the total Standard Model expectation. The Standard Model expectation shown here is the input to the final fit, and is derived from simulation only, normalized to the theoretical cross sections. The uncertainty band around the Standard Model expectation combines the statistical uncertainty on the simulated event samples with the systematic uncertainties on the jet energy scale, b tagging, data-driven multijet background, and luminosity. The systematic uncertainties are largely correlated from bin to bin. An example of the distribution for a simulated signal is also shown (not stacked); the signal point is chosen to be near the exclusion limit of the analysis in Ref. [16].

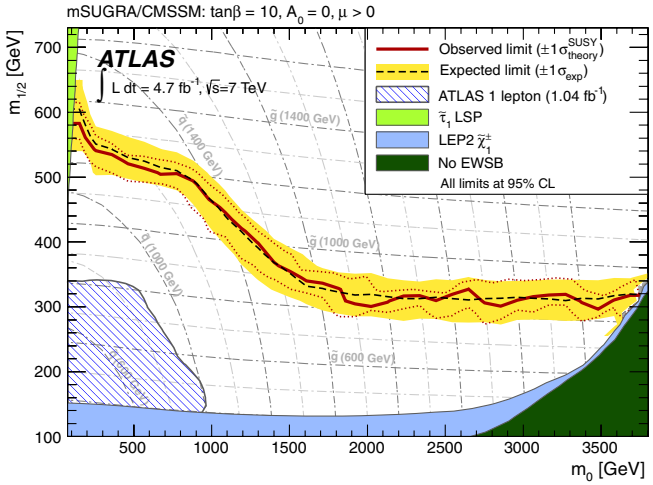

FIG. 8 (color online). Expected and observed 95% CL exclusion limits in the MSUGRA/CMSSM model with $\tan\beta = 10$, $A_0 = 0$ and the sign of μ taken to be positive. The results are obtained by combining ten signal regions from the hard single-lepton and multilepton channels. The band around the median expected limit shows the $\pm 1\sigma$ variations, including all uncertainties except theoretical uncertainties on the signal. The dotted lines around the observed limit indicate the sensitivity to $\pm 1\sigma$ variations on these theoretical uncertainties. The dashed grid shows contours of constant squark (curved lines) and gluino (nearly horizontal lines) masses. The previous limit from ATLAS [16] and the results from the LEP experiments [84] are also shown.

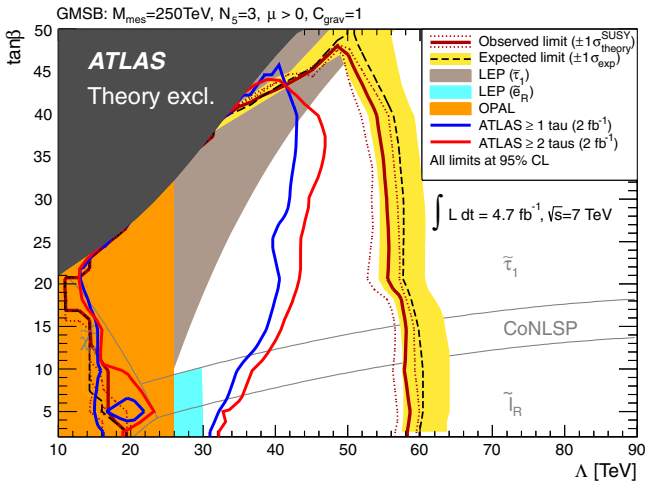

FIG. 9 (color online). Expected and observed 95% CL exclusion limits in the minimal GMSB model, combining six signal regions from the multilepton channels. The band around the median expected limit shows the $\pm 1\sigma$ variations, including all uncertainties except theoretical uncertainties on the signal. The dotted lines around the observed limit indicate the sensitivity to $\pm 1\sigma$ variations on these theoretical uncertainties. The different NLSP regions are indicated. The coNLSP region denotes the region where $\tilde{\tau}_1$ and $\tilde{\ell}_R$ are nearly mass degenerate. Previous OPAL and ATLAS limits in this model can be found in Refs. [85] and [82,83], respectively. Limits derived from the LEP slepton mass limits [86] are also shown.

(3) The high transverse mass validation region is defined by $m_T > 100$ GeV and $40\ \text{GeV} < E_{\text{T}}^{\text{miss}} < 250$ GeV. This region tests the validity of the background yields from dileptonic $t\bar{t}$ events.

For the soft-lepton channel, the validation region is based on the sum of the W + jets and $t\bar{t}$ control regions but with the transverse mass selection changed to $80\ \text{GeV} < m_{\text{T}} < 100$ GeV (from [40, 80] GeV).

For the multilepton channels, two Z + jets validation regions and two $t\bar{t}$ validation regions are defined:

(1) The two-jet Z + jets validation region is similar to the Z + jets control region with ≥ 2 jets, but the leading two jets are required to have $p_{\text{T}} > 120$ GeV (instead of 80 GeV and 50 GeV); the fourth leading jet (if present) is required to have $p_{\text{T}} < 50$ GeV.

(2) The four-jet Z + jets validation region is similar to the control region with ≥ 4 jets but the leading jet p_{T} requirement is tightened to $p_{\text{T}} > 80$ GeV (instead of 50 GeV).

(3) The two-jet $t\bar{t}$ validation region is similar to the $t\bar{t}$ control region with ≥ 2 jets but the leading two jets are required to have $p_{\text{T}} > 120$ GeV (instead of 80 GeV and 50 GeV); the fourth leading jet (if present) is required to have $p_{\text{T}} < 50$ GeV. The $E_{\text{T}}^{\text{miss}}$ requirement is changed to $100\ \text{GeV} < E_{\text{T}}^{\text{miss}} < 300$ GeV.

(4) The four-jet $t\bar{t}$ validation region is similar to the $t\bar{t}$ control region with ≥ 4 jets but the leading jet p_{T} requirement is tightened to $p_{\text{T}} > 80$ GeV (instead of 50 GeV). The $E_{\text{T}}^{\text{miss}}$ requirement is tightened to $80\ \text{GeV} < E_{\text{T}}^{\text{miss}} < 100$ GeV.

In both Z + jets validation regions the $E_{\text{T}}^{\text{miss}}$ requirement is tightened to $50\ \text{GeV} < E_{\text{T}}^{\text{miss}} < 100$ GeV, and the number of b-tagged jets is required to be zero in order to suppress the $t\bar{t}$ contamination. The selection requirements for the validation regions are summarized in Tables IV and V for the single-lepton and multilepton channels, respectively.

The results of the fit to the control regions, as well as the comparison of observed versus predicted event counts in the validation regions, are summarized in Fig. 6. The difference between the observed and predicted event counts is normalized by the total (statistical and systematic) uncertainty on the prediction. The agreement between predicted and observed yields is good.

X. RESULTS AND INTERPRETATION

The predicted background in the signal regions and the observed numbers of events are shown in Tables VI and VII. The data are consistent with SM expectations in all signal regions.

The dominant background uncertainty comes from the limited number of events in the background

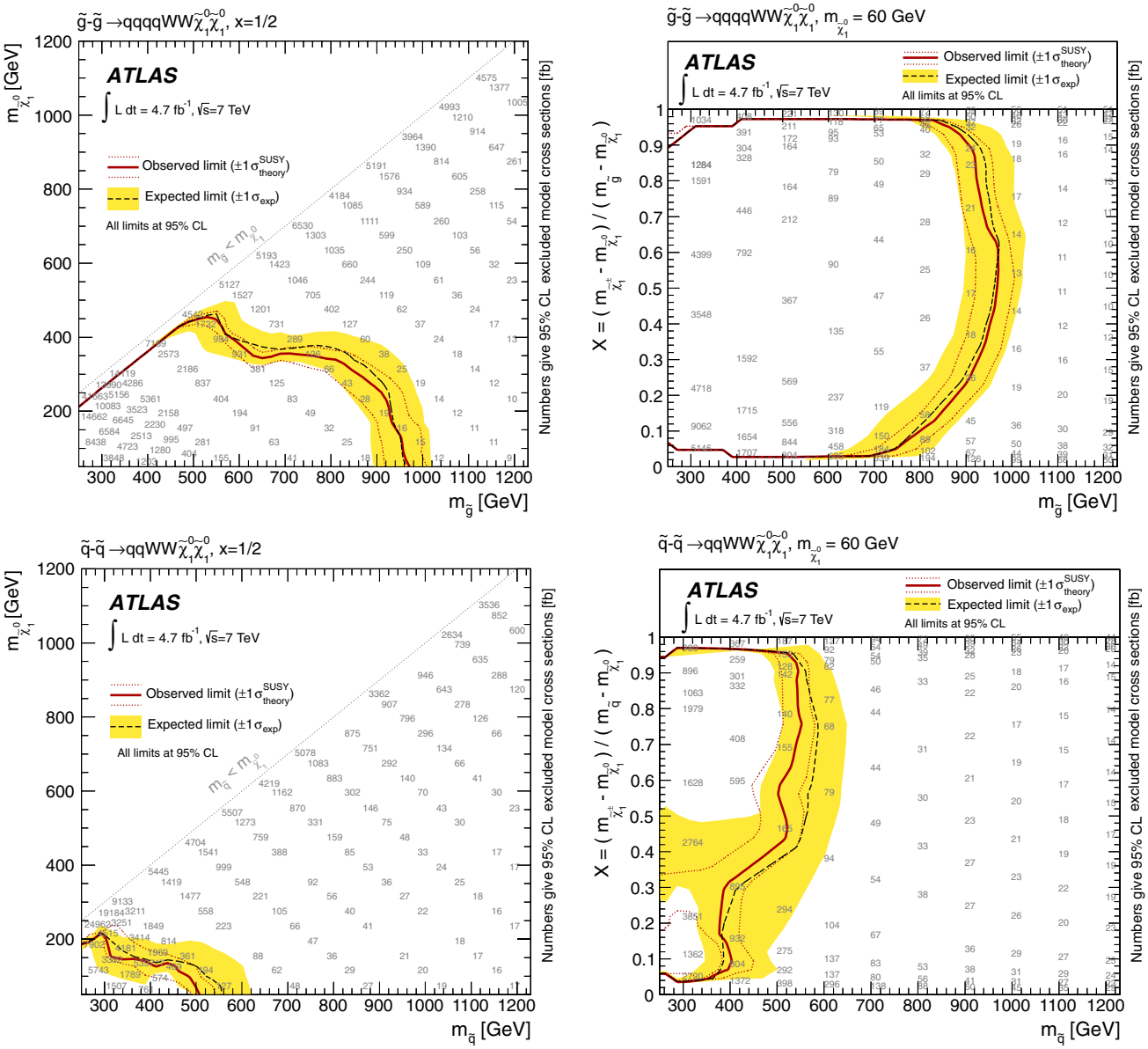

FIG. 10 (color online). Excluded regions at 95% confidence level in the parameter space of one-step simplified models. Top row: gluino pair production with $\tilde{g} \to q\bar{q}'\tilde{\chi}_1^\pm \to q\bar{q}'W^\pm\tilde{\chi}_1^0$. Bottom row: squark pair production with $\tilde{q}_L \to q'\tilde{\chi}_1^\pm \to q'W^\pm\tilde{\chi}_1^0$. In the left column, the chargino mass is set to be halfway between the gluino (top) or squark (bottom) and LSP masses. In the right column, the LSP mass is fixed at 60 GeV and the masses of the chargino and gluino (top) or squark (bottom) are varied. The band around the median expected limit shows the $\pm 1\sigma$ variations, including all uncertainties except theoretical uncertainties on the signal. The dotted lines around the observed limit indicate the sensitivity to $\pm 1\sigma$ variations on these theoretical uncertainties. The plots are from the combination of the hard and soft single-lepton channels. The numbers indicate the excluded cross section in fb. A smaller excluded cross section implies a more stringent limit.

simulation samples in the signal region. Uncertainties on the jet energy scale and the scale uncertainties for the $t\bar{t}$ background at high jet multiplicity are also significant. In the soft-lepton channel, an important contribution comes from the evaluation of the multijet background.

For the signal prediction, the dominant uncertainties at the highest excluded SUSY masses arise from the PDFs (30%–40%) and the JES (10%–20%); the former reflect the uncertainty in the gluon distribution at high values of x. In the simplified models with small mass differences, typical uncertainties from ISR variations are approximately 30%.

Model-independent limits on the visible cross section (i.e. the cross section evaluated inside a given signal region) are derived by including the number of events

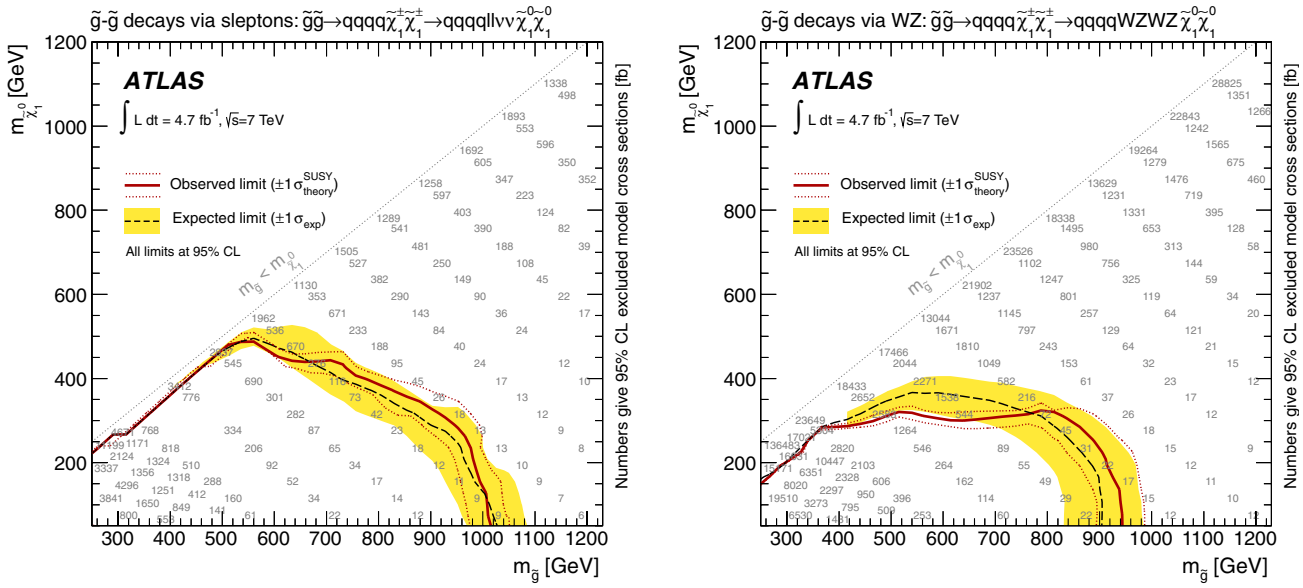

FIG. 11 (color online). Excluded regions at 95% confidence level in the parameter space of two-step simplified models with gluino pair production. Left panel: both gluinos decay via $\tilde{g} \to q\bar{q}'\tilde{\chi}_1^{\pm} \to q\bar{q}'\ell^{\pm}\tilde{\nu}_L \to q\bar{q}'\ell^{\pm}\nu\tilde{\chi}_1^0$ or $\tilde{g} \to q\bar{q}'\tilde{\chi}_1^{\pm} \to q\bar{q}'\nu\tilde{\ell}_L^{\pm} \to q\bar{q}'\nu\ell^{\pm}\tilde{\chi}_1^0$. Right panel: both gluinos decay via $\tilde{g} \to q\bar{q}'\tilde{\chi}_1^{\pm} \to q\bar{q}'W^{(*)\pm}\tilde{\chi}_2^0 \to W^{(*)\pm}Z^{(*)}\tilde{\chi}_1^0$. The band around the median expected limit shows the $\pm 1\sigma$ variations, including all uncertainties except theoretical uncertainties on the signal. The dotted lines around the observed limit indicate the sensitivity to $\pm 1\sigma$ variations on these theoretical uncertainties. The plots are dominated by the multilepton channels. The numbers indicate the excluded cross section in fb. A smaller excluded cross section implies a more stringent limit.

observed in that region as an input to the fit and deriving an additional parameter, representing the non-SM signal strength (constrained to be non-negative), as the output of the fit. Potential signal contamination in the control regions is ignored. Limits on the number of non-SM events in the signal region, derived using the CL_s [81] prescription, are divided by the integrated luminosity to obtain the constraints on the visible cross section. The limits at 95% confidence level (CL) are shown in Table VIII.

For excluding specific models of new physics, the fit in the signal regions proceeds in the same way except that in this case the signal contamination in control regions is treated by providing transfer factors from the signal regions to the control regions as further input to the fit. In addition, the likelihood fit makes use of the $m_{\mathrm{eff}}^{\mathrm{inc}}$ shape information ($E_{\mathrm{T}}^{\mathrm{miss}}/m_{\mathrm{eff}}$ for the soft-lepton channel) in the signal region as a further discriminant. Examples of these distributions are shown in Fig. 7 (the figure shows the distributions summed over lepton flavors, while the fit treats each lepton flavor channel independently). The likelihood is extended to include bin-by-bin $m_{\mathrm{eff}}^{\mathrm{inc}}$ or $E_{\mathrm{T}}^{\mathrm{miss}}/m_{\mathrm{eff}}$ information by dividing the signal region into several bins of $m_{\mathrm{eff}}^{\mathrm{inc}}$ or $E_{\mathrm{T}}^{\mathrm{miss}}/m_{\mathrm{eff}}$.

The ten statistically independent hard-lepton and multilepton channels are combined to set limits in the MSUGRA/CMSSM model. For the minimal GMSB model, only the multilepton channels are used. The soft-lepton channels are used together with the hard-lepton and multilepton channels to set limits in the one- and two-step simplified models.

The limit in the plane of $m_{1/2}$ versus m_0 in the MSUGRA/CMSSM model is shown in Fig. 8. The band around the expected limit includes all uncertainties except theoretical uncertainties on the signal prediction while the band on the observed limit indicates the sensitivity to the theoretical uncertainties on the signal. A large improvement in exclusion coverage over the previous analysis [16] can be seen. The simultaneous fit to the ten signal regions and the inclusion of the shapes of the $m_{\mathrm{eff}}^{\mathrm{inc}}$ distributions increase the expected reach in $m_{1/2}$ and m_0 by about 100 GeV, approximately uniformly across the plane. Along the line of equal masses between squarks and gluinos in the MSUGRA/CMSSM model, masses below approximately 1200 GeV are excluded at 95% CL.

For the minimal GMSB model, the limit in the plane of $\tan\beta$ versus Λ is shown in Fig. 9. The exclusion reach is dominated by the dilepton plus two jets channel. Values of Λ below about 50 TeV are excluded at 95% CL for $\tan\beta < 45$, improving on previous constraints.

Exclusion limits in the one-step simplified models are shown in Fig. 10. The figures also show the cross section excluded at 95% CL. The exclusion limits in the two-step simplified models are shown in Fig. 11 for gluino pair production and Fig. 12 for squark pair production. Simplified models with varying chargino mass and two-step simplified models are considered here for the first time

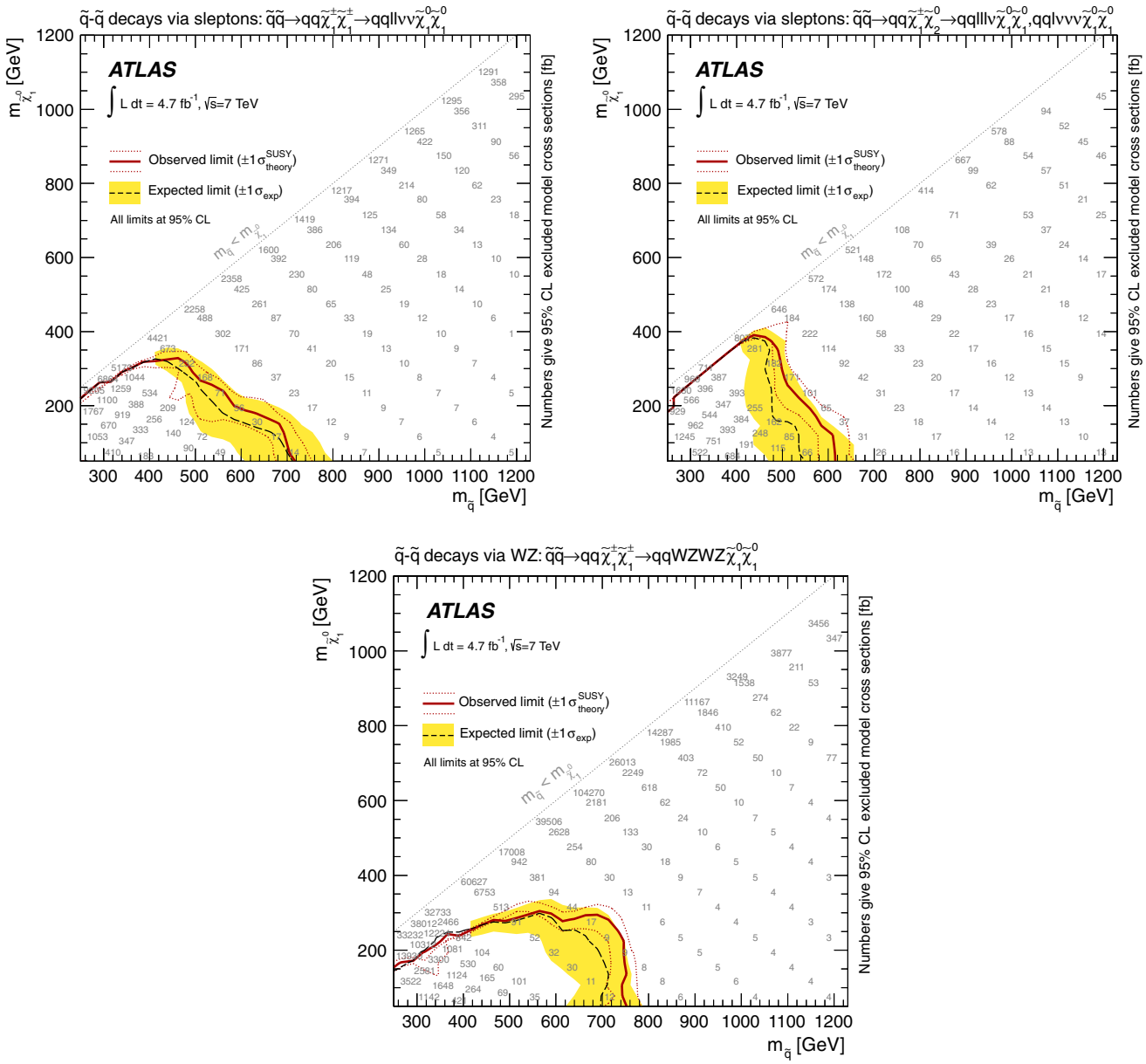

FIG. 12 (color online). Excluded regions at 95% confidence level in the parameter space of two-step simplified models with squark pair production. Top left panel: both squarks decay via $\tilde{q}_L \to q'\tilde{\chi}_1^\pm \to q'\ell^\pm\tilde{\nu}_L \to q'\ell^\pm\nu\tilde{\chi}_1^0$ or $\tilde{q}_L \to q'\tilde{\chi}_1^\pm \to q'\tilde{\ell}^\pm\nu \to q'\ell^\pm\nu\tilde{\chi}_1^0$. Top right panel: one squark decays via $\tilde{q}_L \to q'\tilde{\chi}_1^\pm \to q'\ell^\pm\tilde{\nu}_L \to q'\ell^\pm\nu\tilde{\chi}_1^0$ or $\tilde{q}_L \to q'\tilde{\chi}_1^\pm \to q'\tilde{\ell}^\pm\nu \to q'\ell^\pm\nu\tilde{\chi}_1^0$ and the other squark decays via $\tilde{q}_L \to q\tilde{\chi}_2^0 \to q\ell^\pm\tilde{\ell}_L^\mp \to q\ell^\pm\ell^\mp\tilde{\chi}_1^0$ or $\tilde{q}_L \to q\tilde{\chi}_2^0 \to q\nu\tilde{\nu}_L \to q\nu\nu\tilde{\chi}_1^0$. Bottom panel: both squarks decay via $\tilde{q}_L \to q'\tilde{\chi}_1^\pm \to W^{(*)\pm}\tilde{\chi}_2^0 \to W^{(*)\pm}Z^{(*)}\tilde{\chi}_1^0$. The band around the median expected limit shows the $\pm 1\sigma$ variations, including all uncertainties except theoretical uncertainties on the signal. The dotted lines around the observed limit indicate the sensitivity to $\pm 1\sigma$ variations on these theoretical uncertainties. The plots are dominated by the multilepton channels. The numbers indicate the excluded cross section in fb. A smaller excluded cross section implies a more stringent limit.

in leptonic SUSY searches. For both one- and two-step models, for the case of low LSP masses, gluinos with masses below approximately 900–1000 GeV and squarks with masses below approximately 500–600 GeV are excluded. Squark limits are considerably weaker, primarily due to the lower production cross section. Furthermore in the one-step model, gluinos with mass below 550 GeV are excluded for essentially all values of the LSP mass if the latter is more than 30 GeV smaller than the gluino mass. Care has to be taken when interpreting the simplified model limit in the context of a MSSM scenario, where the mass of the sneutrino is lighter than the mass of the left-handed slepton, as this can lead to modification of the lepton momenta.

XI. CONCLUSION

A new search with the ATLAS detector for SUSY in final states containing jets, one or more isolated leptons (electron or muon) and $E_{\mathrm{T}}^{\mathrm{miss}}$ has been presented. Data from the full 2011 data-taking period, corresponding to an integrated luminosity of 4.7 fb^{-1}, have been analyzed. Single-lepton and multilepton channels are treated in one analysis. A signal region with a soft lepton and soft jets has been introduced to increase the sensitivity to SUSY decay spectra involving small mass differences ("compressed SUSY"), where the sensitivity is improved by a factor of 10–30 compared to the hard-lepton channel. A simultaneous fit is performed to the event yield in multiple signal and control regions and to the shapes of distributions in those regions.

Observations are in good agreement with SM expectations, and constraints have been set on the visible cross section for new physics processes. Exclusion limits have also been extended for the MSUGRA/CMSSM and minimal GMSB models as well as for a number of simplified models. In MSUGRA/CMSSM, squark and gluino masses below approximately 1200 GeV are excluded at 95% CL (for equal squark and gluino masses). In minimal GMSB, values of Λ below about 50 TeV are excluded for $\tan\beta < 45$.

In one-step simplified models (with the chargino mass halfway between the masses of the gluino/squark and LSP) gluinos are excluded for masses below approximately 900 GeV for low values of the LSP mass. Gluinos with mass below 550 GeV are excluded for essentially all values of the LSP mass if the latter is more than 30 GeV smaller than the mass of the gluino. In the one-step simplified model with a fixed LSP mass and varying chargino and gluino (squark) masses, gluinos below approximately 950 GeV are excluded for a wide range of chargino masses; squarks are excluded below 500 GeV, albeit for a narrower range of chargino masses.

A variety of two-step simplified models have been considered. Limits on gluino masses range from about 900 GeV to 1000 GeV, while squark mass limits range from about 500 GeV to 600 GeV, all for low LSP masses.

These results improve significantly on previous constraints.

ACKNOWLEDGMENTS

We thank CERN for the very successful operation of the LHC, as well as the support staff from our institutions without whom ATLAS could not be operated efficiently. We acknowledge the support of ANPCyT, Argentina; YerPhI, Armenia; ARC, Australia; BMWF, Austria; ANAS, Azerbaijan; SSTC, Belarus; CNPq and FAPESP, Brazil; NSERC, NRC and CFI, Canada; CERN; CONICYT, Chile; CAS, MOST and NSFC, China; COLCIENCIAS, Colombia; MSMT CR, MPO CR and VSC CR, Czech Republic; DNRF, DNSRC and Lundbeck Foundation, Denmark; EPLANET and ERC, European Union; IN2P3-CNRS, CEA-DSM/IRFU, France; GNSF, Georgia; BMBF, DFG, HGF, MPG and AvH Foundation, Germany; GSRT, Greece; ISF, MINERVA, GIF, DIP and Benoziyo Center, Israel; INFN, Italy; MEXT and JSPS, Japan; CNRST, Morocco; FOM and NWO, Netherlands; RCN, Norway; MNiSW, Poland; GRICES and FCT, Portugal; MERYS (MECTS), Romania; MES of Russia and ROSATOM, Russian Federation; JINR; MSTD, Serbia; MSSR, Slovakia; ARRS and MVZT, Slovenia; DST/NRF, South Africa; MICINN, Spain; SRC and Wallenberg Foundation, Sweden; SER, SNSF and Cantons of Bern and Geneva, Switzerland; NSC, Taiwan; TAEK, Turkey; STFC, the Royal Society and Leverhulme Trust, United Kingdom; DOE and NSF, United States of America. The crucial computing support from all WLCG partners is acknowledged gratefully, in particular from CERN and the ATLAS Tier-1 facilities at TRIUMF (Canada), NDGF (Denmark, Norway, Sweden), CC-IN2P3 (France), KIT/GridKA (Germany), INFN-CNAF (Italy), NL-T1 (Netherlands), PIC (Spain), ASGC (Taiwan), RAL (UK) and BNL (USA) and in the Tier-2 facilities worldwide.

[1] H. Miyazawa, Prog. Theor. Phys. **36**, 1266 (1966).
[2] P. Ramond, Phys. Rev. D **3**, 2415 (1971).
[3] Y. A. Golfand and E. P. Likhtman, Pis'ma Zh. Eksp. Teor. Fiz. **13**, 452 (1971) [JETP Lett. **13**, 323 (1971)].
[4] A. Neveu and J. H. Schwarz, Nucl. Phys. **B31**, 86 (1971).
[5] A. Neveu and J. H. Schwarz, Phys. Rev. D **4**, 1109 (1971).
[6] J. Gervais and B. Sakita, Nucl. Phys. **B34**, 632 (1971).
[7] D. V. Volkov and V. P. Akulov, Phys. Lett. **46B**, 109 (1973).
[8] J. Wess and B. Zumino, Phys. Lett. **49B**, 52 (1974).
[9] J. Wess and B. Zumino, Nucl. Phys. **B70**, 39 (1974).
[10] L. Evans and P. Bryant, JINST **3**, S08001 (2008).
[11] P. Fayet, Phys. Lett. **64B**, 159 (1976).
[12] P. Fayet, Phys. Lett. **69B**, 489 (1977).
[13] G. R. Farrar and P. Fayet, Phys. Lett. **76B**, 575 (1978).
[14] P. Fayet, Phys. Lett. **84B**, 416 (1979).
[15] S. Dimopoulos and H. Georgi, Nucl. Phys. **B193**, 150 (1981).
[16] ATLAS Collaboration, Phys. Rev. D **85**, 012006 (2012).
[17] ATLAS Collaboration, Phys. Lett. B **709**, 137 (2012).
[18] ATLAS Collaboration, Phys. Rev. Lett. **108**, 241802 (2012).
[19] S. Chatrchyan *et al.* (CMS Collaboration), J. High Energy Phys. 08 (2011) 156.

[20] S. Chatrchyan *et al.* (CMS Collaboration), J. High Energy Phys. 06 (2012) 169.
[21] S. Chatrchyan *et al.* (CMS Collaboration), Phys. Rev. Lett. **109**, 071803 (2012).
[22] S. Chatrchyan *et al.* (CMS Collaboration), arXiv:1206.3949.
[23] ATLAS Collaboration, JINST **3**, S08003 (2008).
[24] ATLAS Collaboration, Report No. CERN-OPEN-2008-020 (arXiv:0901.0512).
[25] A. H. Chamseddine, R. L. Arnowitt, and P. Nath, Phys. Rev. Lett. **49**, 970 (1982); R. Barbieri, S. Ferrara, and C. A. Savoy, Phys. Lett. **119B**, 343 (1982); L. E. Ibanez, Phys. Lett. **118B**, 73 (1982); L. J. Hall, J. D. Lykken, and S. Weinberg, Phys. Rev. D **27**, 2359 (1983); N. Ohta, Prog. Theor. Phys. **70**, 542 (1983).
[26] G. L. Kane, C. F. Kolda, L. Roszkowski, and J. D. Wells, Phys. Rev. D **49**, 6173 (1994).
[27] L. Alvarez-Gaume, M. Claudson, and M. B. Wise, Nucl. Phys. **B207**, 96 (1982).
[28] M. Dine, W. Fischler, and M. Srednicki, Nucl. Phys. **B189**, 575 (1981).
[29] S. Dimopoulos and S. Raby, Nucl. Phys. **B192**, 353 (1981).
[30] C. R. Nappi and B. A. Ovrut, Phys. Lett. **113B**, 175 (1982).
[31] M. Dine and A. E. Nelson, Phys. Rev. D **48**, 1277 (1993).
[32] J. Alwall, P. Schuster, and N. Toro, Phys. Rev. D **79**, 075020 (2009).
[33] D. Alves *et al.* (LHC New Physics Working Group Collaboration), J. Phys. G **39**, 105005 (2012).
[34] M. Bahr, S. Gieseke, M. Gigg, D. Grellscheid, K. Hamilton *et al.*, Eur. Phys. J. C **58**, 639 (2008).
[35] A. Sherstnev and R. Thorne, Eur. Phys. J. C **55**, 553 (2008).
[36] F. E. Paige, S. D. Protopopescu, H. Baer, and X. Tata, arXiv:hep-ph/0312045.
[37] J. Alwall, M. Herquet, F. Maltoni, O. Mattelaer, and T. Stelzer, J. High Energy Phys. 06 (2011) 128.
[38] T. Sjöstrand, S. Mrenna, and P. Skands, J. High Energy Phys. 05 (2006) 026.
[39] J. Pumplin, D. Stump, J. Huston, H. Lai, P. M. Nadolsky, and W. Tung, J. High Energy Phys. 07 (2002) 012.
[40] J. Alwall, S. Hoche, F. Krauss, N. Lavesson, L. Lonnblad *et al.*, Eur. Phys. J. C **53**, 473 (2008).
[41] W. Beenakker, R. Hopker, M. Spira, and P. Zerwas, Nucl. Phys. **B492**, 51 (1997).
[42] A. Kulesza and L. Motyka, Phys. Rev. Lett. **102**, 111802 (2009).
[43] A. Kulesza and L. Motyka, Phys. Rev. D **80**, 095004 (2009).
[44] W. Beenakker, S. Brensing, M. Kramer, A. Kulesza, E. Laenen, and I. Niessen, J. High Energy Phys. 12 (2009) 041.
[45] W. Beenakker, S. Brensing, M. Kramer, A. Kulesza, E. Laenen L. Motyka, and I. Niessen, Int. J. Mod. Phys. A **26**, 2637 (2011).
[46] M. L. Mangano, M. Moretti, F. Piccinini, R. Pittau, and A. D. Polosa, J. High Energy Phys. 07 (2003) 001.
[47] M. Aliev, H. Lacker, U. Langenfeld, S. Moch, P. Uwer, and M. Wiedermann, Comput. Phys. Commun. **182**, 1034 (2011).
[48] K. Melnikov and F. Petriello, Phys. Rev. D **74**, 114017 (2006).
[49] B. P. Kersevan and E. Richter-Was, Comput. Phys. Commun. **149**, 142 (2003).
[50] S. Frixione and B. R. Webber, J. High Energy Phys. 06 (2002) 029.
[51] G. Corcella, I. Knowles, G. Marchesini, S. Moretti, K. Odagiri, P. Richardson, M. H. Seymour, and B. R. Webber, J. High Energy Phys. 01 (2001) 010.
[52] J. M. Campbell, R. K. Ellis, and C. Williams, J. High Energy Phys. 07 (2011) 018.
[53] J. M. Campbell and R. K. Ellis, J. High Energy Phys. 07 (2012) 052.
[54] A. Lazopoulos, T. McElmurry, K. Melnikov, and F. Petriello, Phys. Lett. B **666**, 62 (2008).
[55] ATLAS Collaboration, Eur. Phys. J. C **72**, 2039 (2012).
[56] A. Martin, W. Stirling, R. Thorne, and G. Watt, Phys. Lett. B **652**, 292 (2007).
[57] J. Butterworth, J. R. Forshaw, and M. Seymour, Z. Phys. C **72**, 637 (1996).
[58] H.-L. Lai, M. Guzzi, J. Huston, Z. Li, P. M. Nadolsky, J. Pumplin, and C.-P. Yuan, Phys. Rev. D **82**, 074024 (2010).
[59] A. Sherstnev and R. Thorne, arXiv:0807.2132.
[60] ATLAS Collaboration, Report No. ATL-PHYS-PUB-2011-009, 2011, https://cdsweb.cern.ch/record/1363300.
[61] ATLAS Collaboration, Eur. Phys. J. C **70**, 823 (2010).
[62] S. Agostinelli *et al.* (GEANT4 Collaboration), Nucl. Instrum. Methods Phys. Res., Sect. A **506**, 250 (2003).
[63] ATLAS Collaboration, Report No. ATLAS-CONF-2010-069, 2010, https://cdsweb.cern.ch/record/1281344.
[64] ATLAS Collaboration, Eur. Phys. J. C **72**, 1909 (2012).
[65] ATLAS Collaboration, Report No. ATLAS-CONF-2011-021, 2011, https://cdsweb.cern.ch/record/1336750.
[66] ATLAS Collaboration, Report No. ATLAS-CONF-2011-063, 2011, https://cdsweb.cern.ch/record/1345743.
[67] M. Cacciari, G. P. Salam, and G. Soyez, J. High Energy Phys. 04 (2008) 063.
[68] M. Cacciari and G. P. Salam, Phys. Lett. B **641**, 57 (2006).
[69] ATLAS Collaboration, arXiv:1112.6426 [Eur. Phys. J. C (to be published)].
[70] ATLAS Collaboration, Report No. ATLAS-CONF-2011-102, 2011, https://cdsweb.cern.ch/record/1369219.
[71] ATLAS Collaboration, Eur. Phys. J. C **71**, 1630 (2011).
[72] ATLAS Collaboration, Report No. ATLAS-CONF-2011-116, 2011, https://cdsweb.cern.ch/record/1376384.
[73] ATLAS Collaboration, Eur. Phys. J. C **72**, 1844 (2012).
[74] ATLAS Collaboration, Report No. ATLAS-CONF-2012-043, 2012, https://cdsweb.cern.ch/record/1435197.
[75] ATLAS Collaboration, Report No. ATLAS-CONF-2011-143, 2011, https://cdsweb.cern.ch/record/1386703.
[76] ATLAS Collaboration, Report No. ATLAS-CONF-2012-040, 2012, https://cdsweb.cern.ch/record/1435194.
[77] ATLAS Collaboration, Report No. ATLAS-CONF-2012-039, 2012, https://cdsweb.cern.ch/record/1435193.
[78] P. Z. Skands, Phys. Rev. D **82**, 074018 (2010).
[79] M. Kramer, A. Kulesza, R. van der Leeuw, M. Mangano, S. Padhi *et al.*, arXiv:1206.2892.
[80] G. Cowan, K. Cranmer, E. Gross, and O. Vitells, Eur. Phys. J. C **71**, 1554 (2011).
[81] A. L. Read, J. Phys. G **28**, 2693 (2002).

[82] ATLAS Collaboration, Phys. Lett. B **714**, 197 (2012).
[83] ATLAS Collaboration, Phys. Lett. B **714**, 180 (2012).
[84] LEP SUSY Working Group (ALEPH, DELPHI L3, OPAL), Report No. LEPSUSYWG/01-03.1, http://lepsusy.web.cern.ch/lepsusy/Welcome.html.
[85] G. Abbiendi *et al.* (OPAL Collaboration), Eur. Phys. J. C **46**, 307 (2006).
[86] LEP SUSY Working Group (ALEPH, DELPHI L3, OPAL), Report No. LEPSUSYWG/04-01.1, http://lepsusy.web.cern.ch/lepsusy/Welcome.html.

G. Aad,[48] T. Abajyan,[21] B. Abbott,[111] J. Abdallah,[12] S. Abdel Khalek,[115] A. A. Abdelalim,[49] O. Abdinov,[11] R. Aben,[105] B. Abi,[112] M. Abolins,[88] O. S. AbouZeid,[158] H. Abramowicz,[153] H. Abreu,[136] B. S. Acharya,[164a,164b] L. Adamczyk,[38] D. L. Adams,[25] T. N. Addy,[56] J. Adelman,[176] S. Adomeit,[98] P. Adragna,[75] T. Adye,[129] S. Aefsky,[23] J. A. Aguilar-Saavedra,[124b,b] M. Agustoni,[17] M. Aharrouche,[81] S. P. Ahlen,[22] F. Ahles,[48] A. Ahmad,[148] M. Ahsan,[41] G. Aielli,[133a,133b] T. Akdogan,[19a] T. P. A. Åkesson,[79] G. Akimoto,[155] A. V. Akimov,[94] M. S. Alam,[2] M. A. Alam,[76] J. Albert,[169] S. Albrand,[55] M. Aleksa,[30] I. N. Aleksandrov,[64] F. Alessandria,[89a] C. Alexa,[26a] G. Alexander,[153] G. Alexandre,[49] T. Alexopoulos,[10] M. Alhroob,[164a,164c] M. Aliev,[16] G. Alimonti,[89a] J. Alison,[120] B. M. M. Allbrooke,[18] P. P. Allport,[73] S. E. Allwood-Spiers,[53] J. Almond,[82] A. Aloisio,[102a,102b] R. Alon,[172] A. Alonso,[79] F. Alonso,[70] A. Altheimer,[35] B. Alvarez Gonzalez,[88] M. G. Alviggi,[102a,102b] K. Amako,[65] C. Amelung,[23] V. V. Ammosov,[128,a] S. P. Amor Dos Santos,[124a] A. Amorim,[124a,c] N. Amram,[153] C. Anastopoulos,[30] L. S. Ancu,[17] N. Andari,[115] T. Andeen,[35] C. F. Anders,[58b] G. Anders,[58a] K. J. Anderson,[31] A. Andreazza,[89a,89b] V. Andrei,[58a] M-L. Andrieux,[55] X. S. Anduaga,[70] P. Anger,[44] A. Angerami,[35] F. Anghinolfi,[30] A. Anisenkov,[107] N. Anjos,[124a] A. Annovi,[47] A. Antonaki,[9] M. Antonelli,[47] A. Antonov,[96] J. Antos,[144b] F. Anulli,[132a] M. Aoki,[101] S. Aoun,[83] L. Aperio Bella,[5] R. Apolle,[118,d] G. Arabidze,[88] I. Aracena,[143] Y. Arai,[65] A. T. H. Arce,[45] S. Arfaoui,[148] J-F. Arguin,[15] E. Arik,[19a,a] M. Arik,[19a] A. J. Armbruster,[87] O. Arnaez,[81] V. Arnal,[80] C. Arnault,[115] A. Artamonov,[95] G. Artoni,[132a,132b] D. Arutinov,[21] S. Asai,[155] R. Asfandiyarov,[173] S. Ask,[28] B. Åsman,[146a,146b] L. Asquith,[6] K. Assamagan,[25] A. Astbury,[169] M. Atkinson,[165] B. Aubert,[5] E. Auge,[115] K. Augsten,[127] M. Aurousseau,[145a] G. Avolio,[163] R. Avramidou,[10] D. Axen,[168] G. Azuelos,[93,e] Y. Azuma,[155] M. A. Baak,[30] G. Baccaglioni,[89a] C. Bacci,[134a,134b] A. M. Bach,[15] H. Bachacou,[136] K. Bachas,[30] M. Backes,[49] M. Backhaus,[21] J. Backus Mayes,[143] E. Badescu,[26a] P. Bagnaia,[132a,132b] S. Bahinipati,[3] Y. Bai,[33a] D. C. Bailey,[158] T. Bain,[158] J. T. Baines,[129] O. K. Baker,[176] M. D. Baker,[25] S. Baker,[77] E. Banas,[39] P. Banerjee,[93] Sw. Banerjee,[173] D. Banfi,[30] A. Bangert,[150] V. Bansal,[169] H. S. Bansil,[18] L. Barak,[172] S. P. Baranov,[94] A. Barbaro Galtieri,[15] T. Barber,[48] E. L. Barberio,[86] D. Barberis,[50a,50b] M. Barbero,[21] D. Y. Bardin,[64] T. Barillari,[99] M. Barisonzi,[175] T. Barklow,[143] N. Barlow,[28] B. M. Barnett,[129] R. M. Barnett,[15] A. Baroncelli,[134a] G. Barone,[49] A. J. Barr,[118] F. Barreiro,[80] J. Barreiro Guimarães da Costa,[57] P. Barrillon,[115] R. Bartoldus,[143] A. E. Barton,[71] V. Bartsch,[149] A. Basye,[165] R. L. Bates,[53] L. Batkova,[144a] J. R. Batley,[28] A. Battaglia,[17] M. Battistin,[30] F. Bauer,[136] H. S. Bawa,[143,f] S. Beale,[98] T. Beau,[78] P. H. Beauchemin,[161] R. Beccherle,[50a] P. Bechtle,[21] H. P. Beck,[17] A. K. Becker,[175] S. Becker,[98] M. Beckingham,[138] K. H. Becks,[175] A. J. Beddall,[19c] A. Beddall,[19c] S. Bedikian,[176] V. A. Bednyakov,[64] C. P. Bee,[83] L. J. Beemster,[105] M. Begel,[25] S. Behar Harpaz,[152] P. K. Behera,[62] M. Beimforde,[99] C. Belanger-Champagne,[85] P. J. Bell,[49] W. H. Bell,[49] G. Bella,[153] L. Bellagamba,[20a] F. Bellina,[30] M. Bellomo,[30] A. Belloni,[57] O. Beloborodova,[107,g] K. Belotskiy,[96] O. Beltramello,[30] O. Benary,[153] D. Benchekroun,[135a] K. Bendtz,[146a,146b] N. Benekos,[165] Y. Benhammou,[153] E. Benhar Noccioli,[49] J. A. Benitez Garcia,[159b] D. P. Benjamin,[45] M. Benoit,[115] J. R. Bensinger,[23] K. Benslama,[130] S. Bentvelsen,[105] D. Berge,[30] E. Bergeaas Kuutmann,[42] N. Berger,[5] F. Berghaus,[169] E. Berglund,[105] J. Beringer,[15] P. Bernat,[77] R. Bernhard,[48] C. Bernius,[25] T. Berry,[76] C. Bertella,[83] A. Bertin,[20a,20b] F. Bertolucci,[122a,122b] M. I. Besana,[89a,89b] G. J. Besjes,[104] N. Besson,[136] S. Bethke,[99] W. Bhimji,[46] R. M. Bianchi,[30] M. Bianco,[72a,72b] O. Biebel,[98] S. P. Bieniek,[77] K. Bierwagen,[54] J. Biesiada,[15] M. Biglietti,[134a] H. Bilokon,[47] M. Bindi,[20a,20b] S. Binet,[115] A. Bingul,[19c] C. Bini,[132a,132b] C. Biscarat,[178] B. Bittner,[99] K. M. Black,[22] R. E. Blair,[6] J.-B. Blanchard,[136] G. Blanchot,[30] T. Blazek,[144a] I. Bloch,[42] C. Blocker,[23] J. Blocki,[39] A. Blondel,[49] W. Blum,[81] U. Blumenschein,[54] G. J. Bobbink,[105] V. B. Bobrovnikov,[107] S. S. Bocchetta,[79] A. Bocci,[45] C. R. Boddy,[118] M. Boehler,[48] J. Boek,[175] N. Boelaert,[36] J. A. Bogaerts,[30] A. Bogdanchikov,[107] A. Bogouch,[90,a] C. Bohm,[146a] J. Bohm,[125] V. Boisvert,[76] T. Bold,[38] V. Boldea,[26a] N. M. Bolnet,[136] M. Bomben,[78] M. Bona,[75] M. Boonekamp,[136] S. Bordoni,[78] C. Borer,[17] A. Borisov,[128] G. Borissov,[71] I. Borjanovic,[13a] M. Borri,[82] S. Borroni,[87] V. Bortolotto,[134a,134b] K. Bos,[105] D. Boscherini,[20a] M. Bosman,[12] H. Boterenbrood,[105] J. Bouchami,[93] J. Boudreau,[123] E. V. Bouhova-Thacker,[71] D. Boumediene,[34] C. Bourdarios,[115] N. Bousson,[83] A. Boveia,[31] J. Boyd,[30] I. R. Boyko,[64] I. Bozovic-Jelisavcic,[13b] J. Bracinik,[18] P. Branchini,[134a] G. W. Brandenburg,[57] A. Brandt,[8]

G. Brandt,[118] O. Brandt,[54] U. Bratzler,[156] B. Brau,[84] J. E. Brau,[114] H. M. Braun,[175,a] S. F. Brazzale,[164a,164c] B. Brelier,[158] J. Bremer,[30] K. Brendlinger,[120] R. Brenner,[166] S. Bressler,[172] D. Britton,[53] F. M. Brochu,[28] I. Brock,[21] R. Brock,[88] F. Broggi,[89a] C. Bromberg,[88] J. Bronner,[99] G. Brooijmans,[35] T. Brooks,[76] W. K. Brooks,[32b] G. Brown,[82] H. Brown,[8] P. A. Bruckman de Renstrom,[39] D. Bruncko,[144b] R. Bruneliere,[48] S. Brunet,[60] A. Bruni,[20a] G. Bruni,[20a] M. Bruschi,[20a] T. Buanes,[14] Q. Buat,[55] F. Bucci,[49] J. Buchanan,[118] P. Buchholz,[141] R. M. Buckingham,[118] A. G. Buckley,[46] S. I. Buda,[26a] I. A. Budagov,[64] B. Budick,[108] V. Büscher,[81] L. Bugge,[117] O. Bulekov,[96] A. C. Bundock,[73] M. Bunse,[43] T. Buran,[117] H. Burckhart,[30] S. Burdin,[73] T. Burgess,[14] S. Burke,[129] E. Busato,[34] P. Bussey,[53] C. P. Buszello,[166] B. Butler,[143] J. M. Butler,[22] C. M. Buttar,[53] J. M. Butterworth,[77] W. Buttinger,[28] S. Cabrera Urbán,[167] D. Caforio,[20a,20b] O. Cakir,[4a] P. Calafiura,[15] G. Calderini,[78] P. Calfayan,[98] R. Calkins,[106] L. P. Caloba,[24a] R. Caloi,[132a,132b] D. Calvet,[34] S. Calvet,[34] R. Camacho Toro,[34] P. Camarri,[133a,133b] D. Cameron,[117] L. M. Caminada,[15] R. Caminal Armadans,[12] S. Campana,[30] M. Campanelli,[77] V. Canale,[102a,102b] F. Canelli,[31,h] A. Canepa,[159a] J. Cantero,[80] R. Cantrill,[76] L. Capasso,[102a,102b] M. D. M. Capeans Garrido,[30] I. Caprini,[26a] M. Caprini,[26a] D. Capriotti,[99] M. Capua,[37a,37b] R. Caputo,[81] R. Cardarelli,[133a] T. Carli,[30] G. Carlino,[102a] L. Carminati,[89a,89b] B. Caron,[85] S. Caron,[104] E. Carquin,[32b] G. D. Carrillo Montoya,[173] A. A. Carter,[75] J. R. Carter,[28] J. Carvalho,[124a,i] D. Casadei,[108] M. P. Casado,[12] M. Cascella,[122a,122b] C. Caso,[50a,50b,a] A. M. Castaneda Hernandez,[173,j] E. Castaneda-Miranda,[173] V. Castillo Gimenez,[167] N. F. Castro,[124a] G. Cataldi,[72a] P. Catastini,[57] A. Catinaccio,[30] J. R. Catmore,[30] A. Cattai,[30] G. Cattani,[133a,133b] S. Caughron,[88] V. Cavaliere,[165] P. Cavalleri,[78] D. Cavalli,[89a] M. Cavalli-Sforza,[12] V. Cavasinni,[122a,122b] F. Ceradini,[134a,134b] A. S. Cerqueira,[24b] A. Cerri,[30] L. Cerrito,[75] F. Cerutti,[47] S. A. Cetin,[19b] A. Chafaq,[135a] D. Chakraborty,[106] I. Chalupkova,[126] K. Chan,[3] P. Chang,[165] B. Chapleau,[85] J. D. Chapman,[28] J. W. Chapman,[87] E. Chareyre,[78] D. G. Charlton,[18] V. Chavda,[82] C. A. Chavez Barajas,[30] S. Cheatham,[85] S. Chekanov,[6] S. V. Chekulaev,[159a] G. A. Chelkov,[64] M. A. Chelstowska,[104] C. Chen,[63] H. Chen,[25] S. Chen,[33c] X. Chen,[173] Y. Chen,[35] A. Cheplakov,[64] R. Cherkaoui El Moursli,[135e] V. Chernyatin,[25] E. Cheu,[7] S. L. Cheung,[158] L. Chevalier,[136] G. Chiefari,[102a,102b] L. Chikovani,[51a,a] J. T. Childers,[30] A. Chilingarov,[71] G. Chiodini,[72a] A. S. Chisholm,[18] R. T. Chislett,[77] A. Chitan,[26a] M. V. Chizhov,[64] G. Choudalakis,[31] S. Chouridou,[137] I. A. Christidi,[77] A. Christov,[48] D. Chromek-Burckhart,[30] M. L. Chu,[151] J. Chudoba,[125] G. Ciapetti,[132a,132b] A. K. Ciftci,[4a] R. Ciftci,[4a] D. Cinca,[34] V. Cindro,[74] C. Ciocca,[20a,20b] A. Ciocio,[15] M. Cirilli,[87] P. Cirkovic,[13b] Z. H. Citron,[172] M. Citterio,[89a] M. Ciubancan,[26a] A. Clark,[49] P. J. Clark,[46] R. N. Clarke,[15] W. Cleland,[123] J. C. Clemens,[83] B. Clement,[55] C. Clement,[146a,146b] Y. Coadou,[83] M. Cobal,[164a,164c] A. Coccaro,[138] J. Cochran,[63] L. Coffey,[23] J. G. Cogan,[143] J. Coggeshall,[165] E. Cogneras,[178] J. Colas,[5] S. Cole,[106] A. P. Colijn,[105] N. J. Collins,[18] C. Collins-Tooth,[53] J. Collot,[55] T. Colombo,[119a,119b] G. Colon,[84] P. Conde Muiño,[124a] E. Coniavitis,[118] M. C. Conidi,[12] S. M. Consonni,[89a,89b] V. Consorti,[48] S. Constantinescu,[26a] C. Conta,[119a,119b] G. Conti,[57] F. Conventi,[102a,k] M. Cooke,[15] B. D. Cooper,[77] A. M. Cooper-Sarkar,[118] K. Copic,[15] T. Cornelissen,[175] M. Corradi,[20a] F. Corriveau,[85,l] A. Cortes-Gonzalez,[165] G. Cortiana,[99] G. Costa,[89a] M. J. Costa,[167] D. Costanzo,[139] D. Côté,[30] L. Courneyea,[169] G. Cowan,[76] C. Cowden,[28] B. E. Cox,[82] K. Cranmer,[108] F. Crescioli,[122a,122b] M. Cristinziani,[21] G. Crosetti,[37a,37b] S. Crépé-Renaudin,[55] C.-M. Cuciuc,[26a] C. Cuenca Almenar,[176] T. Cuhadar Donszelmann,[139] M. Curatolo,[47] C. J. Curtis,[18] C. Cuthbert,[150] P. Cwetanski,[60] H. Czirr,[141] P. Czodrowski,[44] Z. Czyczula,[176] S. D'Auria,[53] M. D'Onofrio,[73] A. D'Orazio,[132a,132b] M. J. Da Cunha Sargedas De Sousa,[124a] C. Da Via,[82] W. Dabrowski,[38] A. Dafinca,[118] T. Dai,[87] C. Dallapiccola,[84] M. Dam,[36] M. Dameri,[50a,50b] D. S. Damiani,[137] H. O. Danielsson,[30] V. Dao,[49] G. Darbo,[50a] G. L. Darlea,[26b] J. A. Dassoulas,[42] W. Davey,[21] T. Davidek,[126] N. Davidson,[86] R. Davidson,[71] E. Davies,[118,d] M. Davies,[93] O. Davignon,[78] A. R. Davison,[77] Y. Davygora,[58a] E. Dawe,[142] I. Dawson,[139] R. K. Daya-Ishmukhametova,[23] K. De,[8] R. de Asmundis,[102a] S. De Castro,[20a,20b] S. De Cecco,[78] J. de Graat,[98] N. De Groot,[104] P. de Jong,[105] C. De La Taille,[115] H. De la Torre,[80] F. De Lorenzi,[63] L. de Mora,[71] L. De Nooij,[105] D. De Pedis,[132a] A. De Salvo,[132a] U. De Sanctis,[164a,164c] A. De Santo,[149] J. B. De Vivie De Regie,[115] G. De Zorzi,[132a,132b] W. J. Dearnaley,[71] R. Debbe,[25] C. Debenedetti,[46] B. Dechenaux,[55] D. V. Dedovich,[64] J. Degenhardt,[120] C. Del Papa,[164a,164c] J. Del Peso,[80] T. Del Prete,[122a,122b] T. Delemontex,[55] M. Deliyergiyev,[74] A. Dell'Acqua,[30] L. Dell'Asta,[22] M. Della Pietra,[102a,k] D. della Volpe,[102a,102b] M. Delmastro,[5] P. A. Delsart,[55] C. Deluca,[105] S. Demers,[176] M. Demichev,[64] B. Demirkoz,[12,m] J. Deng,[163] S. P. Denisov,[128] D. Derendarz,[39] J. E. Derkaoui,[135d] F. Derue,[78] P. Dervan,[73] K. Desch,[21] E. Devetak,[148] P. O. Deviveiros,[105] A. Dewhurst,[129] B. DeWilde,[148] S. Dhaliwal,[158] R. Dhullipudi,[25,n] A. Di Ciaccio,[133a,133b] L. Di Ciaccio,[5] A. Di Girolamo,[30] B. Di Girolamo,[30] S. Di Luise,[134a,134b] A. Di Mattia,[173] B. Di Micco,[30] R. Di Nardo,[47] A. Di Simone,[133a,133b] R. Di Sipio,[20a,20b] M. A. Diaz,[32a] E. B. Diehl,[87]

J. Dietrich,[42] T. A. Dietzsch,[58a] S. Diglio,[86] K. Dindar Yagci,[40] J. Dingfelder,[21] F. Dinut,[26a] C. Dionisi,[132a,132b] P. Dita,[26a] S. Dita,[26a] F. Dittus,[30] F. Djama,[83] T. Djobava,[51b] M. A. B. do Vale,[24c] A. Do Valle Wemans,[124a,o] T. K. O. Doan,[5] M. Dobbs,[85] R. Dobinson,[30,a] D. Dobos,[30] E. Dobson,[30,p] J. Dodd,[35] C. Doglioni,[49] T. Doherty,[53] Y. Doi,[65,a] J. Dolejsi,[126] I. Dolenc,[74] Z. Dolezal,[126] B. A. Dolgoshein,[96,a] T. Dohmae,[155] M. Donadelli,[24d] J. Donini,[34] J. Dopke,[30] A. Doria,[102a] A. Dos Anjos,[173] A. Dotti,[122a,122b] M. T. Dova,[70] A. D. Doxiadis,[105] A. T. Doyle,[53] N. Dressnandt,[120] M. Dris,[10] J. Dubbert,[99] S. Dube,[15] E. Duchovni,[172] G. Duckeck,[98] D. Duda,[175] A. Dudarev,[30] F. Dudziak,[63] M. Dührssen,[30] I. P. Duerdoth,[82] L. Duflot,[115] M-A. Dufour,[85] L. Duguid,[76] M. Dunford,[30] H. Duran Yildiz,[4a] R. Duxfield,[139] M. Dwuznik,[38] F. Dydak,[30] M. Düren,[52] W. L. Ebenstein,[45] J. Ebke,[98] S. Eckweiler,[81] K. Edmonds,[81] W. Edson,[2] C. A. Edwards,[76] N. C. Edwards,[53] W. Ehrenfeld,[42] T. Eifert,[143] G. Eigen,[14] K. Einsweiler,[15] E. Eisenhandler,[75] T. Ekelof,[166] M. El Kacimi,[135c] M. Ellert,[166] S. Elles,[5] F. Ellinghaus,[81] K. Ellis,[75] N. Ellis,[30] J. Elmsheuser,[98] M. Elsing,[30] D. Emeliyanov,[129] R. Engelmann,[148] A. Engl,[98] B. Epp,[61] J. Erdmann,[54] A. Ereditato,[17] D. Eriksson,[146a] J. Ernst,[2] M. Ernst,[25] J. Ernwein,[136] D. Errede,[165] S. Errede,[165] E. Ertel,[81] M. Escalier,[115] H. Esch,[43] C. Escobar,[123] X. Espinal Curull,[12] B. Esposito,[47] F. Etienne,[83] A. I. Etienvre,[136] E. Etzion,[153] D. Evangelakou,[54] H. Evans,[60] L. Fabbri,[20a,20b] C. Fabre,[30] R. M. Fakhrutdinov,[128] S. Falciano,[132a] Y. Fang,[173] M. Fanti,[89a,89b] A. Farbin,[8] A. Farilla,[134a] J. Farley,[148] T. Farooque,[158] S. Farrell,[163] S. M. Farrington,[170] P. Farthouat,[30] F. Fassi,[167] P. Fassnacht,[30] D. Fassouliotis,[9] B. Fatholahzadeh,[158] A. Favareto,[89a,89b] L. Fayard,[115] S. Fazio,[37a,37b] R. Febbraro,[34] P. Federic,[144a] O. L. Fedin,[121] W. Fedorko,[88] M. Fehling-Kaschek,[48] L. Feligioni,[83] D. Fellmann,[6] C. Feng,[33d] E. J. Feng,[6] A. B. Fenyuk,[128] J. Ferencei,[144b] W. Fernando,[6] S. Ferrag,[53] J. Ferrando,[53] V. Ferrara,[42] A. Ferrari,[166] P. Ferrari,[105] R. Ferrari,[119a] D. E. Ferreira de Lima,[53] A. Ferrer,[167] D. Ferrere,[49] C. Ferretti,[87] A. Ferretto Parodi,[50a,50b] M. Fiascaris,[31] F. Fiedler,[81] A. Filipčič,[74] F. Filthaut,[104] M. Fincke-Keeler,[169] M. C. N. Fiolhais,[124a,i] L. Fiorini,[167] A. Firan,[40] G. Fischer,[42] M. J. Fisher,[109] M. Flechl,[48] I. Fleck,[141] J. Fleckner,[81] P. Fleischmann,[174] S. Fleischmann,[175] T. Flick,[175] A. Floderus,[79] L. R. Flores Castillo,[173] M. J. Flowerdew,[99] T. Fonseca Martin,[17] A. Formica,[136] A. Forti,[82] D. Fortin,[159a] D. Fournier,[115] A. J. Fowler,[45] H. Fox,[71] P. Francavilla,[12] M. Franchini,[20a,20b] S. Franchino,[119a,119b] D. Francis,[30] T. Frank,[172] S. Franz,[30] M. Fraternali,[119a,119b] S. Fratina,[120] S. T. French,[28] C. Friedrich,[42] F. Friedrich,[44] R. Froeschl,[30] D. Froidevaux,[30] J. A. Frost,[28] C. Fukunaga,[156] E. Fullana Torregrosa,[30] B. G. Fulsom,[143] J. Fuster,[167] C. Gabaldon,[30] O. Gabizon,[172] T. Gadfort,[25] S. Gadomski,[49] G. Gagliardi,[50a,50b] P. Gagnon,[60] C. Galea,[98] B. Galhardo,[124a] E. J. Gallas,[118] V. Gallo,[17] B. J. Gallop,[129] P. Gallus,[125] K. K. Gan,[109] Y. S. Gao,[143,f] A. Gaponenko,[15] F. Garberson,[176] M. Garcia-Sciveres,[15] C. García,[167] J. E. García Navarro,[167] R. W. Gardner,[31] N. Garelli,[30] H. Garitaonandia,[105] V. Garonne,[30] C. Gatti,[47] G. Gaudio,[119a] B. Gaur,[141] L. Gauthier,[136] P. Gauzzi,[132a,132b] I. L. Gavrilenko,[94] C. Gay,[168] G. Gaycken,[21] E. N. Gazis,[10] P. Ge,[33d] Z. Gecse,[168] C. N. P. Gee,[129] D. A. A. Geerts,[105] Ch. Geich-Gimbel,[21] K. Gellerstedt,[146a,146b] C. Gemme,[50a] A. Gemmell,[53] M. H. Genest,[55] S. Gentile,[132a,132b] M. George,[54] S. George,[76] P. Gerlach,[175] A. Gershon,[153] C. Geweniger,[58a] H. Ghazlane,[135b] N. Ghodbane,[34] B. Giacobbe,[20a] S. Giagu,[132a,132b] V. Giakoumopoulou,[9] V. Giangiobbe,[12] F. Gianotti,[30] B. Gibbard,[25] A. Gibson,[158] S. M. Gibson,[30] D. Gillberg,[29] A. R. Gillman,[129] D. M. Gingrich,[3,e] J. Ginzburg,[153] N. Giokaris,[9] M. P. Giordani,[164c] R. Giordano,[102a,102b] F. M. Giorgi,[16] P. Giovannini,[99] P. F. Giraud,[136] D. Giugni,[89a] M. Giunta,[93] P. Giusti,[20a] B. K. Gjelsten,[117] L. K. Gladilin,[97] C. Glasman,[80] J. Glatzer,[48] A. Glazov,[42] K. W. Glitza,[175] G. L. Glonti,[64] J. R. Goddard,[75] J. Godfrey,[142] J. Godlewski,[30] M. Goebel,[42] T. Göpfert,[44] C. Goeringer,[81] C. Gössling,[43] S. Goldfarb,[87] T. Golling,[176] A. Gomes,[124a,c] L. S. Gomez Fajardo,[42] R. Gonçalo,[76] J. Goncalves Pinto Firmino Da Costa,[42] L. Gonella,[21] S. González de la Hoz,[167] G. Gonzalez Parra,[12] M. L. Gonzalez Silva,[27] S. Gonzalez-Sevilla,[49] J. J. Goodson,[148] L. Goossens,[30] P. A. Gorbounov,[95] H. A. Gordon,[25] I. Gorelov,[103] G. Gorfine,[175] B. Gorini,[30] E. Gorini,[72a,72b] A. Gorišek,[74] E. Gornicki,[39] B. Gosdzik,[42] A. T. Goshaw,[6] M. Gosselink,[105] M. I. Gostkin,[64] I. Gough Eschrich,[163] M. Gouighri,[135a] D. Goujdami,[135c] M. P. Goulette,[49] A. G. Goussiou,[138] C. Goy,[5] S. Gozpinar,[23] I. Grabowska-Bold,[38] P. Grafström,[20a,20b] K-J. Grahn,[42] F. Grancagnolo,[72a] S. Grancagnolo,[16] V. Grassi,[148] V. Gratchev,[121] N. Grau,[35] H. M. Gray,[30] J. A. Gray,[148] E. Graziani,[134a] O. G. Grebenyuk,[121] T. Greenshaw,[73] Z. D. Greenwood,[25,n] K. Gregersen,[36] I. M. Gregor,[42] P. Grenier,[143] J. Griffiths,[8] N. Grigalashvili,[64] A. A. Grillo,[137] S. Grinstein,[12] Ph. Gris,[34] Y. V. Grishkevich,[97] J.-F. Grivaz,[115] E. Gross,[172] J. Grosse-Knetter,[54] J. Groth-Jensen,[172] K. Grybel,[141] D. Guest,[176] C. Guicheney,[34] S. Guindon,[54] U. Gul,[53] J. Gunther,[125] B. Guo,[158] J. Guo,[35] P. Gutierrez,[111] N. Guttman,[153] O. Gutzwiller,[173] C. Guyot,[136] C. Gwenlan,[118] C. B. Gwilliam,[73] A. Haas,[143] S. Haas,[30] C. Haber,[15] H. K. Hadavand,[40] D. R. Hadley,[18] P. Haefner,[21] F. Hahn,[30] S. Haider,[30] Z. Hajduk,[39] H. Hakobyan,[177] D. Hall,[118] J. Haller,[54] K. Hamacher,[175]

P. Hamal,[113] M. Hamer,[54] A. Hamilton,[145b,q] S. Hamilton,[161] L. Han,[33b] K. Hanagaki,[116] K. Hanawa,[160] M. Hance,[15] C. Handel,[81] P. Hanke,[58a] J. R. Hansen,[36] J. B. Hansen,[36] J. D. Hansen,[36] P. H. Hansen,[36] P. Hansson,[143] K. Hara,[160] G. A. Hare,[137] T. Harenberg,[175] S. Harkusha,[90] D. Harper,[87] R. D. Harrington,[46] O. M. Harris,[138] J. Hartert,[48] F. Hartjes,[105] T. Haruyama,[65] A. Harvey,[56] S. Hasegawa,[101] Y. Hasegawa,[140] S. Hassani,[136] S. Haug,[17] M. Hauschild,[30] R. Hauser,[88] M. Havranek,[21] C. M. Hawkes,[18] R. J. Hawkings,[30] A. D. Hawkins,[79] T. Hayakawa,[66] T. Hayashi,[160] D. Hayden,[76] C. P. Hays,[118] H. S. Hayward,[73] S. J. Haywood,[129] S. J. Head,[18] V. Hedberg,[79] L. Heelan,[8] S. Heim,[88] B. Heinemann,[15] S. Heisterkamp,[36] L. Helary,[22] C. Heller,[98] M. Heller,[30] S. Hellman,[146a,146b] D. Hellmich,[21] C. Helsens,[12] R. C. W. Henderson,[71] M. Henke,[58a] A. Henrichs,[54] A. M. Henriques Correia,[30] S. Henrot-Versille,[115] C. Hensel,[54] T. Henß,[175] C. M. Hernandez,[8] Y. Hernández Jiménez,[167] R. Herrberg,[16] G. Herten,[48] R. Hertenberger,[98] L. Hervas,[30] G. G. Hesketh,[77] N. P. Hessey,[105] E. Higón-Rodriguez,[167] J. C. Hill,[28] K. H. Hiller,[42] S. Hillert,[21] S. J. Hillier,[18] I. Hinchliffe,[15] E. Hines,[120] M. Hirose,[116] F. Hirsch,[43] D. Hirschbuehl,[175] J. Hobbs,[148] N. Hod,[153] M. C. Hodgkinson,[139] P. Hodgson,[139] A. Hoecker,[30] M. R. Hoeferkamp,[103] J. Hoffman,[40] D. Hoffmann,[83] M. Hohlfeld,[81] M. Holder,[141] S. O. Holmgren,[146a] T. Holy,[127] J. L. Holzbauer,[88] T. M. Hong,[120] L. Hooft van Huysduynen,[108] S. Horner,[48] J-Y. Hostachy,[55] S. Hou,[151] A. Hoummada,[135a] J. Howard,[118] J. Howarth,[82] I. Hristova,[16] J. Hrivnac,[115] T. Hryn'ova,[5] P. J. Hsu,[81] S.-C. Hsu,[15] D. Hu,[35] Z. Hubacek,[127] F. Hubaut,[83] F. Huegging,[21] A. Huettmann,[42] T. B. Huffman,[118] E. W. Hughes,[35] G. Hughes,[71] M. Huhtinen,[30] M. Hurwitz,[15] N. Huseynov,[64,r] J. Huston,[88] J. Huth,[57] G. Iacobucci,[49] G. Iakovidis,[10] M. Ibbotson,[82] I. Ibragimov,[141] L. Iconomidou-Fayard,[115] J. Idarraga,[115] P. Iengo,[102a] O. Igonkina,[105] Y. Ikegami,[65] M. Ikeno,[65] D. Iliadis,[154] N. Ilic,[158] T. Ince,[21] J. Inigo-Golfin,[30] P. Ioannou,[9] M. Iodice,[134a] K. Iordanidou,[9] V. Ippolito,[132a,132b] A. Irles Quiles,[167] C. Isaksson,[166] M. Ishino,[67] M. Ishitsuka,[157] R. Ishmukhametov,[40] C. Issever,[118] S. Istin,[19a] A. V. Ivashin,[128] W. Iwanski,[39] H. Iwasaki,[65] J. M. Izen,[41] V. Izzo,[102a] B. Jackson,[120] J. N. Jackson,[73] P. Jackson,[1] M. R. Jaekel,[30] V. Jain,[60] K. Jakobs,[48] S. Jakobsen,[36] T. Jakoubek,[125] J. Jakubek,[127] D. O. Jamin,[151] D. K. Jana,[111] E. Jansen,[77] H. Jansen,[30] A. Jantsch,[99] M. Janus,[48] G. Jarlskog,[79] L. Jeanty,[57] I. Jen-La Plante,[31] D. Jennens,[86] P. Jenni,[30] A. E. Loevschall-Jensen,[36] P. Ježˇ,[36] S. Jézéquel,[5] M. K. Jha,[20a] H. Ji,[173] W. Ji,[81] J. Jia,[148] Y. Jiang,[33b] M. Jimenez Belenguer,[42] S. Jin,[33a] O. Jinnouchi,[157] M. D. Joergensen,[36] D. Joffe,[40] M. Johansen,[146a,146b] K. E. Johansson,[146a] P. Johansson,[139] S. Johnert,[42] K. A. Johns,[7] K. Jon-And,[146a,146b] G. Jones,[170] R. W. L. Jones,[71] T. J. Jones,[73] C. Joram,[30] P. M. Jorge,[124a] K. D. Joshi,[82] J. Jovicevic,[147] T. Jovin,[13b] X. Ju,[173] C. A. Jung,[43] R. M. Jungst,[30] V. Juranek,[125] P. Jussel,[61] A. Juste Rozas,[12] S. Kabana,[17] M. Kaci,[167] A. Kaczmarska,[39] P. Kadlecik,[36] M. Kado,[115] H. Kagan,[109] M. Kagan,[57] E. Kajomovitz,[152] S. Kalinin,[175] L. V. Kalinovskaya,[64] S. Kama,[40] N. Kanaya,[155] M. Kaneda,[30] S. Kaneti,[28] T. Kanno,[157] V. A. Kantserov,[96] J. Kanzaki,[65] B. Kaplan,[108] A. Kapliy,[31] J. Kaplon,[30] D. Kar,[53] M. Karagounis,[21] K. Karakostas,[10] M. Karnevskiy,[42] V. Kartvelishvili,[71] A. N. Karyukhin,[128] L. Kashif,[173] G. Kasieczka,[58b] R. D. Kass,[109] A. Kastanas,[14] M. Kataoka,[5] Y. Kataoka,[155] E. Katsoufis,[10] J. Katzy,[42] V. Kaushik,[7] K. Kawagoe,[69] T. Kawamoto,[155] G. Kawamura,[81] M. S. Kayl,[105] S. Kazama,[155] V. A. Kazanin,[107] M. Y. Kazarinov,[64] R. Keeler,[169] P. T. Keener,[120] R. Kehoe,[40] M. Keil,[54] G. D. Kekelidze,[64] J. S. Keller,[138] M. Kenyon,[53] O. Kepka,[125] N. Kerschen,[30] B. P. Kerševan,[74] S. Kersten,[175] K. Kessoku,[155] J. Keung,[158] F. Khalil-zada,[11] H. Khandanyan,[146a,146b] A. Khanov,[112] D. Kharchenko,[64] A. Khodinov,[96] A. Khomich,[58a] T. J. Khoo,[28] G. Khoriauli,[21] A. Khoroshilov,[175] V. Khovanskiy,[95] E. Khramov,[64] J. Khubua,[51b] H. Kim,[146a,146b] S. H. Kim,[160] N. Kimura,[171] O. Kind,[16] B. T. King,[73] M. King,[66] R. S. B. King,[118] J. Kirk,[129] A. E. Kiryunin,[99] T. Kishimoto,[66] D. Kisielewska,[38] T. Kitamura,[66] T. Kittelmann,[123] K. Kiuchi,[160] E. Kladiva,[144b] M. Klein,[73] U. Klein,[73] K. Kleinknecht,[81] M. Klemetti,[85] A. Klier,[172] P. Klimek,[146a,146b] A. Klimentov,[25] R. Klingenberg,[43] J. A. Klinger,[82] E. B. Klinkby,[36] T. Klioutchnikova,[30] P. F. Klok,[104] S. Klous,[105] E.-E. Kluge,[58a] T. Kluge,[73] P. Kluit,[105] S. Kluth,[99] N. S. Knecht,[158] E. Kneringer,[61] E. B. F. G. Knoops,[83] A. Knue,[54] B. R. Ko,[45] T. Kobayashi,[155] M. Kobel,[44] M. Kocian,[143] P. Kodys,[126] K. Köneke,[30] A. C. König,[104] S. Koenig,[81] L. Köpke,[81] F. Koetsveld,[104] P. Koevesarki,[21] T. Koffas,[29] E. Koffeman,[105] L. A. Kogan,[118] S. Kohlmann,[175] F. Kohn,[54] Z. Kohout,[127] T. Kohriki,[65] T. Koi,[143] G. M. Kolachev,[107,a] H. Kolanoski,[16] V. Kolesnikov,[64] I. Koletsou,[89a] J. Koll,[88] A. A. Komar,[94] Y. Komori,[155] T. Kondo,[65] T. Kono,[42,s] A. I. Kononov,[48] R. Konoplich,[108,t] N. Konstantinidis,[77] S. Koperny,[38] K. Korcyl,[39] K. Kordas,[154] A. Korn,[118] A. Korol,[107] I. Korolkov,[12] E. V. Korolkova,[139] V. A. Korotkov,[128] O. Kortner,[99] S. Kortner,[99] V. V. Kostyukhin,[21] S. Kotov,[99] V. M. Kotov,[64] A. Kotwal,[45] C. Kourkoumelis,[9] V. Kouskoura,[154] A. Koutsman,[159a] R. Kowalewski,[169] T. Z. Kowalski,[38] W. Kozanecki,[136] A. S. Kozhin,[128] V. Kral,[127] V. A. Kramarenko,[97] G. Kramberger,[74] M. W. Krasny,[78] A. Krasznahorkay,[108] J. K. Kraus,[21] S. Kreiss,[108] F. Krejci,[127] J. Kretzschmar,[73] N. Krieger,[54] P. Krieger,[158] K. Kroeninger,[54] H. Kroha,[99] J. Kroll,[120] J. Kroseberg,[21]

J. Krstic,[13a] U. Kruchonak,[64] H. Krüger,[21] T. Kruker,[17] N. Krumnack,[63] Z. V. Krumshteyn,[64] T. Kubota,[86] S. Kuday,[4a] S. Kuehn,[48] A. Kugel,[58c] T. Kuhl,[42] D. Kuhn,[61] V. Kukhtin,[64] Y. Kulchitsky,[90] S. Kuleshov,[32b] C. Kummer,[98] M. Kuna,[78] J. Kunkle,[120] A. Kupco,[125] H. Kurashige,[66] M. Kurata,[160] Y. A. Kurochkin,[90] V. Kus,[125] E. S. Kuwertz,[147] M. Kuze,[157] J. Kvita,[142] R. Kwee,[16] A. La Rosa,[49] L. La Rotonda,[37a,37b] L. Labarga,[80] J. Labbe,[5] S. Lablak,[135a] C. Lacasta,[167] F. Lacava,[132a,132b] H. Lacker,[16] D. Lacour,[78] V. R. Lacuesta,[167] E. Ladygin,[64] R. Lafaye,[5] B. Laforge,[78] T. Lagouri,[176] S. Lai,[48] E. Laisne,[55] M. Lamanna,[30] L. Lambourne,[77] C. L. Lampen,[7] W. Lampl,[7] E. Lancon,[136] U. Landgraf,[48] M. P. J. Landon,[75] V. S. Lang,[58a] C. Lange,[42] A. J. Lankford,[163] F. Lanni,[25] K. Lantzsch,[175] S. Laplace,[78] C. Lapoire,[21] J. F. Laporte,[136] T. Lari,[89a] A. Larner,[118] M. Lassnig,[30] P. Laurelli,[47] V. Lavorini,[37a,37b] W. Lavrijsen,[15] P. Laycock,[73] O. Le Dortz,[78] E. Le Guirriec,[83] E. Le Menedeu,[12] T. LeCompte,[6] F. Ledroit-Guillon,[55] H. Lee,[105] J. S. H. Lee,[116] S. C. Lee,[151] L. Lee,[176] M. Lefebvre,[169] M. Legendre,[136] F. Legger,[98] C. Leggett,[15] M. Lehmacher,[21] G. Lehmann Miotto,[30] X. Lei,[7] M. A. L. Leite,[24d] R. Leitner,[126] D. Lellouch,[172] B. Lemmer,[54] V. Lendermann,[58a] K. J. C. Leney,[145b] T. Lenz,[105] G. Lenzen,[175] B. Lenzi,[30] K. Leonhardt,[44] S. Leontsinis,[10] F. Lepold,[58a] C. Leroy,[93] J-R. Lessard,[169] C. G. Lester,[28] C. M. Lester,[120] J. Levêque,[5] D. Levin,[87] L. J. Levinson,[172] A. Lewis,[118] G. H. Lewis,[108] A. M. Leyko,[21] M. Leyton,[16] B. Li,[83] H. Li,[173,u] S. Li,[33b,v] X. Li,[87] Z. Liang,[118,w] H. Liao,[34] B. Liberti,[133a] P. Lichard,[30] M. Lichtnecker,[98] K. Lie,[165] W. Liebig,[14] C. Limbach,[21] A. Limosani,[86] M. Limper,[62] S. C. Lin,[151,x] F. Linde,[105] J. T. Linnemann,[88] E. Lipeles,[120] A. Lipniacka,[14] T. M. Liss,[165] D. Lissauer,[25] A. Lister,[49] A. M. Litke,[137] C. Liu,[29] D. Liu,[151] H. Liu,[87] J. B. Liu,[87] L. Liu,[87] M. Liu,[33b] Y. Liu,[33b] M. Livan,[119a,119b] S. S. A. Livermore,[118] A. Lleres,[55] J. Llorente Merino,[80] S. L. Lloyd,[75] E. Lobodzinska,[42] P. Loch,[7] W. S. Lockman,[137] T. Loddenkoetter,[21] F. K. Loebinger,[82] A. Loginov,[176] C. W. Loh,[168] T. Lohse,[16] K. Lohwasser,[48] M. Lokajicek,[125] V. P. Lombardo,[5] R. E. Long,[71] L. Lopes,[124a] D. Lopez Mateos,[57] J. Lorenz,[98] N. Lorenzo Martinez,[115] M. Losada,[162] P. Loscutoff,[15] F. Lo Sterzo,[132a,132b] M. J. Losty,[159a,a] X. Lou,[41] A. Lounis,[115] K. F. Loureiro,[162] J. Love,[6] P. A. Love,[71] A. J. Lowe,[143,f] F. Lu,[33a] H. J. Lubatti,[138] C. Luci,[132a,132b] A. Lucotte,[55] A. Ludwig,[44] D. Ludwig,[42] I. Ludwig,[48] J. Ludwig,[48] F. Luehring,[60] G. Luijckx,[105] W. Lukas,[61] L. Luminari,[132a] E. Lund,[117] B. Lund-Jensen,[147] B. Lundberg,[79] J. Lundberg,[146a,146b] O. Lundberg,[146a,146b] J. Lundquist,[36] M. Lungwitz,[81] D. Lynn,[25] E. Lytken,[79] H. Ma,[25] L. L. Ma,[173] G. Maccarrone,[47] A. Macchiolo,[99] B. Maček,[74] J. Machado Miguens,[124a] R. Mackeprang,[36] R. J. Madaras,[15] H. J. Maddocks,[71] W. F. Mader,[44] R. Maenner,[58c] T. Maeno,[25] P. Mättig,[175] S. Mättig,[81] L. Magnoni,[163] E. Magradze,[54] K. Mahboubi,[48] J. Mahlstedt,[105] S. Mahmoud,[73] G. Mahout,[18] C. Maiani,[136] C. Maidantchik,[24a] A. Maio,[124a,c] S. Majewski,[25] Y. Makida,[65] N. Makovec,[115] P. Mal,[136] B. Malaescu,[30] Pa. Malecki,[39] P. Malecki,[39] V. P. Maleev,[121] F. Malek,[55] U. Mallik,[62] D. Malon,[6] C. Malone,[143] S. Maltezos,[10] V. Malyshev,[107] S. Malyukov,[30] R. Mameghani,[98] J. Mamuzic,[13b] A. Manabe,[65] L. Mandelli,[89a] I. Mandić,[74] R. Mandrysch,[16] J. Maneira,[124a] A. Manfredini,[99] P. S. Mangeard,[88] L. Manhaes de Andrade Filho,[24b] J. A. Manjarres Ramos,[136] A. Mann,[54] P. M. Manning,[137] A. Manousakis-Katsikakis,[9] B. Mansoulie,[136] A. Mapelli,[30] L. Mapelli,[30] L. March,[167] J. F. Marchand,[29] F. Marchese,[133a,133b] G. Marchiori,[78] M. Marcisovsky,[125] C. P. Marino,[169] F. Marroquim,[24a] Z. Marshall,[30] F. K. Martens,[158] L. F. Marti,[17] S. Marti-Garcia,[167] B. Martin,[30] B. Martin,[88] J. P. Martin,[93] T. A. Martin,[18] V. J. Martin,[46] B. Martin dit Latour,[49] S. Martin-Haugh,[149] M. Martinez,[12] V. Martinez Outschoorn,[57] A. C. Martyniuk,[169] M. Marx,[82] F. Marzano,[132a] A. Marzin,[111] L. Masetti,[81] T. Mashimo,[155] R. Mashinistov,[94] J. Masik,[82] A. L. Maslennikov,[107] I. Massa,[20a,20b] G. Massaro,[105] N. Massol,[5] P. Mastrandrea,[148] A. Mastroberardino,[37a,37b] T. Masubuchi,[155] P. Matricon,[115] H. Matsunaga,[155] T. Matsushita,[66] C. Mattravers,[118,d] J. Maurer,[83] S. J. Maxfield,[73] A. Mayne,[139] R. Mazini,[151] M. Mazur,[21] L. Mazzaferro,[133a,133b] M. Mazzanti,[89a] J. Mc Donald,[85] S. P. Mc Kee,[87] A. McCarn,[165] R. L. McCarthy,[148] T. G. McCarthy,[29] N. A. McCubbin,[129] K. W. McFarlane,[56,a] J. A. Mcfayden,[139] G. Mchedlidze,[51b] T. Mclaughlan,[18] S. J. McMahon,[129] R. A. McPherson,[169,l] A. Meade,[84] J. Mechnich,[105] M. Mechtel,[175] M. Medinnis,[42] R. Meera-Lebbai,[111] T. Meguro,[116] R. Mehdiyev,[93] S. Mehlhase,[36] A. Mehta,[73] K. Meier,[58a] B. Meirose,[79] C. Melachrinos,[31] B. R. Mellado Garcia,[173] F. Meloni,[89a,89b] L. Mendoza Navas,[162] Z. Meng,[151,u] A. Mengarelli,[20a,20b] S. Menke,[99] E. Meoni,[161] K. M. Mercurio,[57] P. Mermod,[49] L. Merola,[102a,102b] C. Meroni,[89a] F. S. Merritt,[31] H. Merritt,[109] A. Messina,[30,y] J. Metcalfe,[25] A. S. Mete,[163] C. Meyer,[81] C. Meyer,[31] J-P. Meyer,[136] J. Meyer,[174] J. Meyer,[54] T. C. Meyer,[30] J. Miao,[33d] S. Michal,[30] L. Micu,[26a] R. P. Middleton,[129] S. Migas,[73] L. Mijović,[136] G. Mikenberg,[172] M. Mikestikova,[125] M. Mikuž,[74] D. W. Miller,[31] R. J. Miller,[88] W. J. Mills,[168] C. Mills,[57] A. Milov,[172] D. A. Milstead,[146a,146b] D. Milstein,[172] A. A. Minaenko,[128] M. Miñano Moya,[167] I. A. Minashvili,[64] A. I. Mincer,[108] B. Mindur,[38] M. Mineev,[64] Y. Ming,[173] L. M. Mir,[12] G. Mirabelli,[132a] J. Mitrevski,[137] V. A. Mitsou,[167] S. Mitsui,[65]

P. S. Miyagawa,[139] J. U. Mjörnmark,[79] T. Moa,[146a,146b] V. Moeller,[28] K. Mönig,[42] N. Möser,[21] S. Mohapatra,[148] W. Mohr,[48] R. Moles-Valls,[167] A. Molfetas,[30] J. Monk,[77] E. Monnier,[83] J. Montejo Berlingen,[12] F. Monticelli,[70] S. Monzani,[20a,20b] R. W. Moore,[3] G. F. Moorhead,[86] C. Mora Herrera,[49] A. Moraes,[53] N. Morange,[136] J. Morel,[54] G. Morello,[37a,37b] D. Moreno,[81] M. Moreno Llácer,[167] P. Morettini,[50a] M. Morgenstern,[44] M. Morii,[57] A. K. Morley,[30] G. Mornacchi,[30] J. D. Morris,[75] L. Morvaj,[101] H. G. Moser,[99] M. Mosidze,[51b] J. Moss,[109] R. Mount,[143] E. Mountricha,[10,z] S. V. Mouraviev,[94,a] E. J. W. Moyse,[84] F. Mueller,[58a] J. Mueller,[123] K. Mueller,[21] T. A. Müller,[98] T. Mueller,[81] D. Muenstermann,[30] Y. Munwes,[153] W. J. Murray,[129] I. Mussche,[105] E. Musto,[102a,102b] A. G. Myagkov,[128] M. Myska,[125] J. Nadal,[12] K. Nagai,[160] R. Nagai,[157] K. Nagano,[65] A. Nagarkar,[109] Y. Nagasaka,[59] M. Nagel,[99] A. M. Nairz,[30] Y. Nakahama,[30] K. Nakamura,[155] T. Nakamura,[155] I. Nakano,[110] G. Nanava,[21] A. Napier,[161] R. Narayan,[58b] M. Nash,[77,d] T. Nattermann,[21] T. Naumann,[42] G. Navarro,[162] H. A. Neal,[87] P. Yu. Nechaeva,[94] T. J. Neep,[82] A. Negri,[119a,119b] G. Negri,[30] M. Negrini,[20a] S. Nektarijevic,[49] A. Nelson,[163] T. K. Nelson,[143] S. Nemecek,[125] P. Nemethy,[108] A. A. Nepomuceno,[24a] M. Nessi,[30,aa] M. S. Neubauer,[165] M. Neumann,[175] A. Neusiedl,[81] R. M. Neves,[108] P. Nevski,[25] F. M. Newcomer,[120] P. R. Newman,[18] V. Nguyen Thi Hong,[136] R. B. Nickerson,[118] R. Nicolaidou,[136] B. Nicquevert,[30] F. Niedercorn,[115] J. Nielsen,[137] N. Nikiforou,[35] A. Nikiforov,[16] V. Nikolaenko,[128] I. Nikolic-Audit,[78] K. Nikolics,[49] K. Nikolopoulos,[18] H. Nilsen,[48] P. Nilsson,[8] Y. Ninomiya,[155] A. Nisati,[132a] R. Nisius,[99] T. Nobe,[157] L. Nodulman,[6] M. Nomachi,[116] I. Nomidis,[154] S. Norberg,[111] M. Nordberg,[30] P. R. Norton,[129] J. Novakova,[126] M. Nozaki,[65] L. Nozka,[113] I. M. Nugent,[159a] A.-E. Nuncio-Quiroz,[21] G. Nunes Hanninger,[86] T. Nunnemann,[98] E. Nurse,[77] B. J. O'Brien,[46] D. C. O'Neil,[142] V. O'Shea,[53] L. B. Oakes,[98] F. G. Oakham,[29,e] H. Oberlack,[99] J. Ocariz,[78] A. Ochi,[66] S. Oda,[69] S. Odaka,[65] J. Odier,[83] H. Ogren,[60] A. Oh,[82] S. H. Oh,[45] C. C. Ohm,[30] T. Ohshima,[101] H. Okawa,[25] Y. Okumura,[31] T. Okuyama,[155] A. Olariu,[26a] A. G. Olchevski,[64] S. A. Olivares Pino,[32a] M. Oliveira,[124a,i] D. Oliveira Damazio,[25] E. Oliver Garcia,[167] D. Olivito,[120] A. Olszewski,[39] J. Olszowska,[39] A. Onofre,[124a,bb] P. U. E. Onyisi,[31] C. J. Oram,[159a] M. J. Oreglia,[31] Y. Oren,[153] D. Orestano,[134a,134b] N. Orlando,[72a,72b] I. Orlov,[107] C. Oropeza Barrera,[53] R. S. Orr,[158] B. Osculati,[50a,50b] R. Ospanov,[120] C. Osuna,[12] G. Otero y Garzon,[27] J. P. Ottersbach,[105] M. Ouchrif,[135d] E. A. Ouellette,[169] F. Ould-Saada,[117] A. Ouraou,[136] Q. Ouyang,[33a] A. Ovcharova,[15] M. Owen,[82] S. Owen,[139] V. E. Ozcan,[19a] N. Ozturk,[8] A. Pacheco Pages,[12] C. Padilla Aranda,[12] S. Pagan Griso,[15] E. Paganis,[139] C. Pahl,[99] F. Paige,[25] P. Pais,[84] K. Pajchel,[117] G. Palacino,[159b] C. P. Paleari,[7] S. Palestini,[30] D. Pallin,[34] A. Palma,[124a] J. D. Palmer,[18] Y. B. Pan,[173] E. Panagiotopoulou,[10] P. Pani,[105] N. Panikashvili,[87] S. Panitkin,[25] D. Pantea,[26a] A. Papadelis,[146a] Th. D. Papadopoulou,[10] A. Paramonov,[6] D. Paredes Hernandez,[34] W. Park,[25,cc] M. A. Parker,[28] F. Parodi,[50a,50b] J. A. Parsons,[35] U. Parzefall,[48] S. Pashapour,[54] E. Pasqualucci,[132a] S. Passaggio,[50a] A. Passeri,[134a] F. Pastore,[134a,134b,a] Fr. Pastore,[76] G. Pásztor,[49,dd] S. Pataraia,[175] N. Patel,[150] J. R. Pater,[82] S. Patricelli,[102a,102b] T. Pauly,[30] M. Pecsy,[144a] S. Pedraza Lopez,[167] M. I. Pedraza Morales,[173] S. V. Peleganchuk,[107] D. Pelikan,[166] H. Peng,[33b] B. Penning,[31] A. Penson,[35] J. Penwell,[60] M. Perantoni,[24a] K. Perez,[35,ee] T. Perez Cavalcanti,[42] E. Perez Codina,[159a] M. T. Pérez García-Estañ,[167] V. Perez Reale,[35] L. Perini,[89a,89b] H. Pernegger,[30] R. Perrino,[72a] P. Perrodo,[5] V. D. Peshekhonov,[64] K. Peters,[30] B. A. Petersen,[30] J. Petersen,[30] T. C. Petersen,[36] E. Petit,[5] A. Petridis,[154] C. Petridou,[154] E. Petrolo,[132a] F. Petrucci,[134a,134b] D. Petschull,[42] M. Petteni,[142] R. Pezoa,[32b] A. Phan,[86] P. W. Phillips,[129] G. Piacquadio,[30] A. Picazio,[49] E. Piccaro,[75] M. Piccinini,[20a,20b] S. M. Piec,[42] R. Piegaia,[27] D. T. Pignotti,[109] J. E. Pilcher,[31] A. D. Pilkington,[82] J. Pina,[124a,c] M. Pinamonti,[164a,164c] A. Pinder,[118] J. L. Pinfold,[3] B. Pinto,[124a] C. Pizio,[89a,89b] M. Plamondon,[169] M.-A. Pleier,[25] E. Plotnikova,[64] A. Poblaguev,[25] S. Poddar,[58a] F. Podlyski,[34] L. Poggioli,[115] D. Pohl,[21] M. Pohl,[49] G. Polesello,[119a] A. Policicchio,[37a,37b] A. Polini,[20a] J. Poll,[75] V. Polychronakos,[25] D. Pomeroy,[23] K. Pommès,[30] L. Pontecorvo,[132a] B. G. Pope,[88] G. A. Popeneciu,[26a] D. S. Popovic,[13a] A. Poppleton,[30] X. Portell Bueso,[30] G. E. Pospelov,[99] S. Pospisil,[127] I. N. Potrap,[99] C. J. Potter,[149] C. T. Potter,[114] G. Poulard,[30] J. Poveda,[60] V. Pozdnyakov,[64] R. Prabhu,[77] P. Pralavorio,[83] A. Pranko,[15] S. Prasad,[30] R. Pravahan,[25] S. Prell,[63] K. Pretzl,[17] D. Price,[60] J. Price,[73] L. E. Price,[6] D. Prieur,[123] M. Primavera,[72a] K. Prokofiev,[108] F. Prokoshin,[32b] S. Protopopescu,[25] J. Proudfoot,[6] X. Prudent,[44] M. Przybycien,[38] H. Przysiezniak,[5] S. Psoroulas,[21] E. Ptacek,[114] E. Pueschel,[84] J. Purdham,[87] M. Purohit,[25,cc] P. Puzo,[115] Y. Pylypchenko,[62] J. Qian,[87] A. Quadt,[54] D. R. Quarrie,[15] W. B. Quayle,[173] F. Quinonez,[32a] M. Raas,[104] V. Radeka,[25] V. Radescu,[42] P. Radloff,[114] T. Rador,[19a] F. Ragusa,[89a,89b] G. Rahal,[178] A. M. Rahimi,[109] D. Rahm,[25] S. Rajagopalan,[25] M. Rammensee,[48] M. Rammes,[141] A. S. Randle-Conde,[40] K. Randrianarivony,[29] F. Rauscher,[98] T. C. Rave,[48] M. Raymond,[30] A. L. Read,[117] D. M. Rebuzzi,[119a,119b] A. Redelbach,[174] G. Redlinger,[25] R. Reece,[120] K. Reeves,[41] E. Reinherz-Aronis,[153] A. Reinsch,[114] I. Reisinger,[43] C. Rembser,[30] Z. L. Ren,[151] A. Renaud,[115] M. Rescigno,[132a]

S. Resconi,[89a] B. Resende,[136] P. Reznicek,[98] R. Rezvani,[158] R. Richter,[99] E. Richter-Was,[5,ff] M. Ridel,[78] M. Rijpstra,[105] M. Rijssenbeek,[148] A. Rimoldi,[119a,119b] L. Rinaldi,[20a] R. R. Rios,[40] I. Riu,[12] G. Rivoltella,[89a,89b] F. Rizatdinova,[112] E. Rizvi,[75] S. H. Robertson,[85,l] A. Robichaud-Veronneau,[118] D. Robinson,[28] J. E. M. Robinson,[82] A. Robson,[53] J. G. Rocha de Lima,[106] C. Roda,[122a,122b] D. Roda Dos Santos,[30] A. Roe,[54] S. Roe,[30] O. Røhne,[117] S. Rolli,[161] A. Romaniouk,[96] M. Romano,[20a,20b] G. Romeo,[27] E. Romero Adam,[167] N. Rompotis,[138] L. Roos,[78] E. Ros,[167] S. Rosati,[132a] K. Rosbach,[49] A. Rose,[149] M. Rose,[76] G. A. Rosenbaum,[158] E. I. Rosenberg,[63] P. L. Rosendahl,[14] O. Rosenthal,[141] L. Rosselet,[49] V. Rossetti,[12] E. Rossi,[132a,132b] L. P. Rossi,[50a] M. Rotaru,[26a] I. Roth,[172] J. Rothberg,[138] D. Rousseau,[115] C. R. Royon,[136] A. Rozanov,[83] Y. Rozen,[152] X. Ruan,[33a,gg] F. Rubbo,[12] I. Rubinskiy,[42] N. Ruckstuhl,[105] V. I. Rud,[97] C. Rudolph,[44] G. Rudolph,[61] F. Rühr,[7] A. Ruiz-Martinez,[63] L. Rumyantsev,[64] Z. Rurikova,[48] N. A. Rusakovich,[64] J. P. Rutherfoord,[7] P. Ruzicka,[125] Y. F. Ryabov,[121] M. Rybar,[126] G. Rybkin,[115] N. C. Ryder,[118] A. F. Saavedra,[150] I. Sadeh,[153] H. F-W. Sadrozinski,[137] R. Sadykov,[64] F. Safai Tehrani,[132a] H. Sakamoto,[155] G. Salamanna,[75] A. Salamon,[133a] M. Saleem,[111] D. Salek,[30] D. Salihagic,[99] A. Salnikov,[143] J. Salt,[167] B. M. Salvachua Ferrando,[6] D. Salvatore,[37a,37b] F. Salvatore,[149] A. Salvucci,[104] A. Salzburger,[30] D. Sampsonidis,[154] B. H. Samset,[117] A. Sanchez,[102a,102b] V. Sanchez Martinez,[167] H. Sandaker,[14] H. G. Sander,[81] M. P. Sanders,[98] M. Sandhoff,[175] T. Sandoval,[28] C. Sandoval,[162] R. Sandstroem,[99] D. P. C. Sankey,[129] A. Sansoni,[47] C. Santamarina Rios,[85] C. Santoni,[34] R. Santonico,[133a,133b] H. Santos,[124a] J. G. Saraiva,[124a] T. Sarangi,[173] E. Sarkisyan-Grinbaum,[8] F. Sarri,[122a,122b] G. Sartisohn,[175] O. Sasaki,[65] Y. Sasaki,[155] N. Sasao,[67] I. Satsounkevitch,[90] G. Sauvage,[5,a] E. Sauvan,[5] J. B. Sauvan,[115] P. Savard,[158,e] V. Savinov,[123] D. O. Savu,[30] L. Sawyer,[25,n] D. H. Saxon,[53] J. Saxon,[120] C. Sbarra,[20a] A. Sbrizzi,[20a,20b] D. A. Scannicchio,[163] M. Scarcella,[150] J. Schaarschmidt,[115] P. Schacht,[99] D. Schaefer,[120] U. Schäfer,[81] S. Schaepe,[21] S. Schaetzel,[58b] A. C. Schaffer,[115] D. Schaile,[98] R. D. Schamberger,[148] A. G. Schamov,[107] V. Scharf,[58a] V. A. Schegelsky,[121] D. Scheirich,[87] M. Schernau,[163] M. I. Scherzer,[35] C. Schiavi,[50a,50b] J. Schieck,[98] M. Schioppa,[37a,37b] S. Schlenker,[30] E. Schmidt,[48] K. Schmieden,[21] C. Schmitt,[81] S. Schmitt,[58b] M. Schmitz,[21] B. Schneider,[17] U. Schnoor,[44] A. Schoening,[58b] A. L. S. Schorlemmer,[54] M. Schott,[30] D. Schouten,[159a] J. Schovancova,[125] M. Schram,[85] C. Schroeder,[81] N. Schroer,[58c] M. J. Schultens,[21] J. Schultes,[175] H.-C. Schultz-Coulon,[58a] H. Schulz,[16] M. Schumacher,[48] B. A. Schumm,[137] Ph. Schune,[136] C. Schwanenberger,[82] A. Schwartzman,[143] Ph. Schwegler,[99] Ph. Schwemling,[78] R. Schwienhorst,[88] R. Schwierz,[44] J. Schwindling,[136] T. Schwindt,[21] M. Schwoerer,[5] G. Sciolla,[23] W. G. Scott,[129] J. Searcy,[114] G. Sedov,[42] E. Sedykh,[121] S. C. Seidel,[103] A. Seiden,[137] F. Seifert,[44] J. M. Seixas,[24a] G. Sekhniaidze,[102a] S. J. Sekula,[40] K. E. Selbach,[46] D. M. Seliverstov,[121] B. Sellden,[146a] G. Sellers,[73] M. Seman,[144b] N. Semprini-Cesari,[20a,20b] C. Serfon,[98] L. Serin,[115] L. Serkin,[54] R. Seuster,[99] H. Severini,[111] A. Sfyrla,[30] E. Shabalina,[54] M. Shamim,[114] L. Y. Shan,[33a] J. T. Shank,[22] Q. T. Shao,[86] M. Shapiro,[15] P. B. Shatalov,[95] K. Shaw,[164a,164c] D. Sherman,[176] P. Sherwood,[77] S. Shimizu,[101] M. Shimojima,[100] T. Shin,[56] M. Shiyakova,[64] A. Shmeleva,[94] M. J. Shochet,[31] D. Short,[118] S. Shrestha,[63] E. Shulga,[96] M. A. Shupe,[7] P. Sicho,[125] A. Sidoti,[132a] F. Siegert,[48] Dj. Sijacki,[13a] O. Silbert,[172] J. Silva,[124a] Y. Silver,[153] D. Silverstein,[143] S. B. Silverstein,[146a] V. Simak,[127] O. Simard,[136] Lj. Simic,[13a] S. Simion,[115] E. Simioni,[81] B. Simmons,[77] R. Simoniello,[89a,89b] M. Simonyan,[36] P. Sinervo,[158] N. B. Sinev,[114] V. Sipica,[141] G. Siragusa,[174] A. Sircar,[25] A. N. Sisakyan,[64,a] S. Yu. Sivoklokov,[97] J. Sjölin,[146a,146b] T. B. Sjursen,[14] L. A. Skinnari,[15] H. P. Skottowe,[57] K. Skovpen,[107] P. Skubic,[111] M. Slater,[18] T. Slavicek,[127] K. Sliwa,[161] V. Smakhtin,[172] B. H. Smart,[46] L. Smestad,[117] S. Yu. Smirnov,[96] Y. Smirnov,[96] L. N. Smirnova,[97] O. Smirnova,[79] B. C. Smith,[57] D. Smith,[143] K. M. Smith,[53] M. Smizanska,[71] K. Smolek,[127] A. A. Snesarev,[94] S. W. Snow,[82] J. Snow,[111] S. Snyder,[25] R. Sobie,[169,l] J. Sodomka,[127] A. Soffer,[153] C. A. Solans,[167] M. Solar,[127] J. Solc,[127] E. Yu. Soldatov,[96] U. Soldevila,[167] E. Solfaroli Camillocci,[132a,132b] A. A. Solodkov,[128] O. V. Solovyanov,[128] V. Solovyev,[121] N. Soni,[1] V. Sopko,[127] B. Sopko,[127] M. Sosebee,[8] R. Soualah,[164a,164c] A. Soukharev,[107] S. Spagnolo,[72a,72b] F. Spanò,[76] R. Spighi,[20a] G. Spigo,[30] R. Spiwoks,[30] M. Spousta,[126,hh] T. Spreitzer,[158] B. Spurlock,[8] R. D. St. Denis,[53] J. Stahlman,[120] R. Stamen,[58a] E. Stanecka,[39] R. W. Stanek,[6] C. Stanescu,[134a] M. Stanescu-Bellu,[42] M. M. Stanitzki,[42] S. Stapnes,[117] E. A. Starchenko,[128] J. Stark,[55] P. Staroba,[125] P. Starovoitov,[42] R. Staszewski,[39] A. Staude,[98] P. Stavina,[144a,a] G. Steele,[53] P. Steinbach,[44] P. Steinberg,[25] I. Stekl,[127] B. Stelzer,[142] H. J. Stelzer,[88] O. Stelzer-Chilton,[159a] H. Stenzel,[52] S. Stern,[99] G. A. Stewart,[30] J. A. Stillings,[21] M. C. Stockton,[85] K. Stoerig,[48] G. Stoicea,[26a] S. Stonjek,[99] P. Strachota,[126] A. R. Stradling,[8] A. Straessner,[44] J. Strandberg,[147] S. Strandberg,[146a,146b] A. Strandlie,[117] M. Strang,[109] E. Strauss,[143] M. Strauss,[111] P. Strizenec,[144b] R. Ströhmer,[174] D. M. Strom,[114] J. A. Strong,[76,a] R. Stroynowski,[40] B. Stugu,[14] I. Stumer,[25,a] J. Stupak,[148] P. Sturm,[175] N. A. Styles,[42] D. A. Soh,[151,w] D. Su,[143] HS. Subramania,[3] A. Succurro,[12] Y. Sugaya,[116] C. Suhr,[106]

M. Suk,[126] V. V. Sulin,[94] S. Sultansoy,[4d] T. Sumida,[67] X. Sun,[55] J. E. Sundermann,[48] K. Suruliz,[139] G. Susinno,[37a,37b] M. R. Sutton,[149] Y. Suzuki,[65] Y. Suzuki,[66] M. Svatos,[125] S. Swedish,[168] I. Sykora,[144a] T. Sykora,[126] J. Sánchez,[167] D. Ta,[105] K. Tackmann,[42] A. Taffard,[163] R. Tafirout,[159a] N. Taiblum,[153] Y. Takahashi,[101] H. Takai,[25] R. Takashima,[68] H. Takeda,[66] T. Takeshita,[140] Y. Takubo,[65] M. Talby,[83] A. Talyshev,[107,g] M. C. Tamsett,[25] J. Tanaka,[155] R. Tanaka,[115] S. Tanaka,[131] S. Tanaka,[65] A. J. Tanasijczuk,[142] K. Tani,[66] N. Tannoury,[83] S. Tapprogge,[81] D. Tardif,[158] S. Tarem,[152] F. Tarrade,[29] G. F. Tartarelli,[89a] P. Tas,[126] M. Tasevsky,[125] E. Tassi,[37a,37b] M. Tatarkhanov,[15] Y. Tayalati,[135d] C. Taylor,[77] F. E. Taylor,[92] G. N. Taylor,[86] W. Taylor,[159b] M. Teinturier,[115] F. A. Teischinger,[30] M. Teixeira Dias Castanheira,[75] P. Teixeira-Dias,[76] K. K. Temming,[48] H. Ten Kate,[30] P. K. Teng,[151] S. Terada,[65] K. Terashi,[155] J. Terron,[80] M. Testa,[47] R. J. Teuscher,[158,l] J. Therhaag,[21] T. Theveneaux-Pelzer,[78] S. Thoma,[48] J. P. Thomas,[18] E. N. Thompson,[35] P. D. Thompson,[18] P. D. Thompson,[158] A. S. Thompson,[53] L. A. Thomsen,[36] E. Thomson,[120] M. Thomson,[28] W. M. Thong,[86] R. P. Thun,[87] F. Tian,[35] M. J. Tibbetts,[15] T. Tic,[125] V. O. Tikhomirov,[94] Y. A. Tikhonov,[107,g] S. Timoshenko,[96] P. Tipton,[176] S. Tisserant,[83] T. Todorov,[5] S. Todorova-Nova,[161] B. Toggerson,[163] J. Tojo,[69] S. Tokár,[144a] K. Tokushuku,[65] K. Tollefson,[88] M. Tomoto,[101] L. Tompkins,[31] K. Toms,[103] A. Tonoyan,[14] C. Topfel,[17] N. D. Topilin,[64] I. Torchiani,[30] E. Torrence,[114] H. Torres,[78] E. Torró Pastor,[167] J. Toth,[83,dd] F. Touchard,[83] D. R. Tovey,[139] T. Trefzger,[174] L. Tremblet,[30] A. Tricoli,[30] I. M. Trigger,[159a] S. Trincaz-Duvoid,[78] M. F. Tripiana,[70] N. Triplett,[25] W. Trischuk,[158] B. Trocmé,[55] C. Troncon,[89a] M. Trottier-McDonald,[142] M. Trzebinski,[39] A. Trzupek,[39] C. Tsarouchas,[30] J. C-L. Tseng,[118] M. Tsiakiris,[105] P. V. Tsiareshka,[90] D. Tsionou,[5,ii] G. Tsipolitis,[10] S. Tsiskaridze,[12] V. Tsiskaridze,[48] E. G. Tskhadadze,[51a] I. I. Tsukerman,[95] V. Tsulaia,[15] J.-W. Tsung,[21] S. Tsuno,[65] D. Tsybychev,[148] A. Tua,[139] A. Tudorache,[26a] V. Tudorache,[26a] J. M. Tuggle,[31] M. Turala,[39] D. Turecek,[127] I. Turk Cakir,[4e] E. Turlay,[105] R. Turra,[89a,89b] P. M. Tuts,[35] A. Tykhonov,[74] M. Tylmad,[146a,146b] M. Tyndel,[129] G. Tzanakos,[9] K. Uchida,[21] I. Ueda,[155] R. Ueno,[29] M. Ugland,[14] M. Uhlenbrock,[21] M. Uhrmacher,[54] F. Ukegawa,[160] G. Unal,[30] A. Undrus,[25] G. Unel,[163] Y. Unno,[65] D. Urbaniec,[35] P. Urquijo,[21] G. Usai,[8] M. Uslenghi,[119a,119b] L. Vacavant,[83] V. Vacek,[127] B. Vachon,[85] S. Vahsen,[15] J. Valenta,[125] S. Valentinetti,[20a,20b] A. Valero,[167] S. Valkar,[126] E. Valladolid Gallego,[167] S. Vallecorsa,[152] J. A. Valls Ferrer,[167] R. Van Berg,[120] P. C. Van Der Deijl,[105] R. van der Geer,[105] H. van der Graaf,[105] R. Van Der Leeuw,[105] E. van der Poel,[105] D. van der Ster,[30] N. van Eldik,[30] P. van Gemmeren,[6] I. van Vulpen,[105] M. Vanadia,[99] W. Vandelli,[30] A. Vaniachine,[6] P. Vankov,[42] F. Vannucci,[78] R. Vari,[132a] T. Varol,[84] D. Varouchas,[15] A. Vartapetian,[8] K. E. Varvell,[150] V. I. Vassilakopoulos,[56] F. Vazeille,[34] T. Vazquez Schroeder,[54] G. Vegni,[89a,89b] J. J. Veillet,[115] F. Veloso,[124a] R. Veness,[30] S. Veneziano,[132a] A. Ventura,[72a,72b] D. Ventura,[84] M. Venturi,[48] N. Venturi,[158] V. Vercesi,[119a] M. Verducci,[138] W. Verkerke,[105] J. C. Vermeulen,[105] A. Vest,[44] M. C. Vetterli,[142,e] I. Vichou,[165] T. Vickey,[145b,jj] O. E. Vickey Boeriu,[145b] G. H. A. Viehhauser,[118] S. Viel,[168] M. Villa,[20a,20b] M. Villaplana Perez,[167] E. Vilucchi,[47] M. G. Vincter,[29] E. Vinek,[30] V. B. Vinogradov,[64] M. Virchaux,[136,a] J. Virzi,[15] O. Vitells,[172] M. Viti,[42] I. Vivarelli,[48] F. Vives Vaque,[3] S. Vlachos,[10] D. Vladoiu,[98] M. Vlasak,[127] A. Vogel,[21] P. Vokac,[127] G. Volpi,[47] M. Volpi,[86] G. Volpini,[89a] H. von der Schmitt,[99] H. von Radziewski,[48] E. von Toerne,[21] V. Vorobel,[126] V. Vorwerk,[12] M. Vos,[167] R. Voss,[30] T. T. Voss,[175] J. H. Vossebeld,[73] N. Vranjes,[136] M. Vranjes Milosavljevic,[105] V. Vrba,[125] M. Vreeswijk,[105] T. Vu Anh,[48] R. Vuillermet,[30] I. Vukotic,[31] W. Wagner,[175] P. Wagner,[120] H. Wahlen,[175] S. Wahrmund,[44] J. Wakabayashi,[101] S. Walch,[87] J. Walder,[71] R. Walker,[98] W. Walkowiak,[141] R. Wall,[176] P. Waller,[73] B. Walsh,[176] C. Wang,[45] H. Wang,[173] H. Wang,[33b,kk] J. Wang,[151] J. Wang,[55] R. Wang,[103] S. M. Wang,[151] T. Wang,[21] A. Warburton,[85] C. P. Ward,[28] M. Warsinsky,[48] A. Washbrook,[46] C. Wasicki,[42] I. Watanabe,[66] P. M. Watkins,[18] A. T. Watson,[18] I. J. Watson,[150] M. F. Watson,[18] G. Watts,[138] S. Watts,[82] A. T. Waugh,[150] B. M. Waugh,[77] M. S. Weber,[17] P. Weber,[54] A. R. Weidberg,[118] P. Weigell,[99] J. Weingarten,[54] C. Weiser,[48] P. S. Wells,[30] T. Wenaus,[25] D. Wendland,[16] Z. Weng,[151,w] T. Wengler,[30] S. Wenig,[30] N. Wermes,[21] M. Werner,[48] P. Werner,[30] M. Werth,[163] M. Wessels,[58a] J. Wetter,[161] C. Weydert,[55] K. Whalen,[29] S. J. Wheeler-Ellis,[163] A. White,[8] M. J. White,[86] S. White,[122a,122b] S. R. Whitehead,[118] D. Whiteson,[163] D. Whittington,[60] F. Wicek,[115] D. Wicke,[175] F. J. Wickens,[129] W. Wiedenmann,[173] M. Wielers,[129] P. Wienemann,[21] C. Wiglesworth,[75] L. A. M. Wiik-Fuchs,[48] P. A. Wijeratne,[77] A. Wildauer,[99] M. A. Wildt,[42,s] I. Wilhelm,[126] H. G. Wilkens,[30] J. Z. Will,[98] E. Williams,[35] H. H. Williams,[120] W. Willis,[35] S. Willocq,[84] J. A. Wilson,[18] M. G. Wilson,[143] A. Wilson,[87] I. Wingerter-Seez,[5] S. Winkelmann,[48] F. Winklmeier,[30] M. Wittgen,[143] S. J. Wollstadt,[81] M. W. Wolter,[39] H. Wolters,[124a,i] W. C. Wong,[41] G. Wooden,[87] B. K. Wosiek,[39] J. Wotschack,[30] M. J. Woudstra,[82] K. W. Wozniak,[39] K. Wraight,[53] M. Wright,[53] B. Wrona,[73] S. L. Wu,[173] X. Wu,[49] Y. Wu,[33b,ll] E. Wulf,[35] B. M. Wynne,[46] S. Xella,[36] M. Xiao,[136] S. Xie,[48] C. Xu,[33b,z] D. Xu,[139] B. Yabsley,[150] S. Yacoob,[145a,mm]

M. Yamada,[65] H. Yamaguchi,[155] A. Yamamoto,[65] K. Yamamoto,[63] S. Yamamoto,[155] T. Yamamura,[155] T. Yamanaka,[155] T. Yamazaki,[155] Y. Yamazaki,[66] Z. Yan,[22] H. Yang,[87] U. K. Yang,[82] Y. Yang,[109] Z. Yang,[146a,146b] S. Yanush,[91] L. Yao,[33a] Y. Yao,[15] Y. Yasu,[65] G. V. Ybeles Smit,[130] J. Ye,[40] S. Ye,[25] M. Yilmaz,[4c] R. Yoosoofmiya,[123] K. Yorita,[171] R. Yoshida,[6] C. Young,[143] C. J. Young,[118] S. Youssef,[22] D. Yu,[25] J. Yu,[8] J. Yu,[112] L. Yuan,[66] A. Yurkewicz,[106] M. Byszewski,[30] B. Zabinski,[39] R. Zaidan,[62] A. M. Zaitsev,[128] Z. Zajacova,[30] L. Zanello,[132a,132b] D. Zanzi,[99] A. Zaytsev,[25] C. Zeitnitz,[175] M. Zeman,[125] A. Zemla,[39] C. Zendler,[21] O. Zenin,[128] T. Ženiš,[144a] Z. Zinonos,[122a,122b] S. Zenz,[15] D. Zerwas,[115] G. Zevi della Porta,[57] Z. Zhan,[33d] D. Zhang,[33b,kk] H. Zhang,[88] J. Zhang,[6] X. Zhang,[33d] Z. Zhang,[115] L. Zhao,[108] T. Zhao,[138] Z. Zhao,[33b] A. Zhemchugov,[64] J. Zhong,[118] B. Zhou,[87] N. Zhou,[163] Y. Zhou,[151] C. G. Zhu,[33d] H. Zhu,[42] J. Zhu,[87] Y. Zhu,[33b] X. Zhuang,[98] V. Zhuravlov,[99] D. Zieminska,[60] N. I. Zimin,[64] R. Zimmermann,[21] S. Zimmermann,[21] S. Zimmermann,[48] M. Ziolkowski,[141] R. Zitoun,[5] L. Živković,[35] V. V. Zmouchko,[128,a] G. Zobernig,[173] A. Zoccoli,[20a,20b] M. zur Nedden,[16] V. Zutshi,[106] and L. Zwalinski[30]

(ATLAS Collaboration)

[1]*School of Chemistry and Physics, University of Adelaide, Adelaide, Australia*
[2]*Physics Department, SUNY Albany, Albany, New York, USA*
[3]*Department of Physics, University of Alberta, Edmonton, Alberta, Canada*
[4a]*Department of Physics, Ankara University, Ankara, Turkey*
[4b]*Department of Physics, Dumlupinar University, Kutahya, Turkey*
[4c]*Department of Physics, Gazi University, Ankara, Turkey*
[4d]*Division of Physics, TOBB University of Economics and Technology, Ankara, Turkey*
[4e]*Turkish Atomic Energy Authority, Ankara, Turkey*
[5]*LAPP, CNRS/IN2P3 and Université de Savoie, Annecy-le-Vieux, France*
[6]*High Energy Physics Division, Argonne National Laboratory, Argonne, Illinois, USA*
[7]*Department of Physics, University of Arizona, Tucson, Arizona, USA*
[8]*Department of Physics, The University of Texas at Arlington, Arlington, Texas, USA*
[9]*Physics Department, University of Athens, Athens, Greece*
[10]*Physics Department, National Technical University of Athens, Zografou, Greece*
[11]*Institute of Physics, Azerbaijan Academy of Sciences, Baku, Azerbaijan*
[12]*Institut de Física d'Altes Energies and Departament de Física de la Universitat Autònoma de Barcelona and ICREA, Barcelona, Spain*
[13a]*Institute of Physics, University of Belgrade, Belgrade, Serbia*
[13b]*Vinca Institute of Nuclear Sciences, University of Belgrade, Belgrade, Serbia*
[14]*Department for Physics and Technology, University of Bergen, Bergen, Norway*
[15]*Physics Division, Lawrence Berkeley National Laboratory and University of California, Berkeley, California, USA*
[16]*Department of Physics, Humboldt University, Berlin, Germany*
[17]*Albert Einstein Center for Fundamental Physics and Laboratory for High Energy Physics, University of Bern, Bern, Switzerland*
[18]*School of Physics and Astronomy, University of Birmingham, Birmingham, United Kingdom*
[19a]*Department of Physics, Bogazici University, Istanbul, Turkey*
[19b]*Division of Physics, Dogus University, Istanbul, Turkey*
[19c]*Department of Physics Engineering, Gaziantep University, Gaziantep, Turkey*
[19d]*Department of Physics, Istanbul Technical University, Istanbul, Turkey*
[20a]*INFN Sezione di Bologna, Italy*
[20b]*Dipartimento di Fisica, Università di Bologna, Bologna, Italy*
[21]*Physikalisches Institut, University of Bonn, Bonn, Germany*
[22]*Department of Physics, Boston University, Boston, Massachusetts, USA*
[23]*Department of Physics, Brandeis University, Waltham, Massachusetts, USA*
[24a]*Universidade Federal do Rio De Janeiro COPPE/EE/IF, Rio de Janeiro, Brazil*
[24b]*Federal University of Juiz de Fora (UFJF), Juiz de Fora, Brazil*
[24c]*Federal University of Sao Joao del Rei (UFSJ), Sao Joao del Rei, Brazil*
[24d]*Instituto de Fisica, Universidade de Sao Paulo, Sao Paulo, Brazil*
[25]*Physics Department, Brookhaven National Laboratory, Upton, New York, USA*
[26a]*National Institute of Physics and Nuclear Engineering, Bucharest, Romania*
[26b]*University Politehnica Bucharest, Bucharest, Romania*
[26c]*West University in Timisoara, Timisoara, Romania*
[27]*Departamento de Física, Universidad de Buenos Aires, Buenos Aires, Argentina*
[28]*Cavendish Laboratory, University of Cambridge, Cambridge, United Kingdom*

[29]*Department of Physics, Carleton University, Ottawa, Ontario, Canada*
[30]*CERN, Geneva, Switzerland*
[31]*Enrico Fermi Institute, University of Chicago, Chicago, Illinois, USA*
[32a]*Departamento de Física, Pontificia Universidad Católica de Chile, Santiago, Chile*
[32b]*Departamento de Física, Universidad Técnica Federico Santa María, Valparaíso, Chile*
[33a]*Institute of High Energy Physics, Chinese Academy of Sciences, Beijing, China*
[33b]*Department of Modern Physics, University of Science and Technology of China, Anhui, China*
[33c]*Department of Physics, Nanjing University, Jiangsu, China*
[33d]*School of Physics, Shandong University, Shandong, China*
[34]*Laboratoire de Physique Corpusculaire, Clermont Université and Université Blaise Pascal and CNRS/IN2P3, Clermont-Ferrand, France*
[35]*Nevis Laboratory, Columbia University, Irvington, New York, USA*
[36]*Niels Bohr Institute, University of Copenhagen, Kobenhavn, Denmark*
[37a]*INFN Gruppo Collegato di Cosenza, Italy*
[37b]*Dipartimento di Fisica, Università della Calabria, Arcavata di Rende, Italy*
[38]*AGH University of Science and Technology, Faculty of Physics and Applied Computer Science, Krakow, Poland*
[39]*The Henryk Niewodniczanski Institute of Nuclear Physics, Polish Academy of Sciences, Krakow, Poland*
[40]*Physics Department, Southern Methodist University, Dallas, Texas, USA*
[41]*Physics Department, University of Texas at Dallas, Richardson, Texas, USA*
[42]*DESY, Hamburg and Zeuthen, Germany*
[43]*Institut für Experimentelle Physik IV, Technische Universität Dortmund, Dortmund, Germany*
[44]*Institut für Kern- und Teilchenphysik, Technical University Dresden, Dresden, Germany*
[45]*Department of Physics, Duke University, Durham, North Carolina, USA*
[46]*SUPA-School of Physics and Astronomy, University of Edinburgh, Edinburgh, United Kingdom*
[47]*INFN Laboratori Nazionali di Frascati, Frascati, Italy*
[48]*Fakultät für Mathematik und Physik, Albert-Ludwigs-Universität, Freiburg, Germany*
[49]*Section de Physique, Université de Genève, Geneva, Switzerland*
[50a]*INFN Sezione di Genova, Italy*
[50b]*Dipartimento di Fisica, Università di Genova, Genova, Italy*
[51a]*E. Andronikashvili Institute of Physics, Tbilisi State University, Tbilisi, Georgia*
[51b]*High Energy Physics Institute, Tbilisi State University, Tbilisi, Georgia*
[52]*II Physikalisches Institut, Justus-Liebig-Universität Giessen, Giessen, Germany*
[53]*SUPA-School of Physics and Astronomy, University of Glasgow, Glasgow, United Kingdom*
[54]*II Physikalisches Institut, Georg-August-Universität, Göttingen, Germany*
[55]*Laboratoire de Physique Subatomique et de Cosmologie, Université Joseph Fourier and CNRS/IN2P3 and Institut National Polytechnique de Grenoble, Grenoble, France*
[56]*Department of Physics, Hampton University, Hampton, Virginia, USA*
[57]*Laboratory for Particle Physics and Cosmology, Harvard University, Cambridge, Massachusetts, USA*
[58a]*Kirchhoff-Institut für Physik, Ruprecht-Karls-Universität Heidelberg, Heidelberg, Germany*
[58b]*Physikalisches Institut, Ruprecht-Karls-Universität Heidelberg, Heidelberg, Germany*
[58c]*ZITI Institut für technische Informatik, Ruprecht-Karls-Universität Heidelberg, Mannheim, Germany*
[59]*Faculty of Applied Information Science, Hiroshima Institute of Technology, Hiroshima, Japan*
[60]*Department of Physics, Indiana University, Bloomington, Indiana, USA*
[61]*Institut für Astro- und Teilchenphysik, Leopold-Franzens-Universität, Innsbruck, Austria*
[62]*University of Iowa, Iowa City, Iowa, USA*
[63]*Department of Physics and Astronomy, Iowa State University, Ames, Iowa, USA*
[64]*Joint Institute for Nuclear Research, JINR Dubna, Dubna, Russia*
[65]*KEK, High Energy Accelerator Research Organization, Tsukuba, Japan*
[66]*Graduate School of Science, Kobe University, Kobe, Japan*
[67]*Faculty of Science, Kyoto University, Kyoto, Japan*
[68]*Kyoto University of Education, Kyoto, Japan*
[69]*Department of Physics, Kyushu University, Fukuoka, Japan*
[70]*Instituto de Física La Plata, Universidad Nacional de La Plata and CONICET, La Plata, Argentina*
[71]*Physics Department, Lancaster University, Lancaster, United Kingdom*
[72a]*INFN Sezione di Lecce, Italy*
[72b]*Dipartimento di Matematica e Fisica, Università del Salento, Lecce, Italy*
[73]*Oliver Lodge Laboratory, University of Liverpool, Liverpool, United Kingdom*
[74]*Department of Physics, Jožef Stefan Institute and University of Ljubljana, Ljubljana, Slovenia*
[75]*School of Physics and Astronomy, Queen Mary University of London, London, United Kingdom*
[76]*Department of Physics, Royal Holloway University of London, Surrey, United Kingdom*
[77]*Department of Physics and Astronomy, University College London, London, United Kingdom*

[78]Laboratoire de Physique Nucléaire et de Hautes Energies, UPMC and Université Paris-Diderot and CNRS/IN2P3, Paris, France
[79]Fysiska institutionen, Lunds universitet, Lund, Sweden
[80]Departamento de Fisica Teorica C-15, Universidad Autonoma de Madrid, Madrid, Spain
[81]Institut für Physik, Universität Mainz, Mainz, Germany
[82]School of Physics and Astronomy, University of Manchester, Manchester, United Kingdom
[83]CPPM, Aix-Marseille Université and CNRS/IN2P3, Marseille, France
[84]Department of Physics, University of Massachusetts, Amherst, Massachusetts, USA
[85]Department of Physics, McGill University, Montreal, Quebec, Canada
[86]School of Physics, University of Melbourne, Victoria, Australia
[87]Department of Physics, The University of Michigan, Ann Arbor, Michigan, USA
[88]Department of Physics and Astronomy, Michigan State University, East Lansing, Michigan, USA
[89a]INFN Sezione di Milano, Italy
[89b]Dipartimento di Fisica, Università di Milano, Milano, Italy
[90]B.I. Stepanov Institute of Physics, National Academy of Sciences of Belarus, Minsk, Republic of Belarus
[91]National Scientific and Educational Centre for Particle and High Energy Physics, Minsk, Republic of Belarus
[92]Department of Physics, Massachusetts Institute of Technology, Cambridge, Massachusetts, USA
[93]Group of Particle Physics, University of Montreal, Montreal, Quebec, Canada
[94]P.N. Lebedev Institute of Physics, Academy of Sciences, Moscow, Russia
[95]Institute for Theoretical and Experimental Physics (ITEP), Moscow, Russia
[96]Moscow Engineering and Physics Institute (MEPhI), Moscow, Russia
[97]Skobeltsyn Institute of Nuclear Physics, Lomonosov Moscow State University, Moscow, Russia
[98]Fakultät für Physik, Ludwig-Maximilians-Universität München, München, Germany
[99]Max-Planck-Institut für Physik (Werner-Heisenberg-Institut), München, Germany
[100]Nagasaki Institute of Applied Science, Nagasaki, Japan
[101]Graduate School of Science and Kobayashi-Maskawa Institute, Nagoya University, Nagoya, Japan
[102a]INFN Sezione di Napoli, Italy
[102b]Dipartimento di Scienze Fisiche, Università di Napoli, Napoli, Italy
[103]Department of Physics and Astronomy, University of New Mexico, Albuquerque, New Mexico, USA
[104]Institute for Mathematics, Astrophysics and Particle Physics, Radboud University Nijmegen/Nikhef, Nijmegen, Netherlands
[105]Nikhef National Institute for Subatomic Physics and University of Amsterdam, Amsterdam, Netherlands
[106]Department of Physics, Northern Illinois University, DeKalb, Illinois, USA
[107]Budker Institute of Nuclear Physics, SB RAS, Novosibirsk, Russia
[108]Department of Physics, New York University, New York, New York, USA
[109]Ohio State University, Columbus, Ohio, USA
[110]Faculty of Science, Okayama University, Okayama, Japan
[111]Homer L. Dodge Department of Physics and Astronomy, University of Oklahoma, Norman, Oklahoma, USA
[112]Department of Physics, Oklahoma State University, Stillwater, Oklahoma, USA
[113]Palacký University, RCPTM, Olomouc, Czech Republic
[114]Center for High Energy Physics, University of Oregon, Eugene, Oregon, USA
[115]LAL, Université Paris-Sud and CNRS/IN2P3, Orsay, France
[116]Graduate School of Science, Osaka University, Osaka, Japan
[117]Department of Physics, University of Oslo, Oslo, Norway
[118]Department of Physics, Oxford University, Oxford, United Kingdom
[119a]INFN Sezione di Pavia, Italy
[119b]Dipartimento di Fisica, Università di Pavia, Pavia, Italy
[120]Department of Physics, University of Pennsylvania, Philadelphia, Pennsylvania, USA
[121]Petersburg Nuclear Physics Institute, Gatchina, Russia
[122a]INFN Sezione di Pisa, Italy
[122b]Dipartimento di Fisica E. Fermi, Università di Pisa, Pisa, Italy
[123]Department of Physics and Astronomy, University of Pittsburgh, Pittsburgh, Pennsylvania, USA
[124a]Laboratorio de Instrumentacao e Fisica Experimental de Particulas-LIP, Lisboa, Portugal
[124b]Departamento de Fisica Teorica y del Cosmos and CAFPE, Universidad de Granada, Granada, Spain
[125]Institute of Physics, Academy of Sciences of the Czech Republic, Praha, Czech Republic
[126]Faculty of Mathematics and Physics, Charles University in Prague, Praha, Czech Republic
[127]Czech Technical University in Prague, Praha, Czech Republic
[128]State Research Center Institute for High Energy Physics, Protvino, Russia
[129]Particle Physics Department, Rutherford Appleton Laboratory, Didcot, United Kingdom
[130]Physics Department, University of Regina, Regina, Saskatchewan, Canada
[131]Ritsumeikan University, Kusatsu, Shiga, Japan
[132a]INFN Sezione di Roma I, Italy
[132b]Dipartimento di Fisica, Università La Sapienza, Roma, Italy

[133a]*INFN Sezione di Roma Tor Vergata, Italy*
[133b]*Dipartimento di Fisica, Università di Roma Tor Vergata, Roma, Italy*
[134a]*INFN Sezione di Roma Tre, Italy*
[134b]*Dipartimento di Fisica, Università Roma Tre, Roma, Italy*
[135a]*Faculté des Sciences Ain Chock, Réseau Universitaire de Physique des Hautes Energies-Université Hassan II, Casablanca, Morocco*
[135b]*Centre National de l'Energie des Sciences Techniques Nucleaires, Rabat, Morocco*
[135c]*Faculté des Sciences Semlalia, Université Cadi Ayyad, LPHEA-Marrakech, Morocco*
[135d]*Faculté des Sciences, Université Mohamed Premier and LPTPM, Oujda, Morocco*
[135e]*Faculté des sciences, Université Mohammed V-Agdal, Rabat, Morocco*
[136]*DSM/IRFU (Institut de Recherches sur les Lois Fondamentales de l'Univers), CEA Saclay (Commissariat a l'Energie Atomique), Gif-sur-Yvette, France*
[137]*Santa Cruz Institute for Particle Physics, University of California Santa Cruz, Santa Cruz, California, USA*
[138]*Department of Physics, University of Washington, Seattle, Washington, USA*
[139]*Department of Physics and Astronomy, University of Sheffield, Sheffield, United Kingdom*
[140]*Department of Physics, Shinshu University, Nagano, Japan*
[141]*Fachbereich Physik, Universität Siegen, Siegen, Germany*
[142]*Department of Physics, Simon Fraser University, Burnaby, British Columbia, Canada*
[143]*SLAC National Accelerator Laboratory, Stanford, California, USA*
[144a]*Faculty of Mathematics, Physics & Informatics, Comenius University, Bratislava, Slovak Republic*
[144b]*Department of Subnuclear Physics, Institute of Experimental Physics of the Slovak Academy of Sciences, Kosice, Slovak Republic*
[145a]*Department of Physics, University of Johannesburg, Johannesburg, South Africa*
[145b]*School of Physics, University of the Witwatersrand, Johannesburg, South Africa*
[146a]*Department of Physics, Stockholm University, Sweden*
[146b]*The Oskar Klein Centre, Stockholm, Sweden*
[147]*Physics Department, Royal Institute of Technology, Stockholm, Sweden*
[148]*Departments of Physics & Astronomy and Chemistry, Stony Brook University, Stony Brook, New York, USA*
[149]*Department of Physics and Astronomy, University of Sussex, Brighton, United Kingdom*
[150]*School of Physics, University of Sydney, Sydney, Australia*
[151]*Institute of Physics, Academia Sinica, Taipei, Taiwan*
[152]*Department of Physics, Technion: Israel Institute of Technology, Haifa, Israel*
[153]*Raymond and Beverly Sackler School of Physics and Astronomy, Tel Aviv University, Tel Aviv, Israel*
[154]*Department of Physics, Aristotle University of Thessaloniki, Thessaloniki, Greece*
[155]*International Center for Elementary Particle Physics and Department of Physics, The University of Tokyo, Tokyo, Japan*
[156]*Graduate School of Science and Technology, Tokyo Metropolitan University, Tokyo, Japan*
[157]*Department of Physics, Tokyo Institute of Technology, Tokyo, Japan*
[158]*Department of Physics, University of Toronto, Toronto, Ontario, Canada*
[159a]*TRIUMF, Vancouver, British Columbia, Canada*
[159b]*Department of Physics and Astronomy, York University, Toronto, Ontario, Canada*
[160]*Faculty of Pure and Applied Sciences, University of Tsukuba, Tsukuba, Japan*
[161]*Department of Physics and Astronomy, Tufts University, Medford, Massachusetts, USA*
[162]*Centro de Investigaciones, Universidad Antonio Narino, Bogota, Colombia*
[163]*Department of Physics and Astronomy, University of California Irvine, Irvine, California, USA*
[164a]*INFN Gruppo Collegato di Udine, Italy*
[164b]*ICTP, Trieste, Italy*
[164c]*Dipartimento di Chimica, Fisica e Ambiente, Università di Udine, Udine, Italy*
[165]*Department of Physics, University of Illinois, Urbana, Illinois, USA*
[166]*Department of Physics and Astronomy, University of Uppsala, Uppsala, Sweden*
[167]*Instituto de Física Corpuscular (IFIC) and Departamento de Física Atómica, Molecular y Nuclear and Departamento de Ingeniería Electrónica and Instituto de Microelectrónica de Barcelona (IMB-CNM), University of Valencia and CSIC, Valencia, Spain*
[168]*Department of Physics, University of British Columbia, Vancouver, British Columbia, Canada*
[169]*Department of Physics and Astronomy, University of Victoria, Victoria, British Columbia, Canada*
[170]*Department of Physics, University of Warwick, Coventry, United Kingdom*
[171]*Waseda University, Tokyo, Japan*
[172]*Department of Particle Physics, The Weizmann Institute of Science, Rehovot, Israel*
[173]*Department of Physics, University of Wisconsin, Madison, Wisconsin, USA*
[174]*Fakultät für Physik und Astronomie, Julius-Maximilians-Universität, Würzburg, Germany*
[175]*Fachbereich C Physik, Bergische Universität Wuppertal, Wuppertal, Germany*
[176]*Department of Physics, Yale University, New Haven, Connecticut, USA*
[177]*Yerevan Physics Institute, Yerevan, Armenia*
[178]*Centre de Calcul de l'Institut National de Physique Nucléaire et de Physique des Particules (IN2P3), Villeurbanne, France*

[a]Deceased.
[b]Also at Laboratorio de Instrumentacao e Fisica Experimental de Particulas-LIP, Lisboa, Portugal.
[c]Also at Faculdade de Ciencias and CFNUL, Universidade de Lisboa, Lisboa, Portugal.
[d]Also at Particle Physics Department, Rutherford Appleton Laboratory, Didcot, United Kingdom.
[e]Also at TRIUMF, Vancouver BC, Canada.
[f]Also at Department of Physics, California State University, Fresno, CA, USA.
[g]Also at Novosibirsk State University, Novosibirsk, Russia.
[h]Also at Fermilab, Batavia, IL, USA.
[i]Also at Department of Physics, University of Coimbra, Coimbra, Portugal.
[j]Also at Department of Physics, UASLP, San Luis Potosi, Mexico.
[k]Also at Università di Napoli Parthenope, Napoli, Italy.
[l]Also at Institute of Particle Physics (IPP), Canada.
[m]Also at Department of Physics, Middle East Technical University, Ankara, Turkey.
[n]Also at Louisiana Tech University, Ruston, LA, USA.
[o]Also at Dep Fisica and CEFITEC of Faculdade de Ciencias e Tecnologia, Universidade Nova de Lisboa, Caparica, Portugal.
[p]Also at Department of Physics and Astronomy, University College London, London, United Kingdom.
[q]Also at Department of Physics, University of Cape Town, Cape Town, South Africa.
[r]Also at Institute of Physics, Azerbaijan Academy of Sciences, Baku, Azerbaijan.
[s]Also at Institut für Experimentalphysik, Universität Hamburg, Hamburg, Germany.
[t]Also at Manhattan College, New York, NY, USA.
[u]Also at School of Physics, Shandong University, Shandong, China.
[v]Also at CPPM, Aix-Marseille Université and CNRS/IN2P3, Marseille, France.
[w]Also at School of Physics and Engineering, Sun Yat-sen University, Guanzhou, China.
[x]Also at Academia Sinica Grid Computing, Institute of Physics, Academia Sinica, Taipei, Taiwan.
[y]Also at Dipartimento di Fisica, Università La Sapienza, Roma, Italy.
[z]Also at DSM/IRFU (Institut de Recherches sur les Lois Fondamentales de l'Univers), CEA Saclay (Commissariat a l'Energie Atomique), Gif-sur-Yvette, France.
[aa]Also at Section de Physique, Université de Genève, Geneva, Switzerland.
[bb]Also at Departamento de Fisica, Universidade de Minho, Braga, Portugal.
[cc]Also at Department of Physics and Astronomy, University of South Carolina, Columbia, SC, USA.
[dd]Also at Institute for Particle and Nuclear Physics, Wigner Research Centre for Physics, Budapest, Hungary.
[ee]Also at California Institute of Technology, Pasadena, CA, USA
[ff]Also at Institute of Physics, Jagiellonian University, Krakow, Poland.
[gg]Also at LAL, Université Paris-Sud and CNRS/IN2P3, Orsay, France.
[hh]Also at Nevis Laboratory, Columbia University, Irvington, NY, USA.
[ii]Also at Department of Physics and Astronomy, University of Sheffield, Sheffield, United Kingdom.
[jj]Also at Department of Physics, Oxford University, Oxford, United Kingdom.
[kk]Also at Institute of Physics, Academia Sinica, Taipei, Taiwan.
[ll]Also at Department of Physics, The University of Michigan, Ann Arbor, MI, USA.
[mm]Also at Discipline of Physics, University of KwaZulu-Natal, Durban, South Africa.